



HAL
open science

Characterization of different pepper resistances to Potato virus Y through quantitative approaches to measure viral load

Pierre Mustin

► **To cite this version:**

Pierre Mustin. Characterization of different pepper resistances to Potato virus Y through quantitative approaches to measure viral load. Life Sciences [q-bio]. 2020. dumas-02997823

HAL Id: dumas-02997823

<https://dumas.ccsd.cnrs.fr/dumas-02997823v1>

Submitted on 10 Nov 2020

HAL is a multi-disciplinary open access archive for the deposit and dissemination of scientific research documents, whether they are published or not. The documents may come from teaching and research institutions in France or abroad, or from public or private research centers.

L'archive ouverte pluridisciplinaire **HAL**, est destinée au dépôt et à la diffusion de documents scientifiques de niveau recherche, publiés ou non, émanant des établissements d'enseignement et de recherche français ou étrangers, des laboratoires publics ou privés.

Année universitaire : 2019 - 2020

Spécialité/Mention : PPEH

Spécialisation/Parcours : Horticulture

Mémoire de fin d'études

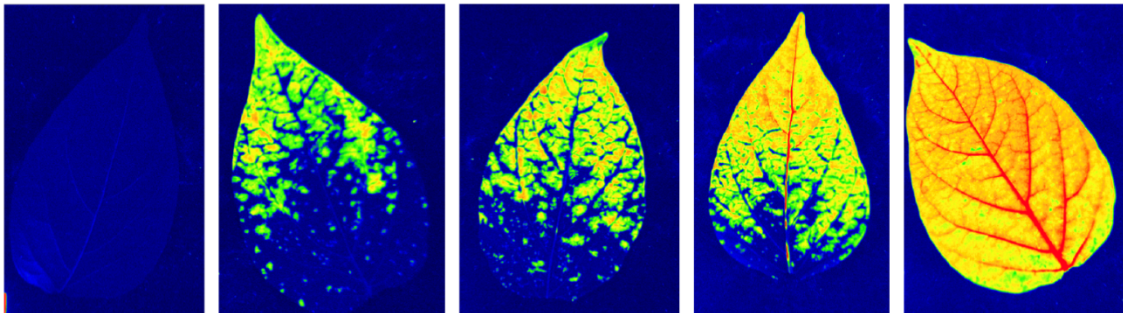
D'ingénieur de l'Institut Supérieur des Sciences agronomiques, agroalimentaires, horticoles et du paysage

De master de l'Institut Supérieur des Sciences agronomiques, agroalimentaires, horticoles et du paysage

D'un autre établissement (étudiant arrivé en M2)

Characterization of different pepper resistances to *Potato virus Y* through quantitative approaches to measure viral load

Par : Pierre MUSTIN



Soutenu à Angers le 24 septembre 2020

Devant le jury composé de :

Président : Bruno Jaloux

Autres membres du jury : Amandine Cunty

Maître de stage : Loup Rimbaud

Enseignant référent : Alexandre Degrave

Les analyses et les conclusions de ce travail d'étudiant n'engagent que la responsabilité de son auteur et non celle d'AGROCAMPUS OUEST

Ce document est soumis aux conditions d'utilisation

«Paternité-Pas d'Utilisation Commerciale-Pas de Modification 4.0 France»

disponible en ligne <http://creativecommons.org/licenses/by-nc-nd/4.0/deed.fr>



Etat de l'art des mécanismes de résistances des plantes aux infections virales et des méthodes de laboratoire pour la détection et la quantification des virus dans les plantes

(Partie supplémentaire rédigée en français, lecture non exigée)

Introduction

L'amélioration des pratiques de protection des cultures contre les organismes nuisibles est l'un des principaux enjeux de la recherche agronomique actuelle. Parmi ceux-ci, les agents pathogènes des plantes sont caractérisés par une diversité d'organismes biologiques comme les nématodes, les champignons, les bactéries et les virus (Oerke, 2005). Cette diversité d'agents pathogènes est liée à diverses façons de réduire la productivité des cultures, depuis la consommation de tissus, l'assimilation de la sève jusqu'aux troubles du métabolisme compromettant au moins 10 % de la production alimentaire mondiale (Boote et al, 1983 ; Strange et Scott, 2005).

Depuis les années 1950, le développement industriel de l'agriculture a conduit à une utilisation massive de produits chimiques de protection des cultures afin de minimiser les pertes causées par les agents pathogènes et les parasites (Savary et al, 2019). Cependant, les maladies causées par les virus diffèrent considérablement des pathologies bactériennes ou fongiques. Les infections virales sont persistantes, généralisées et généralement incurables (Devergne et Albouy, 1991). Par conséquent, les pratiques de protection des cultures sont limitées puisqu'il n'existe pas de traitement chimique pour guérir les plantes infectées par des virus (Moury et al, 2010). Certaines méthodes de prophylaxie telles que la thermothérapie et la protection croisée donnent des résultats prometteurs pour réduire les infections virales, mais sont associées à des procédures coûteuses et exigeantes en main-d'œuvre (Thompson et Tepfer, 2010 ; Varveri et al, 2015 ; Wang et al, 2018). Par ailleurs, l'efficacité de la lutte contre les vecteurs dépend fortement de l'espèce de virus et de son mode de transmission (Perring et al, 1999). Compte tenu de ces limites, des pratiques de protection des cultures efficaces nécessitent la gestion des maladies virales avant l'apparition des foyers de maladie. Par conséquent, l'utilisation des résistances des plantes pourrait être un catalyseur majeur pour proposer des solutions efficaces et à faible apport d'intrants (Moury et al, 2010 ; Boualem et al, 2011). La sélection de résistances végétales est déjà une méthode courante pour limiter les infections virales. Cependant, l'évaluation de l'expression des résistances est une condition préalable à une utilisation durable des résistances des plantes qui peut facilement être compromise par la contre-adaptation du virus ciblé conduisant à la dégradation des résistances, un gaspillage de ressources génétiques associé à de lourdes pertes économiques.

Le sujet de mon stage porte sur la gestion des maladies virales par l'utilisation des résistances des plantes et l'évaluation de leur expression phénotypique sur une étape du cycle viral. Afin de fournir un contexte permettant de mieux comprendre les résultats présentés dans ce rapport, l'introduction est divisée en quatre parties principales. Tout d'abord, le cycle viral sera présenté, ainsi que les principaux mécanismes de la résistance des plantes aux virus. Ensuite, les méthodes actuelles d'évaluation de la résistance des plantes seront présentées, avant d'exposer les objectifs du stage et les connaissances préalables sur l'étude de cas de ce travail : l'interaction entre le piment (*Capsicum annuum*) et le PVY (*Potato virus Y*).

1. Cycle viral et résistance des plantes aux virus

1.1. De l'inoculation du virus à sa transmission ultérieure

Fondamentalement, un cycle viral dans les plantes est constitué de cinq étapes principales (figure 1) : (i) inoculation du virus, (ii) multiplication du virus dans les cellules hôtes, (iii) migration du virus de cellule à cellule, (iv) colonisation systémique du virus et (v) dissémination du virus vers d'autres plantes.

Les espèces virales peuvent avoir plusieurs voies de transmission (Matthews, 1981 ; Astier et al, 2001). Par exemple, les tobamovirus comme le *Tobacco mosaic virus* (TMV) et le *Tomato brown rugose fruit virus* (ToBRFV) sont transmis par les semences, les eaux de circulation et les contacts mécaniques entre les plantes (Salem et al, 2016). Ces contacts mécaniques provoquent des blessures "fraîches" qui permettent à ces virus de surmonter les premières barrières de l'hôte à l'infection (cuticule et paroi cellulaire) (Devergne et Albouy, 1998).

Cependant, la transmission des virus se fait le plus souvent par des insectes vecteurs qui peuvent être telluriques ou aériens (Astier et al, 2001). Les vecteurs telluriques comprennent des groupes restreints de nématodes et de champignons (Walkey, 1991). Les vecteurs aériens comprennent des insectes comme les aleurodes, les cochenilles, les cicadelles et les pucerons (Jones, 1987 ; Astier et al, 2001). Les pucerons sont de loin les vecteurs les plus importants, car ils transmettent environ 30 % de tous les virus végétaux connus à ce jour (Brault et al, 2010). En outre, les stratégies de transmission dépendent d'interactions très spécifiques entre les protéines virales et les récepteurs des insectes, ce qui met en évidence une coévolution intense entre l'agent pathogène et son vecteur (Brault et al, 2010). Il existe deux principaux modes de transmission des virus des plantes par les insectes vecteurs : non circulatoire et circulatoire.

- La transmission non circulatoire est le mode de transmission le plus courant dans les virus des plantes. Les particules virales restent liées aux stylets de pucerons sur des récepteurs spécifiques (Khelifa, 2019). Cette étape est appelée rétention et sa durée peut varier de quelques minutes (non persistante) à quelques heures ou jours (semi-persistante) (Brault et al, 2010). Les particules virales et les styles d'insectes peuvent se lier soit directement grâce à la protéine de capsid (*Cucumber mosaic virus*), soit indirectement par l'intermédiaire d'un composé protéique supplémentaire.

- La transmission circulatoire nécessite la rétention de la particule virale à l'intérieur de son vecteur et le franchissement de différentes barrières pour atteindre l'hémolymphe et les autres organes (glandes salivaires, organes reproducteurs...) (Ng et Perry, 2004 ; Brault et al, 2010). Dans la plupart des cas, la période de rétention peut durer pendant toute la durée de vie du vecteur (Brault et al, 2010). Certains virus peuvent même se multiplier dans leurs cellules vectrices comme les Rhabdoviridae (Sylvester, 1980).

Une fois que le virus a pénétré dans son hôte, il profite de la cellule hôte en utilisant son énergie et sa machinerie pour la synthèse de ses propres protéines et acides nucléiques

(figure 2). Pour les virus végétaux à ARN (+) (environ 75 % de tous les virus végétaux), les acides nucléiques sont séparés de la protéine d'enveloppe (Astier et al, 2001). Ensuite, l'ARN viral s'associe aux ribosomes de l'hôte qui assurent la traduction de l'ARN polymérase virale et de certaines autres protéines spécifiques au virus comme les protéines de l'enveloppe (Matthews, 1981). L'ARN (+) est utilisé comme modèle pour transcrire des copies d'ARN (-) qui assureront ensuite la synthèse de molécules d'ARN (+) complémentaires (Devergne et Albouy, 1998). Les nouvelles particules virales sont composées d'ARN viral nouvellement répliqué et encapsidé par la protéine de capsid (Astier et al, 2001). Lorsque les multiples cycles de réplication et de traduction se produisent, il y a une accumulation d'ARN viral, de particules virales et de protéines virales dans la cellule hôte primaire infectée (Devergne et Albouy, 1998). Le virus peut alors coloniser les plantes par l'intermédiaire des plasmodemes sous forme de particules virales ou de complexes ribonucléoprotéiques (RNP) et initier de nouveaux cycles d'infection virale (Matthews, 1981 ; Dawson et Hilf, 1992, Lucas, 2006). Lorsque le virus atteint le système vasculaire, il colonise l'ensemble de l'organisme, ce qui entraîne une maladie généralisée reconnaissable à ses symptômes (Devergne et Albouy, 1998). Ces symptômes comprennent des anomalies de la pigmentation (mosaïques, aspect tacheté, taches annulaires, jaunisse et panachure des fleurs et/ou du feuillage), un ralentissement de la croissance (rabougrissement), des déformations et des nécroses (Walkey, 1991 ; Astier et al, 2001 ; Valverde et al, 2012). De plus, les infections virales provoquent des changements physiologiques et biochimiques tels qu'une diminution de l'efficacité de la photosynthèse, une augmentation de la fréquence respiratoire, une augmentation de certaines activités enzymatiques (polyphénoloxydases), une accumulation de polyphénols oxydés et enfin une augmentation ou une diminution des régulateurs de croissance des plantes (Matthews, 1981). Tous ces symptômes entraînent une réduction du rendement et de la qualité des cultures, ce qui se traduit par des pertes économiques pour les producteurs.

Enfin, la dernière étape du cycle viral est la transmission à une autre plante (selon l'une des voies décrites précédemment) qui est essentielle pour la survie et la dissémination géographique de la population virale.

1.2. Les résistances des plantes aux virus

Les plantes ont un système immunitaire complexe contre les virus, ce qui leur confère une résistance plus ou moins efficace aux infections. Les principaux mécanismes de résistance peuvent être divisés en trois catégories :

1.2.1. Résistance médiée par l'interférence de l'ARN

L'interférence de l'ARN constitue une défense contre les virus par un mécanisme de régulation de l'expression génétique où l'ARN viral subit une dégradation très spécifique (Astier et al, 2001). Une fois que la cellule végétale est infectée par un virus à ARN, l'ARN

viral se réplique et forme des molécules d'ARN double brin (ARNdb) dont la présence inhabituelle est détectée dans la cellule hôte. Ces ARN double brin sont ensuite transformés par des enzymes de type Dicer en petits ARN interférents (siRNA) dérivés du virus (Sharma et al, 2013). Ces siRNA sont pris dans le complexe de silençage induit par l'ARN (RISC) qui initie le clivage des acides nucléiques viraux ciblés (Sharma et al, 2013, Nicaise, 2014). En outre, l'intégration des siRNA dans le RISC génère un signal de silencieux mobile qui est transféré aux cellules adjacentes et à la plante entière par le biais des plasmodesmes et du phloème et amplifié par un processus d'amplification relais (Nicaise, 2014). Par conséquent, ce signal active l'extinction de l'ARN dans les cellules non infectées. Ce processus est impliqué dans les stratégies de protection croisée, qui empêchent l'infection par une espèce de virus à la suite d'une infection antérieure par une souche apparentée (Sharma et al, 2013).

1.2.2. Résistances qualitatives et quantitatives

Les résistances qualitatives sont connues pour conférer une résistance forte ou complète contre un parasite spécifique. Elles sont principalement basées sur la reconnaissance spécifique d'un facteur d'avirulence codé par un virus (comme la protéine de l'enveloppe) par une protéine R (résistance) végétale, appartenant à la classe des répétitions riches en leucine (NLR) (Nicaise, 2014 ; Boualem et al, 2016). Cette interaction déclenche une cascade de signalisation par la protéine kinase activée par un mitogène (MAPK). L'activation des gènes R déclenche une réponse hypersensible (HR), qui est une induction rapide de la mort cellulaire programmée pour les cellules infectées et leurs voisins. Il en résulte un confinement du virus et empêche toute nouvelle colonisation virale dans la plante (Nicaise, 2014). Elle peut également entraîner une accumulation rapide d'espèces réactives de l'oxygène (ROS) et d'hormones de défense (acides salicylique et jasmonique), ce qui conduit à une résistance systémique acquise (SAR ; Nicaise, 2014 ; Boualem et al, 2016). D'un point de vue sémiologique, cela conduit à l'apparition de taches nécrotiques sur les organes infectés après quelques heures (Astier et al, 2001). En outre, dans certains cas, l'infection virale est totalement éliminée sans aucune réaction de nécrose ; c'est ce qu'on appelle une résistance extrême (Astier et al, 2001). Malgré la rareté des gènes de résistance qualitative, ce type de résistance est fréquemment utilisé par les éleveurs car ces traits génétiques sont faciles à sélectionner (Fraser, 1992). Cependant, comme ils exercent une forte pression sélective sur les virus qui sont connus pour présenter des taux de mutation élevés par rapport à d'autres organismes biologiques, ces résistances peuvent être facilement surmontées par les virus (Gago et al, 2009) via la mutation de leurs facteurs d'avirulence. En revanche, les résistances partielles ou quantitatives ne font qu'adoucir l'infection des agents pathogènes (réduisant ainsi l'impact sur le rendement ou la qualité des plantes) sans empêcher l'infection. Elles sont plus abondantes dans les collections génétiques des cultures. Ces résistances ne sont pas liées à un mécanisme moléculaire spécifique et leur déterminisme génétique repose sur de nombreux QTL (Quantitative Trait Loci) (Lindhout,

2002). La résistance quantitative est souvent supposée plus durable que la résistance qualitative, cependant, comme l'utilisation de la résistance quantitative dans les cultures est moins fréquente que la résistance qualitative, peu de données sont disponibles pour documenter cette hypothèse (Lecoq et al, 2004).

1.2.3. Les résistances récessives

Ce type de résistance est plus courant pour les virus que pour les autres agents pathogènes des plantes et représente environ la moitié des 200 gènes de résistance connus (Diaz-Pendon, 2004 ; Nicaise, 2014). Elle repose sur des gènes récessifs codant pour des facteurs d'initiation eucaryotes (eIF) principalement recrutés par les virus (dont notamment les potyvirus) pour leur réplication et leur traduction (Nicaise, 2014). En effet, le cycle viral nécessite une série d'interactions compatibles entre l'hôte et les facteurs viraux à toutes les étapes de l'infection virale, de la traduction et de la réplication de l'ARN viral à la translocation à longue distance dans le système vasculaire (Diaz-Pendon et al, 2004). En conséquence, si un facteur hôte requis fait défaut ou présente une version mutée, le virus ne peut pas achever son cycle, ce qui entraîne une résistance de l'hôte (Astier et al, 2001 ; Diaz-Pendon et al, 2004).

1.3. Intégration des résistances des plantes dans le cycle viral

Comme l'illustrent les paragraphes précédents, il existe de multiples mécanismes de résistance des plantes aux virus qui sont complémentaires en termes de moment de défense (aux premiers ou derniers stades de l'infection), de localisation (dans la première feuille infectée ou dans les tissus systémiques) et de molécules virales ciblées (génome ou protéines virales) (Lecoq et al, 2004 ; Nicaise, 2014). En conséquence, on peut émettre l'hypothèse que différents gènes de résistance peuvent cibler différentes étapes du cycle infectieux viral. Cette hypothèse est étayée par les exemples suivants.

1.3.1. Résistance à l'inoculation ou à l'acquisition de virus par des vecteurs

La résistance à la transmission du virus est associée à une résistance dominante de la plante au vecteur lui-même, ce qui entraîne l'échec de l'inoculation ou de l'acquisition (Pochard, 1977). Ces résistances ont été décrites sur de nombreux vecteurs tels que les nématodes, les champignons et les insectes (Jones, 1987). Par exemple, le gène *Vat* (Virus aphid transmission) du melon interfère avec la transmission du virus par l'espèce de puceron *Aphis gossypii*. Les plantes porteuses du gène *Vat* ne sont pas infectées après une inoculation à médiation par les pucerons avec différents virus mais sont sensibles à ces virus lorsqu'elles sont inoculées mécaniquement ou lorsque d'autres espèces de pucerons sont utilisées pour la transmission (Martin et al, 2005 ; Boissot et al, 2010).

1.3.2. Résistance à la multiplication du virus dans la cellule infectée

La résistance à la multiplication du virus dans la cellule inoculée peut entraîner une absence totale ou une réduction de la réplication virale dans la cellule et peut reposer sur des gènes récessifs ou dominants. Par exemple, dans le cas de l'infection du poivron par le PVY, lorsqu'une plante est porteuse de deux allèles de résistance récessifs comme *pvr2*¹ et *pvr2*², leur présence combinée entraîne une interaction incompatible entre le virus et un facteur de traduction de la plante (eIF4E) conduisant à l'absence de multiplication du virus (Moury et al, 2004).

1.3.3. Résistance au mouvement des cellules du virus et à la colonisation systémique

Dans certains cas, le virus peut se multiplier dans les cellules inoculées mais ne peut pas se déplacer vers les cellules voisines ou ne pas atteindre le système vasculaire. Ici des résistances dominantes ont été identifiées. Par exemple, dans l'écotype Col-0 d'*Arabidopsis thaliana*, le TEV (*Tobacco etch virus*) se multiplie et se déplace de cellule en cellule mais ne peut pas atteindre le système vasculaire. Trois gènes dominants, *RTM1* (Restricted TEV Movement 1), *RTM2* et *RTM3* sont nécessaires pour cette résistance (Chisholm et al, 2001). Malgré les exemples cités ci-dessus, la littérature scientifique sur l'effet de la résistance des plantes aux différentes étapes du cycle infectieux des virus est encore rare. En particulier, il n'a jamais été démontré que différents gènes de résistance peuvent cibler différentes étapes du cycle pour une combinaison plante/virus donnée. Pourtant, la mise en place de résistances adaptées et efficaces dans les plantes cultivées est guidée par les connaissances disponibles sur les mécanismes moléculaires et les effets phénotypiques des résistances des virus des plantes (Nicaise, 2014). La mesure de ces effets phénotypiques à des fins de sélection nécessite des protocoles appropriés, et notamment des outils de diagnostic et de quantification pour évaluer la présence du virus et sa limitation par les mécanismes de résistance.

2. Méthodes de détection et de quantification des virus des plantes

Afin d'évaluer la présence d'un virus dans une plante, les scientifiques disposent d'un arsenal de méthodes qui sont choisies en fonction des objectifs de l'étude et des caractéristiques de la technique, telles que la spécificité (probabilité d'obtention d'un résultat négatif si absence de la cible) et la sensibilité (probabilité d'obtention d'un résultat positif si présence de la cible) (Van Stralen et al, 2009). Cette section couvrira les tests de diagnostic des virus des plantes les plus fréquemment utilisés en laboratoire.

2.1. Les tests d'infectivité

De toutes les méthodes d'évaluation, les tests d'infectivité sont les plus élémentaires puisqu'ils ne reposent que sur l'observation des symptômes après l'inoculation du virus (Matthews, 1981). Historiquement, ces tests étaient considérés comme des facteurs clés pour l'identification des virus car ils pouvaient aider à déterminer la gamme d'hôtes ou la sémiologie d'une espèce de virus inconnue (Walkey, 1991). Dans la pratique, les chercheurs commencent par inoculer biologiquement (via un vecteur) ou mécaniquement le virus à l'une de ses plantes hôtes et surveillent ensuite l'apparition des symptômes (Walkey, 1991). Cependant, l'expression des symptômes dépend fortement de la plante hôte (génotype et état physiologique), de la souche virale, de la date d'inoculation et des conditions environnementales (température, lumière) ; cela indique qu'une extrême prudence est nécessaire pour effectuer et normaliser ces tests (Walkey, 1991 ; Astier et al, 2001). Bien que ces tests soient toujours utilisés en laboratoire, l'introduction de l'essai immuno-enzymatique (ELISA) dans les années 1970-1980 a considérablement raccourci et simplifié la réalisation des diagnostics viraux de routine (Boonham et al, 2014).

2.2. Les techniques sérologiques

Les techniques sérologiques sont fréquemment utilisées pour leur spécificité, leur rapidité et leur facilité de standardisation (Clark et Adams, 1977). Ces techniques sont basées sur des principes de réactivité antigénique reposant sur la liaison spécifique entre deux types de molécules : l'antigène viral et son anticorps provenant de mammifères (Walkey, 1991 ; Astier et al, 2001). En résumé, le système immunitaire des mammifères a la capacité de reconnaître spécifiquement les caractéristiques de surface des macromolécules exogènes ou des micro-organismes appelés antigènes (Crowther, 1995). Les composants des mammifères qui effectuent cette reconnaissance sont appelés anticorps qui peuvent être monoclonaux ou polyclonaux selon qu'ils reconnaissent respectivement un ou plusieurs épitopes du même antigène. En virologie végétale, ces principes d'immunologie sont utilisés dans diverses techniques telles que l'immunoprécipitation ou le test ELISA (Enzyme linked Immunosorbent Assay). L'ELISA repose sur la détection sensible des réactions non précipitantes grâce à des anticorps marqués par une enzyme (Clark et Adams, 1977). En pratique, cette méthode est réalisée dans des plaques de microtitration sur lesquelles les antigènes sont d'abord adsorbés passivement sur la surface interne avant d'être incubés avec des anticorps marqués par des enzymes et suivis par le changement de couleur substrat approprié (Crowther, 1995 ; Sakamoto et al, 2018). Cette adsorption passive des anticorps facilite la séparation des réactifs libres et liés, ce qui permet également une grande souplesse dans la conception des tests (Crowther, 1995). En général, la phosphatase alcaline (ALP) est utilisée comme enzyme chargée de la transformation (en cas de reconnaissance antigène-anticorps) d'un substrat incolore soluble, le *p*-nitrophénylphosphate (PNPP), en *p*-nitrophénol qui peut être détecté à 405 nm (couleur jaune, Astier et al, 2001 ; Sakamoto et al, 2018). La raison de la popularité de l'ELISA réside dans son rapport coût-efficacité, sa robustesse, sa capacité à tester un grand nombre d'échantillons et sa simplicité. Cependant, dans les années 1990, de

nouvelles méthodes ont été développées pour détecter les acides nucléiques viraux (Boonham et al, 2014).

2.3. Les techniques moléculaires

Les techniques moléculaires telles que l'hybridation moléculaire et l'amplification en chaîne par polymérase (PCR) sont basées sur la complémentarité des séquences permettant la liaison des acides nucléiques viraux avec des sondes d'ADN ou d'ARN spécifiques aux séquences (Rubio et al, 2020). La PCR repose sur une succession d'étapes de dénaturation, d'hybridation des amorces et d'extension de la polymérase thermostable qui reproduit la séquence virale cible délimitée par les amorces (Astier et al, 2001). Cependant, pour les virus à ARN, une étape de transcription inverse est nécessaire avant l'amplification par PCR. Elle consiste à synthétiser un brin d'ADN complémentaire (ADNc) basé sur le brin d'ARN du virus grâce à une transcriptase inverse (Astier et al, 2001 ; Webster et al, 2004). À la fin, une migration des produits d'amplification est généralement effectuée par électrophorèse dans un gel d'agarose, qui révèle la présence ou l'absence d'un virus (Astier et al, 2001). La PCR et ses variantes sont très populaires en raison de leur grande sensibilité et de leur spécificité modulable en fonction des objectifs (Webster et al, 2004). En effet, plus les amorces sont conçues dans une région variable de la séquence du virus, plus le test est spécifique pour une espèce ou une souche virale (Astier et al, 2001). Toutefois, comme le test est très sensible, il augmente le risque de résultats faussement positifs dus à des contaminations (Webster et al, 2004 ; Bustin et al, 2009 ; Varveri et al, 2015).

2.4. Potentiel de ces techniques pour la quantification des virus

En plus de leur potentiel de détection qualitative des virus, les techniques de laboratoire décrites ci-dessus ont un potentiel de quantification. Pour les tests d'infectivité, une relation linéaire a été démontrée entre le nombre de lésions locales et la concentration de particules virales infectieuses dans l'extrait d'inoculation (Matthews, 1981 ; Astier et al, 2001). Cela suggère que la notation de la progression des symptômes peut être un moyen d'évaluer quantitativement l'accumulation virale. Le test ELISA peut être utilisé pour la quantification des protéines virales en fonction de l'intensité du signal (Rubio et al, 2020). Comme la densité optique résultante à une longueur d'onde spécifique et après une période d'incubation donnée est proportionnelle à la quantité initiale d'antigène, la concentration virale dans l'extrait de plante est mesurable par spectrophotométrie (Clark et Adams, 1977 ; Astier et al, 2001, Rubio et al, 2020). Pour les acides nucléiques viraux, la PCR quantitative (ou en temps réel) (qPCR) repose sur la quantification d'un signal fluorescent généré lors de l'amplification de l'ADN, soit via un agent d'intercalation (par exemple SYBRGreen), soit via une sonde d'hydrolyse (par exemple Taqman). Elle constitue une méthode très précise pour estimer la concentration d'acides nucléiques avec une grande sensibilité (Tse et Capeau, 2010).

3. Contexte du stage : méthodes de quantification pour l'étude des résistances du poivron contre le virus Y de la pomme de terre

Comme décrit ci-dessus, l'absence de virucides et la difficulté de contrôler les insectes vecteurs tout en atténuant les problèmes environnementaux et humains limitent considérablement le potentiel des produits chimiques pour gérer les épidémies de virus. Dans ce contexte, l'utilisation de la résistance des plantes est une stratégie prometteuse (Moury et al, 2010 ; Boualem et al, 2011). L'utilisation de méthodes de quantification fiables de l'infection virale est essentielle pour caractériser le niveau de résistance d'une plante à l'accumulation de virus. Traditionnellement, l'état sanitaire d'une plante est révélé par l'observation des symptômes ou par la détection des composants du virus tels que les protéines (révélées par ELISA) ou les acides nucléiques (révélées par RT-PCR). Ces méthodes sont donc utilisées pour distinguer les géotypes de plantes sensibles des géotypes de plantes résistantes (Lecoq et al, 2004). Cependant, l'estimation quantitative de la présence d'un virus permet d'obtenir une information plus précise sur le niveau de résistance d'une plante. Par exemple, il a été démontré que l'accumulation de virus est un estimateur précis de la résistance quantitative pour le piment (Tamisier et al, 2020). En effet, l'accumulation virale est une étape cruciale car elle contrôle non seulement la quantité de virus au sein de son hôte mais est également essentielle pour toutes les étapes suivantes de la migration cellulaire, de la colonisation systémique et de la transmission du vecteur. Le principal objectif de mon stage était l'évaluation de diverses approches quantitatives pour mesurer l'accumulation du virus Y de la pomme de terre (PVY, Potyvirus) dans le piment afin de caractériser les différentes résistances du poivron au PVY. Ce virus est associé à de lourdes pertes économiques et bénéficie d'une grande expertise au sein du laboratoire "Pathologie Végétale" du Centre INRAE d'Avignon où il est étudié depuis près de 50 ans. Il constitue donc un candidat parfait pour atteindre mes objectifs.

4. Cas d'étude : infection du piment par le virus Y de la pomme de terre

4.1. Le piment

Le piment (*Capsicum* L.) appartient à la famille des Solanacées et a été importé d'Amérique latine. Le genre *Capsicum* est composé de plus de 35 espèces dont 5 espèces sont domestiquées : *Capsicum annuum*, *Capsicum baccatum*, *Capsicum chinense*, *Capsicum frutescens* et *Capsicum pubescens* (Moscone et al, 2006). Actuellement, *C. annuum* est l'espèce la plus cultivée à l'échelle mondiale et est représentée par des milliers de cultivars (Penella et Calatayud, 2018). En raison de leur distribution mondiale, les poivriers sont exposés à de nombreux agents pathogènes, notamment des champignons (*Phytophthora capsici*, *Rhizoctonia solani*, *Verticillium dahlia*, *Fusarium* spp.), des bactéries (*Xanthomonas campestris*), des insectes (acariens, termites, pucerons et thrips), des nématodes (*Meloidogyne incognita*) et des virus (Penella et Calatayud, 2018). En particulier, vingt espèces de virus sont connues pour infecter le poivron, parmi lesquelles dix espèces appartiennent au genre Potyvirus, notamment le virus Y de la pomme de terre (Moury et al, 2005).

4.2. Le *Potato virus Y*

Le virus Y de la pomme de terre (PVY) appartient à la famille des Potyviridae et au genre Potyvirus. Son génome est un ARN simple brin (+), encapsidé dans une particule filamenteuse et flexueuse. Il possède une large gamme d'hôtes parmi lesquels des plantes économiquement importantes de la famille des Solanacées (tomate, tabac, piment, pomme de terre). Pour cette raison et la facilité avec laquelle ce virus peut être manipulé dans des conditions contrôlées, le PVY est signalé comme l'un des dix virus les plus étudiés en pathologie végétale moléculaire (Scholthof et al, 2010). La transmission naturelle du PVY implique des pucerons vecteurs, mais des inoculations mécaniques peuvent être effectuées dans des conditions de laboratoire (Astier et al, 2001). Plus de 40 espèces de pucerons sont connues pour transmettre le PVY de manière non persistante et non circulatoire (Scholthof et al, 2010).

4.3. Résistances du piment au PVY

Les infections à PVY sont fréquentes dans les cultures de piment et peuvent entraîner des pertes économiques considérables (Fereres et al, 1996). Sur le piment, les symptômes du PVY sont caractérisés des mosaïques ou des nécroses selon le génotype du piment et l'isolat du PVY (Dogimont et al, 1996). Selon les estimations, environ 40 % de toutes les accessions de piments sont résistantes aux isolats actuels de PVY, et plusieurs mécanismes de résistance sont impliqués (Charron et al, 2008). Parmi les sources de résistance bien identifiées :

- *Pvr4*, un gène localisé sur le chromosome 10, confère une résistance qualitative au PVY en codant pour une protéine NLR interagissant avec un facteur d'avirulence du PVY, l'ARN polymérase NIb dépendante de l'ARN (Kim et al, 2017).

- *pvr2*, localisé sur le chromosome 4, confère une résistance récessive au PVY. À ce niveau, 34 allèles de résistance sont classés de *pvr2*¹ à *pvr2*³⁴ et un allèle de susceptibilité est noté *pvr2*⁺. Ces allèles codent pour une protéine appartenant à la famille eIF4E (eukaryotic translation initiation factor 4E). Sur un génotype sensible, eIF4E est réquisitionné par la protéine VPg du virus pour initier la traduction ou la réplication de l'ARN viral. Cependant, lorsqu'une plante porte deux allèles de résistance de ce gène, l'infection est inhibée (Ruffel et al, 2004).

- Les QTLs pour les résistances quantitatives au PVY ont été identifiées sur des accessions doubles de piments haploïdes obtenues à partir d'hybrides F1 entre un cultivar de piment résistant, "Perennial" (portant l'allèle de résistance récessif *pvr2*³) et un cultivar sensible "Yolo wonder" (portant un allèle sensible *pvr2*⁺). En raison de la ségrégation des allèles parents au niveau du locus *pvr2*, ces accessions présentent différents niveaux de résistance partielle au PVY.

5. Objectif du stage et stratégie expérimentale

En résumé, le stage a un objectif majeur : évaluer les relations entre les résultats fournis par différentes méthodes de quantification afin de proposer un outil fiable pour le suivi de l'accumulation de virus dans des plants de piments infectés. Pour atteindre cet objectif, l'approche expérimentale consiste à mesurer la charge virale associée à l'infection par le PVY dans les plants de piment par ELISA, RT-qPCR et imagerie de fluorescence, puis à évaluer les corrélations et les relations mathématiques entre les résultats. Historiquement dans le laboratoire de "Pathologie Végétale", la quantification des protéines virales est assurée par des tests ELISA. Récemment, les tests d'infectivité sont remplacés une approche quantitative non destructive basée sur la mesure de fluorescence d'un isolat de PVY modifié mais nécessitant quelques ajustements. Enfin, la quantification des acides nucléiques du PVY nécessite le développement d'un protocole de RT-qPCR.

Characterization of different pepper resistances to *Potato virus Y* through quantitative approaches to measure viral load

Pierre Mustin

Acknowledgements:

First of all, I would like to thank my training supervisor, Loup Rimbaud. Thank you for all the knowledges about plant virology, statistic and modelling you shared with me in a very pedagogical way. I also thank you for your precious tips on the master thesis redaction, your quick mindedness and of course your full support during the lockdown period. I really enjoyed working with you and I will remember all your advices for a long time

I thank also my co-supervisors, Marion Szadkowski and Judith Hirsch. Thank you both for your pedagogy, enthusiasm and your unfailing support. I really appreciated all our videoconference during the lockdown and all our regular meetings during the whole internship. Thank you also, Benoît Moury for all your sound advices during the meetings.

I also thank my referent teacher, Alexandre Degrave and the plant protection head teachers for your pedagogical supervision and your positive words during the confinement.

I thank all the members of the Plant Pathology laboratory for their kindness and communicative joy, Catherine, Gregory, Karine, Magali, Alexandra, Jonathan, Clara, Corinne, Claudine, Pascale and of course Marc Bardin for welcoming me during these six months. And of course, the doctoral students and employees, Paul, Estelle, Thomas and Roxanne for all our interesting daily conversations and laughter.

Thank you again for welcoming me with such open arms, during my unfortunately shortened visit to the Plant Pathology laboratory.

List of figures and tables:

Figure 1: Global infectious cycle of an aphid transmitted non-circulative plant virus

Figure 2: Main steps of the viral cycle at the cellular scale

Figure 3: Genome organization of potyviruses and role of synthesized proteins

Figure 4: Mechanical inoculation of a virus on plants

Figure 5: Mosaic symptoms of PVY on *C. annuum* leaves (©B. Lederer)

Figure 6: DAS-ELISA protocol for detection and quantification of PVYson41p-115k-GFP in leaf extracts.

Figure 7: Scheme of macroscopic Closed Fluorcam FC 800-C/1010-GFP

Figure 8: Relative quantification in a leaf sample (green curve) in comparison to a positive standard (red curve).

Figure 9: RT-PCR protocol for detection and quantification of PVYson41p-115k-GFP in extracted RNA from leaf samples.

Figure 10: Estimation of the viral load of PVYson41p-115k-GFP infected plants by fluorescence imaging followed by semi-quantitative ELISA assay (B, Blank; C, Negative control)

Table 1: PVY isolates used to develop generic RT-qPCR assays

Figure 11: Observed fluorescence on *C. annuum* cv. 'Yolo Wonder' mechanically inoculated with PVY-son41p-115K-GFP (A: leaves, B: stems, C: flowers, D: roots) and mock inoculated (E: stems, F: roots) at 42 dpi.

Figure 12: Observed fluorescence on *C. annuum* cv. 'Perennial' mechanically inoculated with PVY-son41p-115K-GFP (A: stems, B: leaves, C: roots) and mock inoculated (D: stems, E: roots) at 42 dpi.

Table 2: Detection of PVY-son41p-115K-GFP by ELISA in different plant organs for two *C. annuum* cultivars ('Yolo Wonder' and 'Perennial').

Figure 13: Heat map of the normalized OD values, averaged from 3 plates (loaded with *N. tabacum* cv. 'Xanthi' leaf extracts) after 4h of incubation with *p*-nitrophenyl-phosphate at ambient temperature.

Figure 14: Heat map of the normalized OD values, averaged from 9 plates (loaded with *C. annuum* cv. 'Yolo Wonder' leaf extracts) after 4h of incubation with *p*-nitrophenyl-phosphate at ambient temperature

Figure 15: Mean OD values recorded for the 12 wells of each line (from A to H) or the 8 wells of each column (from 1 to 12) of a microtiter plate loaded with 3 different *N. tabacum* cv. 'Xanthi' leaf extract concentrations (Plate 1 = 1:25, Plate 2 = 1:625, Plate 3 = 1:15625) and incubated in light.

Figure 16: Mean OD values recorded for the 12 wells of each line (from A to H) or the 8 wells of each column (from 1 to 12) of a microtiter plate loaded with 3 different *C. annuum* cv. 'Yolo Wonder' leaf extract concentrations (Plate 4 = 1:5, Plate 6 = 1:25, Plate 8 = 1:125) and incubated in light.

Figure 17: Mean OD values recorded for the 12 wells of each line (from A to H) or the 8 wells of each column (from 1 to 12) of a microtiter plate loaded with 3 different *C. annuum* cv. 'Yolo Wonder' leaf extract concentrations (Plate 5 = 1:5, Plate 7 = 1:25, Plate 9 = 1:125) and incubated in the dark.

Figure 18: Mean OD values recorded for the 12 wells of each line (from A to H) or the 8 wells of each column (from 1 to 12) of a microtiter plate loaded with 3 different *C. annuum* cv. 'Yolo Wonder' leaf extract concentrations (Plate 10 = 1:5, Plate 11 = 1:125, Plate 12 = 1:3125).

Table 3: Summary of the results of Welch's t-test assessing the edge effect on OD values and the characterization of the mean OD values curve (Df: Degree of freedom)

Figure 19: Boxplots of normalized OD values measured after 4h of substrate incubation in the light or in the dark.

Figure 20: Boxplots of normalized OD values measured after 4h of substrate incubation for each sample type (Sample, Blank, Negative control) when plant extracts were removed from plates directly in the sink or using a vacuum a pump

Table 4: Results of Welch's *t* test and Kruskal-Wallis *H* test assessing the washing effect on normalized OD values

Table 5: Pearson's correlation coefficient (*r*) between coat protein concentrations and GFP fluorescence (proportion of fluorescent surface and average level of fluorescence) for *C. annuum* cv. 'Yolo Wonder', *N. benthamiana*, *N. tabacum* cv. 'Xanthi'.

Table 6: Summary of RNA isolation from leaf samples using the TRI-Reagent® or the RNeasy® Plant Mini Kit procedure

Figure 21: The 1.0% agarose gel electrophoresis analysis showing the quality of the RNA samples extracted by the TRI-Reagent®-chloroform method (A) or by the RNeasy® Plant Mini kit (B). Lanes 1 to 30 are different RNA samples extracted from 30 different PVY infected *C. annuum* cv. 'Yolo Wonder' leaves.

Table 7: Nucleotide sequences of primers designed and used for RT-PCR to detect PVYson41p-115k-GFP and 22 other PVY isolates

Figure 22: The 1.0% agarose gel electrophoresis analysis showing the detection of PVYson41p-115K-GFP from infected leaf samples of *C. annuum* cv. 'Yolo Wonder' by different primers couples using a RT-PCR assay targeting the coat protein gene and the untranslated 3' region. C = control (RNA extract of a healthy *C. annuum* cv. 'Yolo Wonder').

Figure 23: The 1.5% agarose gel electrophoresis analysis showing the detection of 15 PVY isolates using a RT-PCR with the PM202 (A) and PM2011 (B) primer couple. B = Blank. L = 1kb DNA ladder (Promega®, USA)

Figure 24: Proportion of fluorescent leaf surface (A) and relative coat protein concentration (B) of *C. annuum* cv. 'Yolo Wonder' leaves in relation to their rank (0, cotyledon; 1, first leaf rank; 2, second leaf rank; 3, third leaf rank; 4, fourth leaf rank).

Figure 25: Regression curves between coat protein concentration and the proportion of fluorescent surface in PVYson41p-115K-GFP infected leaves of (A) *C. annuum* cv. 'Yolo Wonder', (B) *N. benthamiana*, (C) *N. tabacum* cv. 'Xanthi'.

Table 8: Mean and 95% confidence interval for the parameters of the non-linear logistic equations estimated for two cultivars of *C. annuum*, 'Yolo Wonder' and 'Perennial'

Figure 26: Kinetics of the proportion of fluorescent leaf surface in PVYson41p-115k-GFP infected leaves of *C. annuum* cv. 'Yolo Wonder' and 'Perennial'.

Table of contents

Acronyms	4
Names of cited viruses followed by their genus	5
Introduction	6
1. Viral cycle and plant resistance against viruses	6
2. Methods for plant virus detection and quantification	10
3. Internship context: quantification methods for studying viral accumulation	13
4. Case of study: infection of pepper by the <i>Potato virus Y</i>	13
5. Internship purpose and experimental strategy	14
Materials and methods	16
1. Plants and viruses	16
2. Quantitative estimations of the viral load	17
3. Assessing the correlation of the variables provided by different quantification methods	21
4. Assessing virus accumulation in pepper	21
5. Statistical analyses	22
Results	23
1. Efficiency of mechanical inoculation of PVY _{SON41p-115K-GFP} on two pepper genotypes 23	
2. Optimizing the semi quantitative ELISA protocol	23
3. Determination of the variable of interest for fluorescence imaging	24
4. Prior results for the future quantification of viral RNA	25
5. Relationship between leaf relative virus coat protein concentrations and proportion of fluorescent leaf surface	26
6. Assessing PVY _{SON41p-115K-GFP} accumulation in two contrasted pepper genotypes	27
Discussion	28
1. A robust quantitative approach to estimate viral load	28
2. Promising prior results for an entire RT-qPCR protocol development	29
3. Fluorescence imaging: a non-destructive and reliable method for virus quantification 29	
4. The proportion of fluorescent surface allows to monitor virus accumulation dynamics confirming known resistance characteristics of pepper cultivars	30

5. <i>C. annuum</i> cv. 'Perennial' resistance to mechanical inoculation of PVYson41p-115K-GFP	31
6. Ambiguous effects inducing OD variations in ELISA plates	31
Conclusion	33
Cited literature	34

Acronyms

AIC	Akaike Information Criterion
ALP	Alkaline phosphatase
BET	Ethidium Bromide
bp	Base pair
cDNA	Complementary deoxyribonucleic acid
CI ₉₅	95% Confidence Interval
eIFs	Eukaryotic initiation factors
ELISA	Enzyme Linked ImmunoSorbent Assay
DAS-ELISA	Double Antibody Sandwich Enzyme Linked ImmunoSorbent Assay
DNA	Deoxyribonucleic acid
dNTP	desoxyribonucleoside triphosphate
dpi	Day post inoculation
GFP	Green Fluorescent Protein
GLM	Generalized Linear Model
GMO	Genetically Modified Organism
HTS	High Throughput Sequencing
MAPK	Mitogen-activated protein kinase
NLR	Nucleotide-binding leucine-rich repeat
OD	Optical Density
PBS	Phosphate-Buffered Saline Solution
PCR	Polymerase Chain Reaction
PNPP	<i>p</i> -nitrophenyl phosphate
PNP	<i>p</i> -nitrophenol
qPCR	quantitative Polymerase Chain Reaction
QTL	Quantitative trait loci
RNA	Ribonucleic acid
RT-qPCR	Reverse Transcription quantitative Polymerase Chain Reaction
dsRNA	Double stranded ribonucleic acid
siRNA	small interfering ribonucleic acid
RISC	Ribonucleic acid induced silencing complex
RNP	Ribonucleoprotein
RTM	Restricted TEV Movement
Vat	Virus aphid transmission
TAE	Tris-Acetate-Ethylenediaminetetraacetic-acid
Taq	Thermus aquaticus polymerase
USA	United States of America

Names of cited viruses followed by their genus

PVY	<i>Potato virus Y</i>	<i>Potyvirus</i>
CMV	<i>Cucumber mosaic virus</i>	<i>Cucumovirus</i>
TMV	<i>Tobacco mosaic virus</i>	<i>Tobamovirus</i>
TEV	<i>Tobacco etch virus</i>	<i>Potyvirus</i>
ToBFRV	<i>Tomato brown rugose fruit virus</i>	<i>Tobamovirus</i>

Introduction

The enhancement of crop protection practices against harmful organisms is one of the main issues of current agronomic research. Among these, plant pathogens are characterized by a diversity of biological organisms like nematodes, fungi, bacteria and viruses (Oerke, 2005). This diversity of pathogens triggers various sources of crop productivity reduction, from tissue consumption, sap assimilation to metabolism disorders, globally compromising at least 10% of the global food production (Boote and al, 1983; Strange and Scott, 2005).

Since the 1950's the industrial development of agriculture has led to a massive use of crop protection chemical products in order to minimise the losses caused by pathogens and pests (Savary and al, 2019). However, the diseases caused by viruses differ significantly from bacterial or fungal pathologies. Viral infections are persistent, generalized and generally incurable (Devergne and Albouy, 1991). Consequently, crop protection practices are limited since no chemical treatment is available to cure plants infected by viruses (Moury and al, 2010). Some prophylaxis methods such as thermotherapy and cross-protection show promising results on reducing viral infections but are associated with labor intensive and expensive procedures (Thompson and Tepfer, 2010; Varveri and al, 2015; Wang and al, 2018). In addition, the efficiency of vector control highly depends on the virus species and its transmission mode (Perring and al, 1999). Taking into account these limits, efficient crop protection practices require the management of viral diseases before disease outbreaks. Hence, the use of plant resistance could be a major catalyst in proposing efficient and low-input solutions (Moury and al, 2010; Boualem and al, 2011). The selection of plant resistance is already a current method to limit virus infections. However, assessing resistance expression is a prerequisite for a sustainable use of plant resistance which can easily be compromised by the counter-adaptation of the targeted virus. Such adaptation leads to resistance breakdown, a waste of rare genetic resources associated with heavy economic losses.

My internship subject pertains to viral disease management by the use of plant resistances and assessment of their phenotypic expression on a step of the viral cycle. In order to provide background to better understand the results presented in this report, the introduction is divided in four main parts. First, the viral cycle will be presented, along with the main mechanisms of plant resistance to viruses. Next, the current methods for plant resistance assessment will be presented, before stating the objectives of the internship and prior knowledge on the case study of this work: the interaction between pepper (*Capsicum annum*) and PVY (Potato virus Y).

1. Viral cycle and plant resistance against viruses

1.1. From virus inoculation to its further transmission

Basically, a viral cycle in plants is constituted of five main steps (figure 1): (i) virus inoculation, (ii) virus multiplication in host cells, (iii) virus cell-to-cell migration, (iv) virus systemic colonization and (v) virus dissemination to other plants.

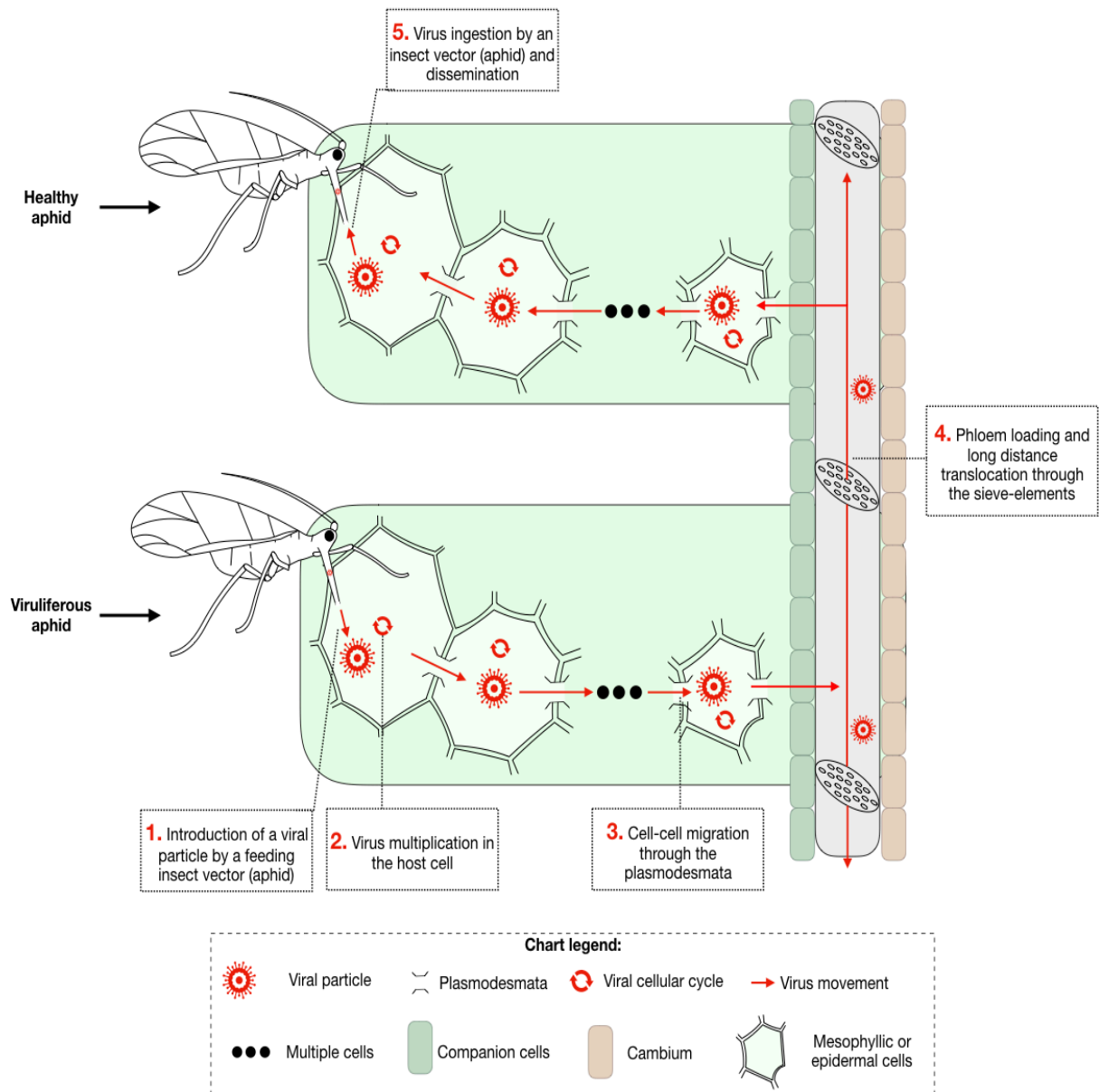


Figure 1: Global infectious cycle of an aphid transmitted non-circulative plant virus (adapted from Hipper, 2013). This viral cycle is a simplified representation of a type “cycle” in the case of a compatible infection of a host by a plant virus. (1) A viruliferous aphid inoculates the virus to a healthy plant. (2) In the inoculated cells, the virus replicates and its genome is translated into viral proteins. (3) The newly formed virus particles and ribonucleoproteins migrate through plasmodesmata. (4) The virus particles and/or RNP reach the sieve elements where they are transported to the distal tips of the plant. The virus enters a new site of infection and continues its replication. (5) The propagation of the virus inside the plant allows its acquisition by an aphid which may transmit it to another plant.

Virus species may have several paths for transmission (Matthews, 1981 ; Astier and al, 2001). For instance, tobamoviruses like the *Tobacco mosaic virus* (TMV) and the emerging *Tomato brown rugose fruit virus* (ToBRFV), are transmitted through seeds, circulating waters and mechanical contacts between plants (Salem and al, 2016). These mechanical contacts cause “fresh” wounds which allows these viruses to overcome the first host barriers to infection (cuticle and cell-wall) (Devergne and Albouy, 1998).

However, the most common way for viruses to be transmitted is via insect vectors which may be telluric or aerial (Astier and al, 2001). Telluric vectors include restricted groups of nematodes and fungi (Walkey, 1991). Aerial vectors include insects like whiteflies, mealybugs, leafhoppers, plant hoppers and aphids (Jones, 1987; Astier and al, 2001). Aphids are by far the most important vectors as they transmit about 30% of all plant viruses known to date (Brault and al, 2010). Besides, transmission strategies depend on highly specific interactions between viral proteins and insect receptors which highlights an intense coevolution between the pathogen and its vector (Brault and al, 2010). There are two main modes of plant virus transmission by insect vectors: non-circulative and circulative.

- **Non-circulative transmission** is the most common mode of transmission in plant viruses. The viral particles remain bound to the aphid stylets on specific receptors (Khelifa, 2019). This step is called retention and its duration can vary from a few minutes (non-persistent) to a few hours or days (semi-persistent) (Brault and al, 2010). The viral particle and insect stylets can either bind directly thanks to the capsid protein (*Cucumber mosaic virus*) or indirectly via an additional protein component, the helper component protein (HC) (Brault and al, 2010). These viruses are not transmitted to the progeny of their insect vector (Astier and al, 2001).
- **Circulative transmission** requires the retention of the viral particle inside its vector and the crossing of different barriers to reach the hemolymph and the other organs (salivary glands, reproductive organs...) (Ng and Perry, 2004; Brault and al, 2010). In most cases, the retention period can last for the vector entire lifespan (Brault and al, 2010). Some viruses can even multiply in their vector cells like the Rhabdoviridae (Sylvester, 1980).

Once the virus has entered its host, it takes advantage of the host cell by utilizing its energy and machinery for the synthesis of its own proteins and nucleic acids (figure 2). For (+) RNA plant viruses (about 75% of all plant viruses) the nucleic acids are separated from the coat protein (Astier and al, 2001). Then the viral RNA associates with the host ribosomes which ensure the translation of the viral RNA polymerase and some other virus-specific proteins like coat proteins (Matthews, 1981). The (+) RNA is used as a template to transcribe copies of (-)RNA which will then ensure the synthesis of complementary (+) RNA molecules (Devergne and Albouy, 1998). New viral particles are composed of newly replicated viral RNA encapsidated by the coat protein (Astier and al, 2001). As the multiple cycles of replication and translation occur, there is an accumulation of viral RNA, viral particles and viral proteins in the primary infected host cell (Devergne and Albouy, 1998). Then the virus can colonize the plants through plasmodesmata as virus particles or as ribonucleoprotein (RNP) complexes and initiate new virus infection cycles (Matthews, 1981; Dawson and Hilf,

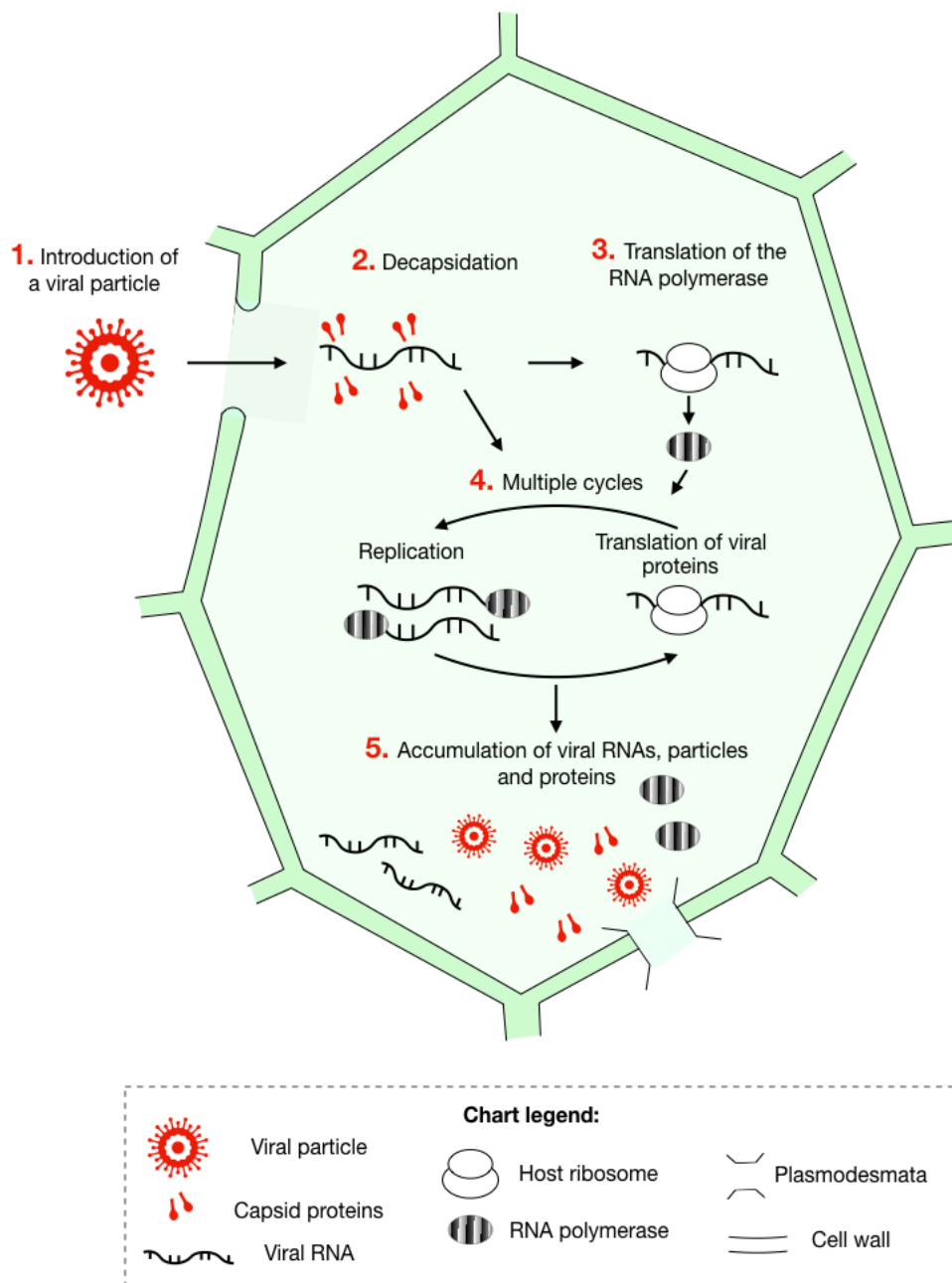


Figure 2: Main steps of the viral cycle at the cellular scale (adapted from Devergne and Albouy, 1998; Astier and al, 2001). (1) The viral particle is introduced to a host cell and its (2) RNA is separated from the coat protein. (3) The RNA polymerase is translated by a host ribosome. (4) The host ribosomes translate viral proteins and the RNA polymerases ensure virus RNAs replication. (5) Viral RNAs, particles and proteins are accumulating in the host cell.

1992, Lucas, 2006). When the virus reaches the vascular system, it colonizes the whole organism leading to a generalized disease recognizable by its symptoms (Devergne and Albouy, 1998). These symptoms include pigmentation anomalies (mosaics, mottled appearance, ring spots, jaundices and flower and/or foliage variegations), reduced growth (stunting), deformations and necrosis (Walkey, 1991; Astier and al, 2001; Valverde and al, 2012). Furthermore, virus infections cause physiological and biochemical changes such as a decrease in photosynthesis efficiency, an increase in respiratory rate, an increase of certain enzyme activities (polyphenoloxidases), an accumulation of oxidized polyphenols and finally an increase or a decrease of plant growth regulators (Matthews, 1981). All these symptoms lead to a reduction in crop yield and quality, resulting in economic losses for producers. Finally, the last step of the viral cycle is the transmission to another plant (according to one of the pathways described previously) which is essential for the survival and geographical dissemination of the viral population.

1.2. Plant resistance against viruses

Plants have a complex immune system against viruses, resulting in a more or less efficient resistance to infection. The main resistance mechanisms can be divided in three categories:

1.2.1. RNA interference mediated-resistance

RNA interference constitutes a defense against viruses by a mechanism of gene expression regulation where the viral RNA undergoes a highly specific degradation (Astier and al, 2001). Once the plant cell is infected by a RNA virus, the viral RNA replicates and forms double stranded RNA molecules (dsRNA) whose unusual presence is detected in the host cell. These dsRNAs are then processed by Dicer-like enzymes into virus-derived small interfering RNAs (siRNAs), (Sharma and al, 2013). These siRNAs are taken into the RNA induced silencing complex (RISC) which initiates the cleavage of the target viral nucleic acids (Sharma and al, 2013, Nicaise, 2014). In addition, the integration of siRNAs in the RISC generates a mobile-silencing signal which is transferred to the adjoining cells and the whole plant through plasmodesmata and the phloem and amplified by a relay-amplification process (Nicaise, 2014). Consequently, this signal activates RNA silencing in non-infected cells. This process is involved in cross-protection strategies, which prevent infection by a virus species following previous infection by a related strain (Sharma and al, 2013).

1.2.2. Qualitative and quantitative resistances

Qualitative resistances are known to confer strong or complete resistance against a specific parasite. They are mostly based on the specific recognition of a virus-encoded avirulence factor (like the coat protein) by a plant R (resistance) protein, belonging to the nucleotide binding leucine-rich repeat (NLR) class (Nicaise, 2014; Boualem and al, 2016). This interaction initiates a mitogen-activated protein kinase (MAPK) signaling cascade. The activation of *R* genes triggers a hypersensitive response (HR), which is a rapid induction of programmed cell death for the infected cells and their surrounding neighbors. It results in a

confinement of the virus and prevents any further viral colonization in the plant (Nicaise, 2014). It can also result in a fast accumulation of reactive oxygen species (ROS) and defense hormones (salicylic and jasmonic acids) leading to a systemic acquired resistance (SAR; Nicaise, 2014; Boualem and al, 2016). From a semiological point of view, this leads to the appearance of necrotic spots on the infected organs after a few hours (Astier and al, 2001). Besides, in some instances, viral infection is totally cleared without any necrosis reaction; this is called extreme resistance (Astier and al, 2001). In spite of the rarity of qualitative resistance genes, this kind of resistance is frequently used by breeders as these genetic traits are easily selected (Fraser, 1992). However, as they apply a strong selective pressure on viruses which are known to present high mutation rates compared to other biological organisms, these resistances may be easily overcome by viruses (Gago and al, 2009) via the mutation of their avirulence factors.

In contrast, partial or quantitative resistances only soften pathogen infection (hence reducing the impact on plant yield or quality) without preventing infection. They are more abundant in crop genetic collections. These resistances are not linked to a specific molecular mechanism and their genetic determinism rely on numerous QTLs (Quantitative Trait Loci) (Lindhout, 2002). Quantitative resistance is often supposed more durable than qualitative resistance, however, as the use of quantitative resistance in cultivated crops is less frequent than qualitative resistance, few data are available to document this hypothesis (Lecoq and al, 2004).

1.2.3. Recessive resistances

This kind of resistance is more common for viruses than for other plant pathogens and represents about one half of the 200 known resistance genes (Diaz-Pendon, 2004; Nicaise, 2014). It relies on recessive genes encoding for eukaryotic initiation factors (eIFs) mainly recruited by viruses (including especially potyviruses) for their replication and translation (Nicaise, 2014). Indeed, the viral cycle requires a series of compatible interactions between host and viral factors along all steps of the viral infection, from viral RNA translation and replication to long-distance translocation through the vascular system (Diaz-Pendon and al, 2004). As a consequence, if a required host factor is lacking or presents a mutated version, the virus cannot complete its cycle, resulting in host resistance (Astier and al, 2001; Diaz-Pendon and al, 2004).

1.3. Plant resistances and viral cycle

As illustrated in the previous paragraphs, there are multiple mechanisms of plant resistance against viruses which are complementary in terms of defense timing (at early or late steps of infection), location (in the first infected leaf or in systemic tissues) and the viral molecules that are targeted (viral genome or proteins) (Lecoq and al, 2004; Nicaise, 2014). As a consequence, it can be hypothesized that different resistance genes may target different steps of the viral infectious cycle. This hypothesis is supported by the following examples.

1.3.1. Resistance to virus inoculation or acquisition by vectors

Resistance to virus transmission is associated with a plant dominant resistance to the vector itself leading to the failure of the inoculation or the acquisition (Pochard, 1977). These resistances were described on many vectors such as nematodes, fungi and insects (Jones, 2006). For instance, the melon *Vat* (*Virus aphid transmission*) gene interferes with virus transmission by the aphid species *Aphis gossypi*. Plants carrying the *Vat* gene are not infected after an aphid-mediated inoculation with different viruses but are susceptible to these viruses when they are mechanically inoculated or when other aphid species are used for the transmission (Martin and al, 2005; Boissot and al, 2010).

1.3.2. Resistance to virus multiplication in the infected cell

Resistance to virus multiplication in the inoculated cell may result in a total absence or a reduction of viral replication in the cell and may rely on recessive or dominant genes. For example, in the case of pepper infection by PVY, when a plant carries two recessive resistance alleles like *pvr2*¹ and *pvr2*², their combined presence results in an incompatible interaction between the virus and a plant translation factor (eIF4E) leading to the absence of virus multiplication (Moury and al, 2004).

1.3.3. Resistance to virus cell to cell movement and systemic colonization

In some cases, the virus may multiply in the inoculated cells but cannot move to the adjoining cells or cannot reach the vascular system. In these cases, dominant resistances were identified. For instance, in the *Arabidopsis thaliana* ecotype Col-0, TEV (*Tobacco etch virus*) multiplies and moves from cell to cell but cannot move through the vascular system. Three dominant genes, *RTM1* (*Restricted TEV Movement 1*), *RTM2* and *RTM3* are required for this resistance (Chisholm and al, 2001)

In spite of the examples listed above, the scientific literature on the effect of plant resistance on the different steps of the viral infectious cycle is still scarce. In particular, it has never been demonstrated that different resistance genes may target different steps of the cycle for a given plant/virus combination. Yet, the implementation of suitable and efficient resistances in crop plants is guided by available knowledge on the molecular mechanisms and phenotypic effects of plant virus resistances (Nicaise, 2014). Measuring these phenotypic effects for breeding purposes requires appropriate protocols, and especially diagnostic and quantification tools to assess the virus presence and its limitation by resistance mechanisms.

2. Methods for plant virus detection and quantification

In order to assess the presence of a virus in a plant, scientists have an arsenal of methods which are chosen depending on the study purposes and the technique features such as the specificity (probability of a negative test among these without the target condition) and the

sensitivity (probability of a positive test result among these having the target condition) (Van Stralen and al, 2009). This section will cover the more frequently used diagnosis tests for plant viruses in laboratory.

2.1. Infectivity tests

Of all assessment methods, infectivity tests are the most basic since they rely only on the observation of symptoms after the inoculation of the virus (Matthews, 1981). Historically, these tests were considered as key factors for virus identification because they might help to determine the host range or the semiology of an unknown virus species (Walkey, 1991). In practice, investigators start by biologically (via vector) or mechanically inoculating the virus to one of its plant host and then monitor the occurrence of symptoms (Walkey, 1991). However, symptom expression strongly depends on the host plant (genotype and physiological state), the viral strain, the date of inoculation and the environmental conditions (temperature, light); this indicates that extreme caution is required to perform and standardize these tests (Walkey, 1991; Astier and al, 2001). Although these tests are still used in laboratories, the introduction of enzyme-linked immunosorbent assay (ELISA) in the 1970-80s deeply shortened and simplified the achievement of routine viral diagnostics (Boonham and al, 2014).

2.2. Serological techniques

Serological techniques are frequently used for their specificity, speed and ease to standardize (Clark and Adams, 1977). These techniques are based upon antigenic reactivity principles relying on the specific binding between two types of molecules: the viral antigen and its related antibody originating from mammals (Walkey, 1991; Astier and al, 2001). In brief, the mammalian immune system has an ability to specifically recognize surface features of exogenous macromolecules or microorganisms called antigens (Crowther, 1995). The mammal components performing this recognition are called antibodies which may be monoclonal or polyclonal depending on whether they recognize respectively one or several epitopes of the same antigen. In plant virology, these immunology principles are used in various techniques such as immunoprecipitation or Enzyme linked Immunosorbent Assay (ELISA). ELISA relies on the sensitive detection of non-precipitating reactions thanks to enzyme labelled antibodies (Clark and Adams, 1977). In practice, this method is achieved in microtiter plates on which antigens are first passively adsorbed on the inner surface before being incubated with enzyme labelled antibodies and followed by color development with the appropriate substrate (Crowther, 1995; Sakamoto and al, 2018). This passive adsorption of antibodies facilitates the separation of free and bound reagents which also allows a great flexibility in assay design (Crowther, 1995). Generally, alkaline phosphatase (ALP) is used as the enzyme in charge of the transformation (in case of antigen-antibody recognition) of a soluble colorless substrate, *p*-nitrophenyl phosphate (PNPP) into *p*-nitrophenol which can be detected at 405 nm (yellow color, Astier and al, 2001; Sakamoto and al, 2018). The reason

for ELISA popularity resides in its cost effectiveness, robustness, capacity of testing large number of samples and simplicity.

However, in the 1990s, new methods were developed to detect viral nucleic acids (Boonham and al, 2014).

2.3. Molecular techniques

Molecular techniques such as molecular hybridization and polymerase chain reaction (PCR) are based on sequence complementarity allowing the binding of viral nucleic acids with sequence-specific DNA or RNA probes (Rubio and al, 2020). The PCR relies on a succession of denaturation, primers hybridization and thermostable polymerase extension steps which replicates the target viral sequence delimited by primers (Astier and al, 2001). However, for RNA viruses, a reverse transcription step is required before the PCR amplification. It consists in synthesizing a complementary DNA (cDNA) strand based on the RNA strand of the virus thanks to a reverse transcriptase (Astier and al, 2001; Webster and al, 2004). This added step is performed prior to the PCR amplification (Astier and al, 2001). At the end, a migration of the amplification products is generally performed with an electrophoresis in an agarose gel, which reveals the presence or absence of a virus (Astier and al, 2001). The PCR and its variants are very popular because of their high sensitivity and modulable specificity depending on the desired objectives (Webster and al, 2004). Indeed, the more the primers are designed in a variable region of the virus sequence, the more specific the test is for a viral species or strain (Astier and al, 2001). However, as the test is highly sensitive, it increases the risk of false positive results due to contaminations (Webster and al, 2004; Bustin and al, 2009; Varveri and al, 2015).

2.4. Potential of these techniques for virus quantification

In addition to their potential for virus detection in a qualitative way, the laboratory techniques described above have a potential for virus quantification. For infectivity tests, a linear relationship has been demonstrated between the number of local lesions and the concentration of infective viral particles in the inoculation extract (Matthews, 1981; Astier and al, 2001). This suggest that scoring the progression of symptoms may be a way to evaluate quantitatively viral accumulation. ELISA can be used for virus protein quantification based on the signal intensity (Rubio and al, 2020). Since the resulting optical density at a specific wavelength and after a given incubation period is proportional to the initial quantity of antigen, the viral concentration in the plant extract is measurable by spectrophotometry (Clark and Adams, 1977; Astier and al, 2001, Rubio and al, 2020). For viral nucleic acids, quantitative (or real-time) PCR (qPCR) relies on the quantification of a fluorescent signal generated during DNA amplification, either via an intercalating agent (e.g. SYBRGreen) or a hydrolysis probe (e.g. Taqman). It constitutes of a very accurate method to estimate nucleic acid titer with a wide dynamic range and high sensitivity (Tse and Capeau, 2010).

There are also other techniques like High Throughput Sequencing (HTS), DNA arrays, lateral flow and molecular hybridization, which allow a quantitative assessment of viral

accumulation (Rubio and al, 2020). As these are beyond the scope of this work, they will not be further detailed.

3. Internship context: quantification methods for studying viral accumulation

As described above, the absence of virucides and the difficulty to control insect vectors while mitigating environmental and health issues considerably limits the potential of chemicals to manage virus epidemics. In this context, the use of plant resistance is a promising strategy (Moury and al, 2010; Boualem and al, 2011). The use of reliable quantification methods of virus infection is essential to characterize the resistance level of a plant to virus accumulation. Traditionally, the sanitary state of a plant is determined by the observation of symptoms or by the detection of virus components such as proteins (revealed by ELISA) or nucleic acids (revealed by RT-PCR). These methods were traditionally used to distinguish susceptible from resistant plant genotypes (Lecoq and al, 2004). However, quantitatively estimating the amount of a virus allows a more precise information on the level of a given plant resistance. For example, it has been shown that virus accumulation is an accurate estimator of quantitative resistance for pepper (Tamisier and al, 2020). Indeed, viral accumulation is a crucial step as it controls not only the virus quantity within its host but is also essential for all the following steps of cell migration, systemic colonization and vector transmission.

The main goal of my internship was the assessment of various quantitative approaches to measure the accumulation of *Potato virus Y* (PVY, Potyvirus) in pepper and destined to characterize different pepper resistances to PVY. This virus is associated with heavy economic losses and benefit from a great expertise at the “Pathologie Végétale” laboratory of the INRAE Center of Avignon where it has been studied for nearly 50 years. It thus provides a perfect candidate to fulfill my objectives.

4. Case of study: infection of pepper by the *Potato virus Y*

4.1. Pepper

Pepper (*Capsicum* L.) belongs to the *Solanaceae* family and was imported from latin America. The *Capsicum* genus is composed of more than 35 species among which 5 species are domesticated: *Capsicum annuum*, *Capsicum baccatum*, *Capsicum chinense*, *Capsicum frutescens* and *Capsicum pubescens* (Moscone and al, 2006). Currently, *C. annuum* is the more cultivated species at a global scale and is represented by thousands or cultivars (Penella and Calatayud, 2018). Due to their worldwide distribution, pepper plants are exposed to numerous pathogens including fungi (*Phytophthora capsici*, *Rhizoctonia solani*, *Verticillium dahlia*, *Fusarium* spp.), bacteria (*Xanthomonas campestris*), insects (mites, termites, aphids and thrips), nematodes (*Meloidogyne incognita*) and viruses (Penella and Calatayud, 2018). In particular, twenty virus species are known to infect pepper, among

which ten species belong to the *Potyvirus* genus, especially the *Potato virus Y* (Moury and al, 2005).

4.2. *Potato virus Y*

Potato virus Y (PVY) belongs to the *Potyviridae* family and the genus *Potyvirus*. Its genome is single stranded (+) RNA, encapsidated in a filamentous and flexuous particle (figure 3). It has a wide host range among which economically important plants from the *Solanacea* family (tomato, tobacco, pepper, potato). For this reason and the ease with which this virus can be manipulated in controlled conditions, PVY is reported as one of the ten most studied virus in molecular plant pathology, according to Scholthof and al (2010). Natural PVY transmission involves aphid vectors, but mechanical inoculations can be performed in laboratory conditions (Astier and al, 2001). More than 40 aphid species are known to transmit PVY in a non-persistent and non-circulative way (Scholthof and al, 2010).

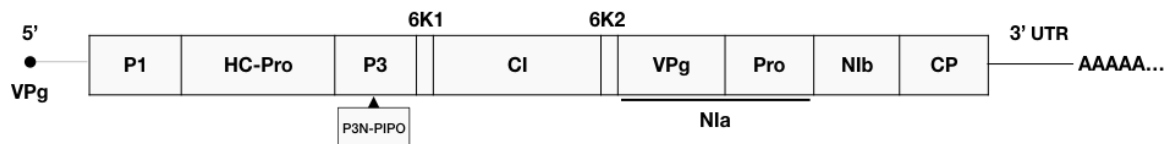
4.3. Pepper resistances to PVY

PVY infection are frequent in pepper and may result in considerable economic losses (Feres and al, 1996). Symptoms are characterized by systemic mosaic or necrotic symptoms depending on the pepper genotype and the PVY isolate (Dogimont and al, 1996). According to estimates, about 40% of all pepper accessions are resistant to current isolates of PVY, and several resistance mechanisms are involved (Charron and al, 2008). Among the well identified resistance sources:

- *Pvr4*, a gene localized on chromosome 10, confers a qualitative resistance to PVY by coding for a NLR protein interacting with an avirulence factor of PVY, the Nib RNA-dependent RNA polymerase (Kim and al, 2017).
- *pvr2*, localized on chromosome 4, confers a recessive resistance to PVY. At this locus, 34 resistance alleles are classified from *pvr2*¹ to *pvr2*³⁴ and a susceptibility allele is noted *pvr2*⁺. These alleles code for a protein belonging to the eIF4E (eukaryotic translation initiation factor 4E) family. On a susceptible genotype, eIF4E is requisitioned by the VPg protein of the virus to initiate the translation or the replication of the viral RNA. However, when a plant carries two resistance alleles of this gene, the infection is inhibited (Ruffel and al, 2004).
- QTLs for quantitative resistances to PVY were identified on doubled haploid pepper accessions obtained from F₁ hybrids between a resistant pepper cultivar, 'Perennial' (carrying the recessive resistance allele *pvr2*³) and a susceptible cultivar 'Yolo wonder' (carrying a susceptible allele *pvr2*⁺). Due to the segregation of parent alleles at the *pvr2* locus, these accessions show different levels of partial resistance to PVY.

5. Internship purpose and experimental strategy

To sum up, the internship held one major purpose: assessing the relationships between the results provided by different quantification methods in order to propose a reliable tool for monitoring virus accumulation in pepper. To address this objective, the experimental



Genomic region	Role
P1 protein	Protease, genome replication
HC-Pro	Aphid transmission, protease, long distance translocation, suppressor of RNA silencing
P3 protein	P3N Genome replication
	PIPO Cell to cell migration
6K1	Unknown
CI	Helicase and cell to cell migration
6K2	Nla and VPg protein attachment
Nla	Protease
	VPg Replication, long distance translocation and RNA binding to the coat protein
Nib	Genome replication
CP	Genome encapsidation, aphid transmission, cell to cell and long distance translocation, genome replication

Figure 3: Genome organization of potyviruses and role of synthesized proteins (Astier and al, 2001)

approach consisted in measuring the viral load associated with PVY infection in pepper plants by ELISA, RT-qPCR and fluorescence imaging and then assessing the correlations and mathematical relationships between the results. Historically in the "Plant Pathology laboratory", the quantification of virus proteins was ensured by ELISA assays. Recently, instead of doing infectivity tests, a non-destructive quantitative approach based on the measurement of a fluorescently tagged PVY isolate, has been developed but required some adjustments. Finally, the quantification of PVY nucleic acids needed the development of a complete RT-qPCR protocol.

However, developing a full RT-qPCR protocol toward this objective was difficult because of the current Covid-19 pandemic and the lockdown period, so it remained incomplete.

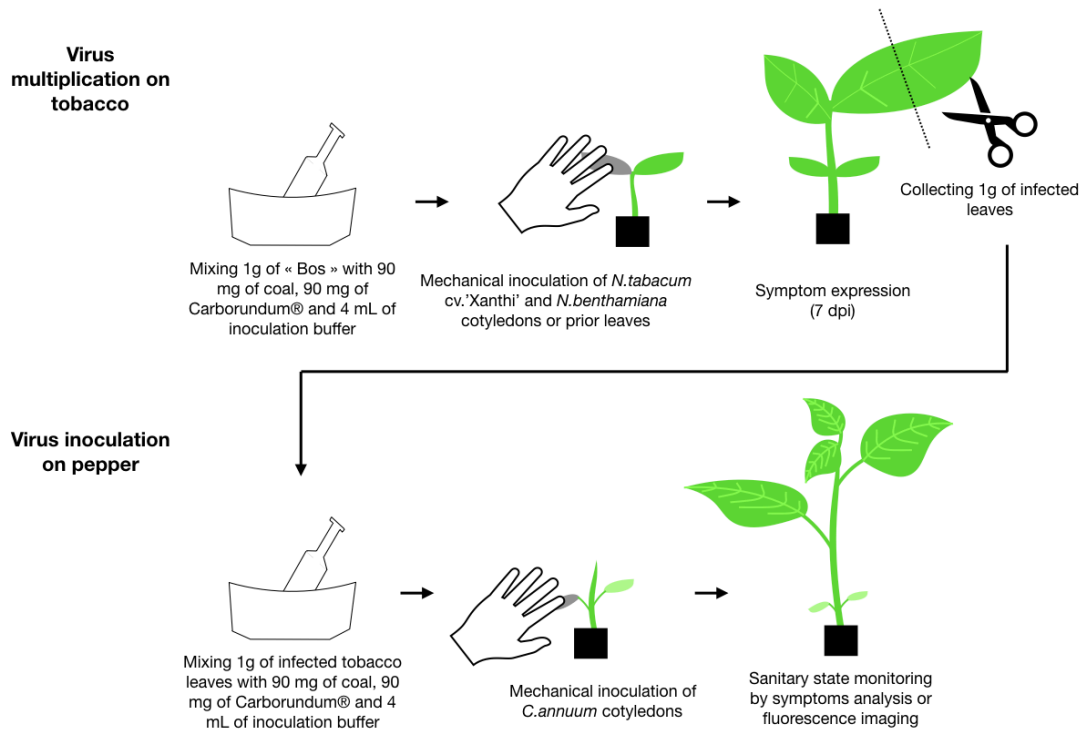


Figure 4: Mechanical inoculation of a virus on plants



Figure 5: Mosaic symptoms of PVY on *C. annuum* leaves (©B. Lederer)

Materials and methods

1. Plants and viruses

1.1. Plant material

Two contrasted pepper genotypes were used for the experiments. The cultivar 'Yolo Wonder' has a susceptible allele (*pvr2*⁺) and so was used as a susceptible genotype whereas 'Perennial' was used as a resistant genotype due to its recessive resistance allele (*pvr2*³) and at least its three QTLs conferring a quantitative resistance to PVY (Montarry and al, 2012; Quenouille and al, 2013). Moreover, *Nicotiana tabacum* cv. 'Xanthi' and *Nicotiana benthamiana* also from the *Solanaceae* family were used for viral multiplication before mechanical inoculation of pepper plants, as well as for some viral quantification tests.

For all plant species and cultivars, the seeds were first manually sown in batches and approximately two weeks after germination, the plantlets were manually disposed in individual pots. All the plants were grown in greenhouses with natural light conditions and no thermic control (except via fans to avoid extreme summer temperatures).

1.2. Virus material

The PVY_{SON41p-115K-GFP} isolate is named after the weed *Solanum nigrum* ('SON'), on which it was originally collected in Montfavet in 1982 (Moury and al, 2003). For years, it was conserved by serial inoculations of *C. annuum* plants in the "Pathologie Végétale" laboratory (hence the letter 'p'). A single amino acid substitution occurred, and the threonine (115th amino acid in the VPg amino acid sequence) was replaced by a lysine (K) allowing the virus to overcome the major resistance allele *pvr2*³ of the pepper cultivar 'Perennial'. More recently, a fluorescent marker, the green fluorescent protein ('GFP') sequence was added to the genome of the isolate in order to be able to visually monitor the colonization of the virus. Consequently, this PVY isolate is considered as a genetically modified organism (GMO) and its maintenance and study follow drastic rules. Accordingly, the plants inoculated with PVY 'son41p-115K-GFP' were disposed in a "S3 type" greenhouse which consists of a high level of confinement to prevent the undesirable dissemination of such material.

The collection of PVY isolates was maintained in the laboratory in the form of dehydrated infected plant material (Bos, 1969). This process relies on thinly cutting one gram of systemically infected leaves and stocking it at 4°C in airtight boxes with calcium chloride.

1.3. Plant inoculation procedures

As the isolate of PVY_{SON41p-115K-GFP} was conserved as a "Bos", it needed to be firstly multiplied on one of its highly susceptible host plants to regenerate fresh viral particles. Thus, we used classical mechanical inoculations of *N. benthamiana* and *N. tabacum* cv 'Xanthi'. For this, the "Bos" was mixed in a mortar bowl with 4 mL of inoculation buffer, 90 mg of coal (to limit the action of RNase enzymes) and 90 mg of Carborundum® (a fine abrasive powder) before being finger rubbed on a leaf (figure 4). The leaves were exposed to the inoculum for 5-10

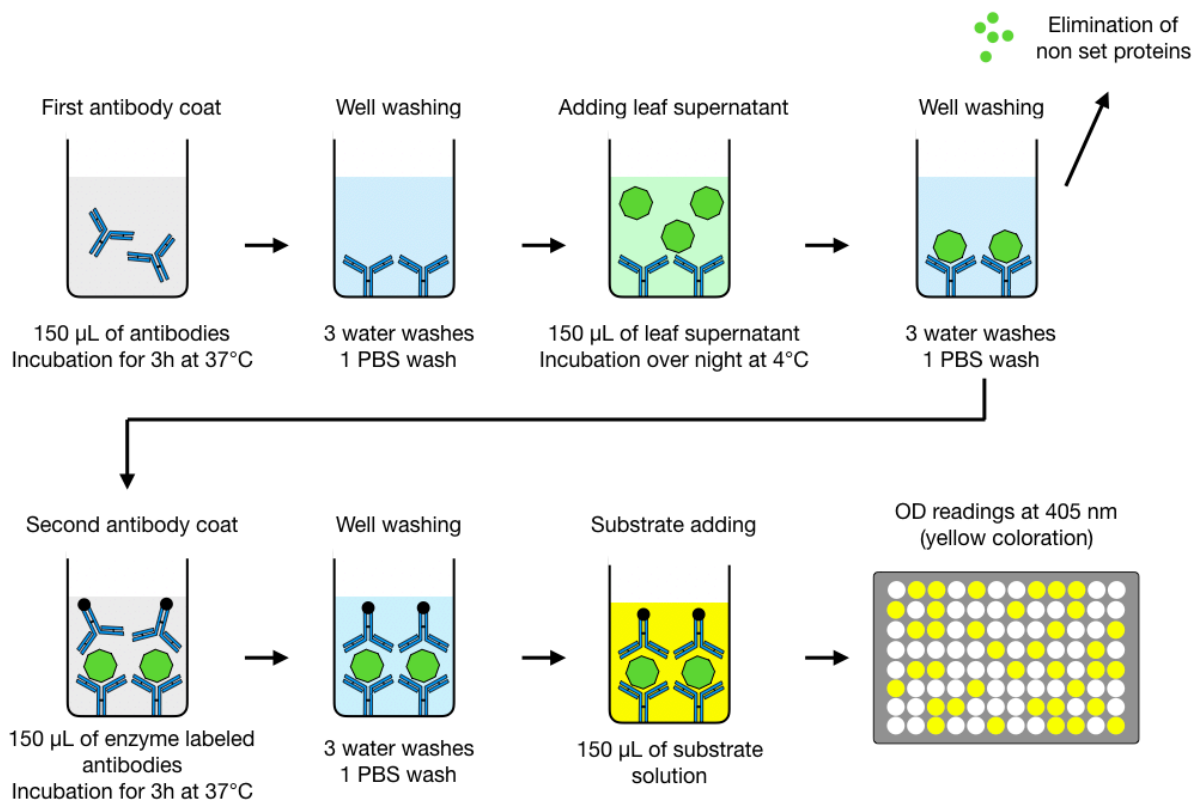


Figure 6: DAS-ELISA protocol for detection and quantification of PVYson41p-115k-GFP in leaf extracts.

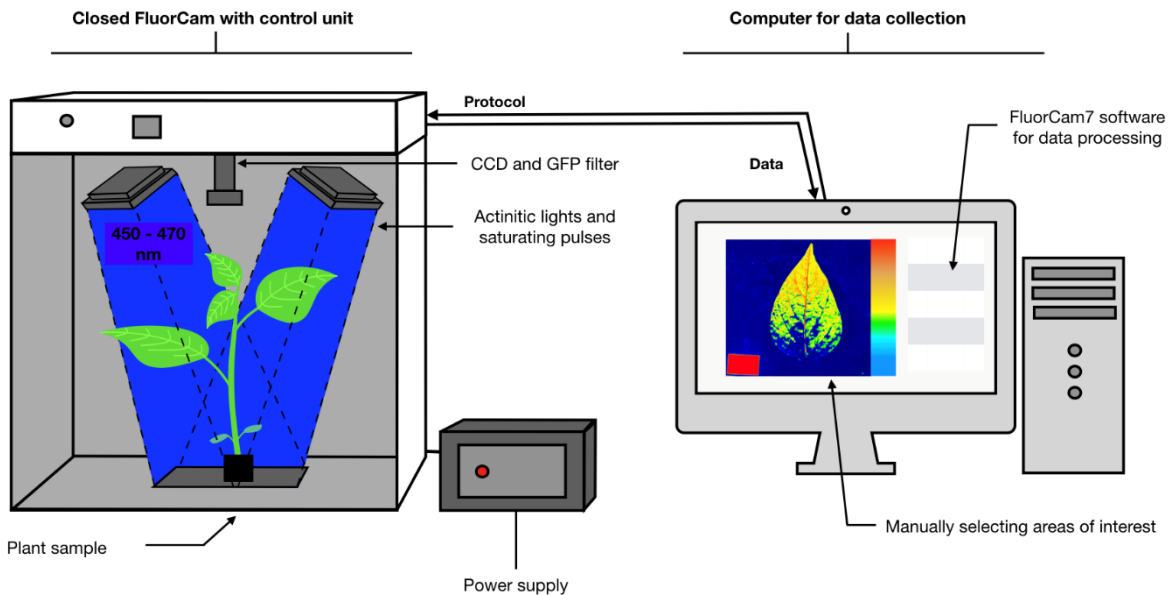


Figure 7: Scheme of macroscopic Closed Fluorcam FC 800-C/1010-GFP

min before being washed with tap water. Approximately seven days post inoculation (dpi), the occurrence of mosaic symptoms (figure 5) on the leaves of *N. benthamiana* and *N. tabacum* cv. 'Xanthi' revealed that the virus had efficiently multiplied. The cotyledons of healthy pepper plants could then be inoculated following the same protocol by using crude extract (1 g) of *N. benthamiana* and *N. tabacum* cv. 'Xanthi' leaves as sources of virus. In the absence of symptoms (i.e. at early stages of infection) the sanitary status of the plants (i.e. PVY infected or not) could be checked by fluorescence imaging or DAS-ELISA. Two types of controls were systematically added: mock-inoculated plants were inoculated only with the inoculation mix (buffer, coal and Carborundum®) and without any viral source, and healthy plant controls were not inoculated at all.

2. Quantitative estimations of the viral load

In the "Plant Pathology laboratory", the assessment of virus accumulation was traditionally performed by semi quantitative ELISA, a reliable method for coat protein quantification. However, as this method is used regularly, manipulators wanted to optimize their protocol by assessing the influences of different factors on ELISA results. Moreover, in order to simplify and increase the efficacy of the quantification, two candidate quantification methods based on fluorescence imaging and RT-qPCR required respectively a further analysis and a full development. Consequently, the three methods used for estimating the viral load and their respective optimization or development were to be described separately.

2.1. ELISA

2.1.1. General DAS-ELISA procedure

For all the experiments, only F96 Maxisorp nun-immuno plate® (Thermo scientific, Denmark) were used. First, the 96 wells of each plate were coated with 150 µL of antibodies (tittered at 1:2000) before being placed in an incubator for 3 hours at 37°C (figure 6). Then the plates were washed three times with water and once with phosphate-buffered saline solution (PBS) and patted dry. Straight after, the wells were filled with 150 µL of leaf extract (1g of leaf ground in 4 mL buffer, see table S1) and placed in a refrigerator at 4°C overnight (about 15 hours). Then the plates were washed again as described above before being filled with 150 µL of the second layer of antibodies (tittered at 1:2000) labelled with an enzyme, the alkaline phosphatase. The plates were incubated again at 37°C for 3 hours before being washed and filled with 150 µL of the substrate solution of *p*-nitrophenyl phosphate diluted in the substrate buffer (1%). During the incubation, a colored reaction occurred when *p*-nitrophenyl phosphate was dephosphorylated by phosphatase activity leading to the formation of the yellow colored *p*-nitrophenol. The optical densities were then measured after four hours of substrate incubation thanks to a Multiskan FC (Thermo scientific, Denmark) microplate reader calibrated at 405 nm.

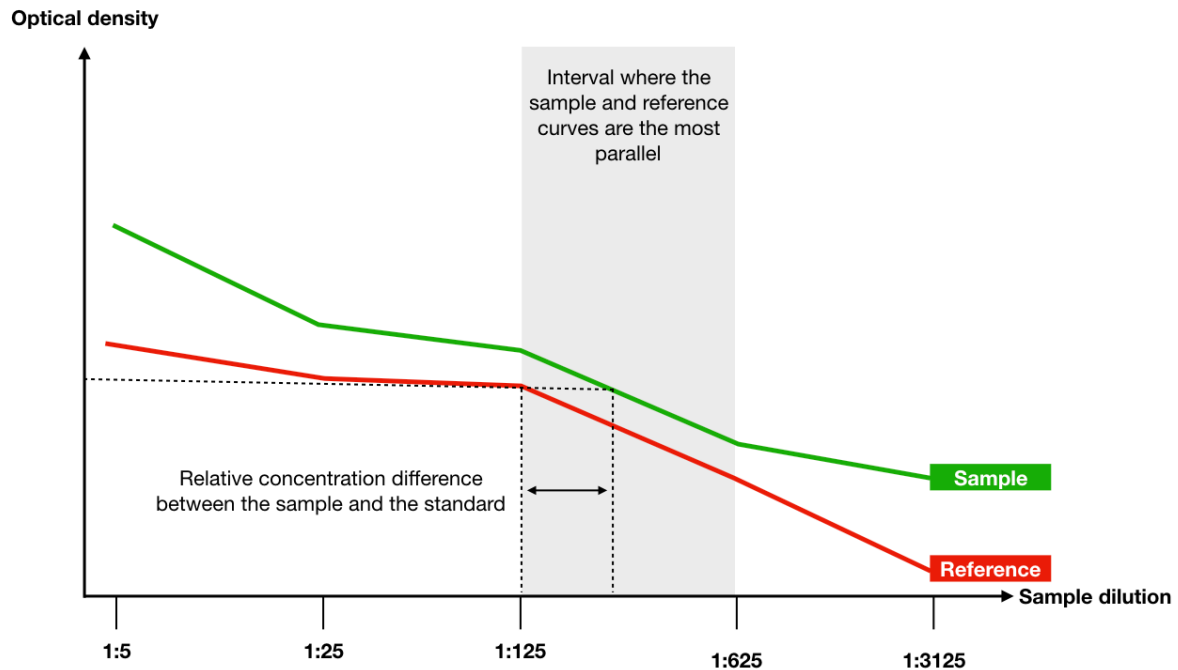


Figure 8: Relative quantification in a leaf sample (green curve) in comparison to a positive standard (red curve). In the grey area, it is possible to determine the relative coat protein concentration in the sample thanks to the difference in the abscissas associated with a given optical density between the two curves.

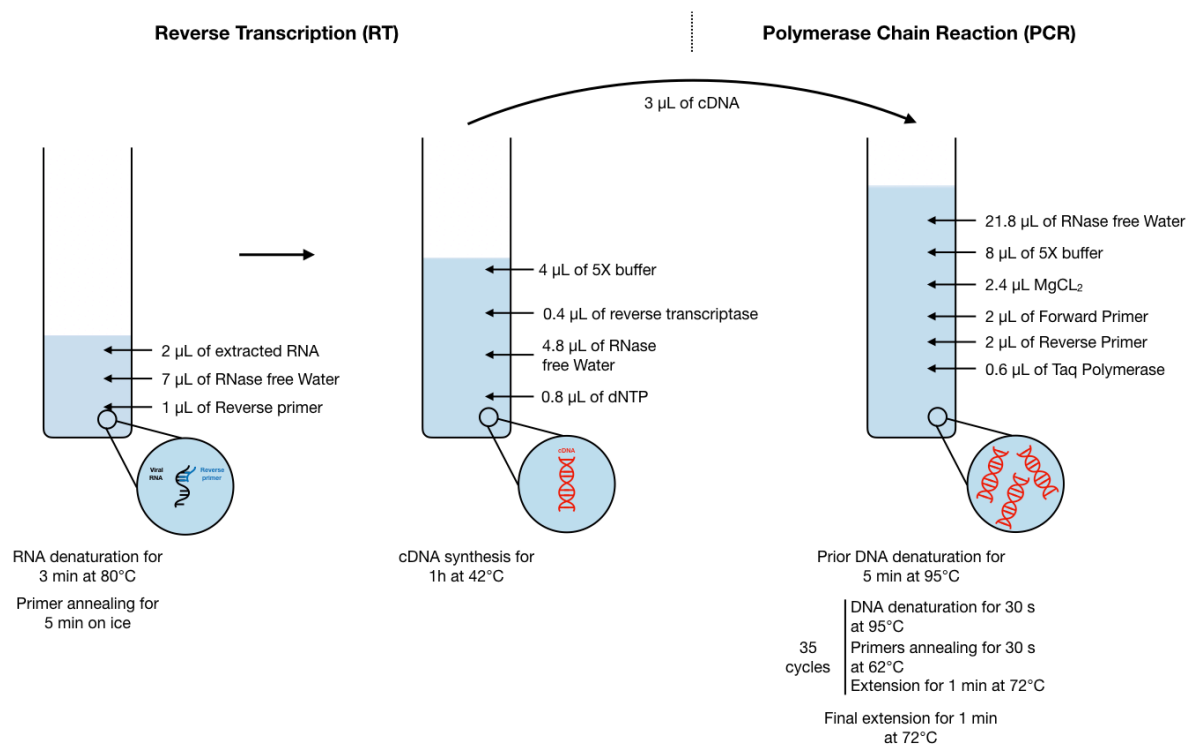


Figure 9: RT-PCR protocol for detection and quantification of PVYson41p-115k-GFP in extracted RNA from leaf samples.

2.1.2. Preliminary experiments: optimizing the semi quantitative ELISA protocol

Several authors reported the existence of optical density (OD) gradients within microtiter plates and reported especially an “edge” effect (Burt and al, 1979; Oliver and al, 1981). Knowing these possible variations, manipulators at the research unit “Plant Pathology laboratory” often choose to avoid the peripheral wells for quantitative ELISA tests. However, this represents a loss of 36 wells by plate. Moreover, protocol differences between manipulators and research units suggested that two other factors could influence the OD values: light condition during the substrate incubation (which may be a cause of the edge effect) and the plates washing method (which could trigger contaminations between neighboring wells).

Consequently, we ran some preliminary experiments to choose the best procedure for quantitative ELISA tests. The PVY_{SON41p-115K-GFP} was mechanically inoculated on pepper (*C. annuum* cv. ‘Yolo Wonder’) and tobacco (*N. tabacum* cv. ‘Xanthi’) plants.

For a given plant species, leaves were bulked to serve as positive samples in ELISA.

To test each factor, different designs were elaborated on ELISA plates:

- The “edge” effect was assessed by filling the 96 wells of 12 plates (no control or blank were added). Each plate was filled using a dilution (1:5 to 1:15625) of the bulk sample. Then the OD values from the peripheral wells (36 wells) and the center wells (60 wells) were compared.
- The “light” effect was assessed by either exposing the plates to natural light or to place them in a dark polystyrene box (doubled with aluminum paper) during the substrate incubation period. The “edge” and “light” effects were tested on the same plates (9 plates were exposed to light, 3 plates were placed in the dark).
- The “washing” effect was assessed by designing two mosaic plates (i.e. alternating positive samples, healthy controls and blanks) in order to control the efficiency of two washing methods to minimize the risk of contamination between the wells: removing the plant extract from the plate directly into the sink or using a vacuum pump. Three different dilutions of the bulk sample were used (1:25, 1:625, 1:15625).

2.1.3. Determining coat protein concentration by semi quantitative ELISA

The relative concentration of PVY_{SON41p-115K-GFP} in infected plants was determined by semi quantitative ELISA, in order to estimate the virus load in the leaves relative to a reference sample. To compare virus concentration between samples, each leaf sample was weighted and an adjusted volume of grinding buffer was added to make a 1:5 dilution. Then, for each sample, 1/5th dilutions in grinding buffer were deposited (dilution factors 1:25 to 1:3125, see figure 10, step 3). A unique reference sample (and associated dilutions) was also added to all the plates. ODs of all wells were obtained using the same protocol as described previously (see section 2.2). Then, for a given sample, the ODs associated with the different dilutions give a curve (ideally linear, figure 8). The comparison of this curve (slope and

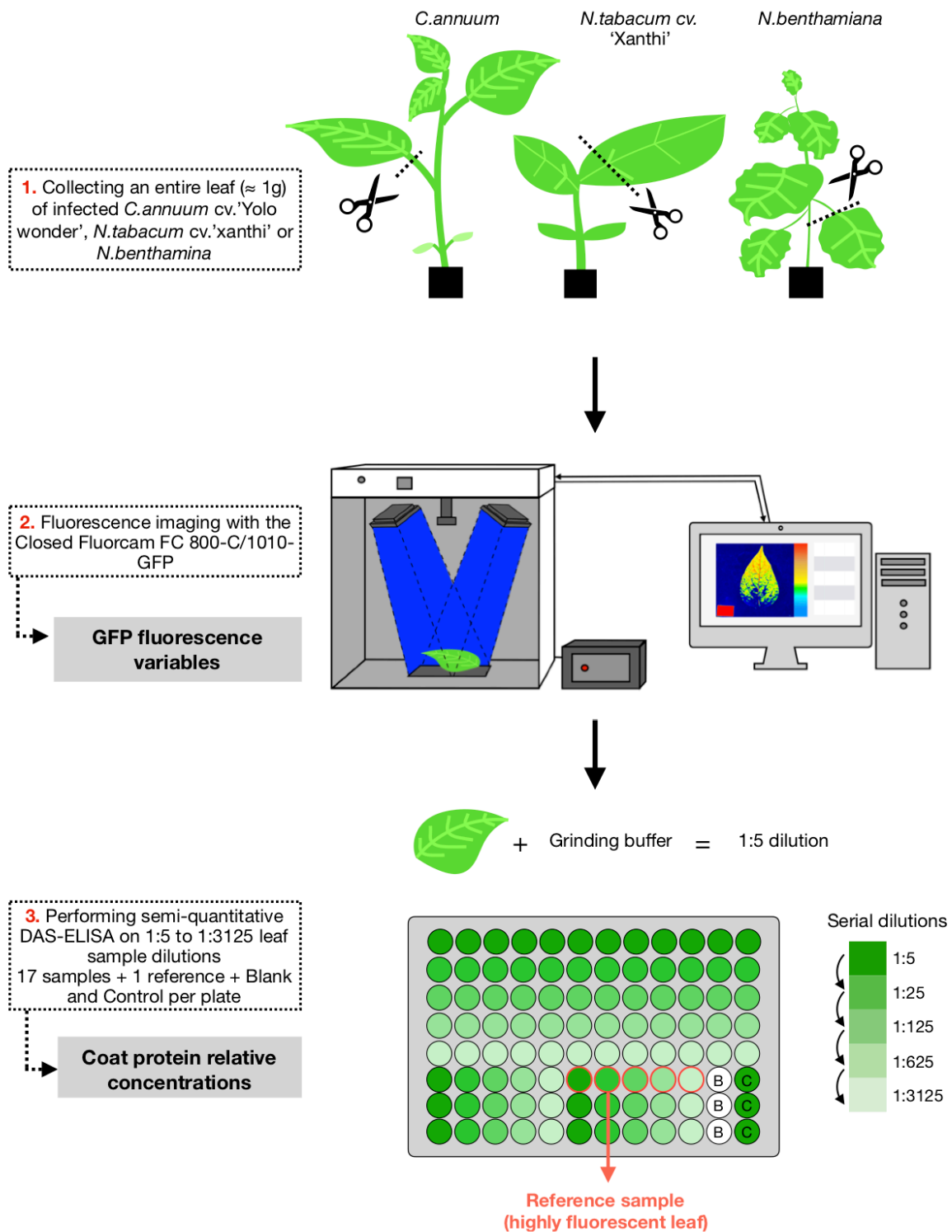


Figure 10: Estimation of the viral load of PVYson41p-115k-GFP infected plants by fluorescence imaging followed by semi-quantitative ELISA assay (B, Blank; C, Negative control)

intercept of one of its segments) with the curve associated with the reference sample allows the estimation of a relative viral concentration. An R script developed by Lucie Tamisier (former PhD student) and enhanced by Loup Rimbaud (Researcher) was used to compute the relative virus concentrations.

An absolute quantification could be obtained if the viral concentration in the reference sample was already known. This could be easily done with a purified virus solution. However, as it would have been labor intensive, no purification of the isolate PVY-son41p-115K-GFP was performed. Consequently, all the obtained concentrations were considered as “relative” concentrations.

2.2. Fluorescence imaging

Here the viral load was estimated by a non-destructive method allowing the measurement of fluorescence associated with the isolate PVY_{SON41p-115K-GFP} infection. The required material was a kinetic imaging fluorometer, the Closed Fluorcam FC 800-C/1010-GFP (Photon System Instruments, Czech Republic) containing a light module and a camera (figure 7). Each plant or plant sample (leaf or other tissues) was exposed to light at 450-470 nm (which matches with the peak of the GFP excitation spectrum) and photographed. The camera was equipped with an optical filter which captures wavelengths around 508 nm (which matches with the peak of the GFP emission spectrum).

All the photos were then treated with the Fluorcam7 software provided by the company. This software associates a level of fluorescence (an arbitrary value between 0 and 8140) to each pixel of the photo, and allowed the measurement of different variables:

- The total leaf surface (in pixels) was determined by manually cutting-out the area of the leaf
- The fluorescent leaf surface, which was the number of pixels whose fluorescent level is above 800 (this threshold had been chosen according to experiments prior to the internship). Then the proportion of fluorescent surface was calculated by dividing the fluorescent leaf surface by the total leaf surface.
- The average fluorescence level is a dimensionless measurement, representing the mean value of fluorescence of all pixels of the leaf area.

2.3. RT-qPCR

Here the purpose was to quantify the PVY nucleic acids in the samples by developing a Reverse Transcription quantitative Polymerase Chain Reaction (RT-qPCR). As the method was not yet used on pepper infected by PVY in the “Pathologie Végétale” laboratory, the whole procedure had to be developed.

2.3.1. Primer design

Primers for virus detection and quantification were designed in the coat protein gene and 3' untranslated region of the genome (figure 3), which is a highly conserved region of the

Table 1: PVY isolates used to develop generic RT-qPCR assays (Quenouille and al, 2013)

PVY clade	Isolate abbreviation	Isolate infectivity on Pepper (<i>Capsicum spp.</i>)
C1	ALGERIE1	Frequent
C1	CAA14	Frequent
C1	CAA1412	Frequent
C1	CAA156	Frequent
C1	CAA157	Frequent
C1	CAA163	Frequent
C1	K4-11-94	Frequent
C1	K47-94	Frequent
C1	LYE245	Frequent
C1	MARTINIQUE3	Frequent
C1	LYE90v	Frequent
C1	LYE72	Frequent
C1	SON41p-115K-GFP	Frequent
C1	LYE84	Frequent
N	N605	Poorly infectious in laboratory
O	O139	Poorly infectious in laboratory
Chile	Chile3	Reported
C2	Cadgen	Not infectious in laboratory
O x N	NTN-H	-
O x N	WilgaP	-
Brazil	Bresil_071034	-
O x N	Pologne_6_puc3_pl2	-
C1	Guadeloupe1Revers	Frequent

potyvirus genome. According to Bustin and Hugget (2017), the primers were designed in such a way that:

- Their length should be between 18 to 25 nucleotides
- Their GC contents should be as close to 50% as possible (40 to 60%)
- Their annealing temperatures should be in the range of 61°C to 65°C
- Their amplicon sizes should be short (around 150 bp)
- Their probability of dimer bands and hybridization with pepper should be as low as possible

In addition, the primers were designed to detect as many PVY isolates as possible. For this, the sequences of a core collection of 23 isolates of PVY (including PVY 141p-115k-GFP, table 1) were aligned using MEGA-X (Kumar, Stecher, Li, Knyaz, and Tamura 2018). Four highly conserved sub regions (presenting only one nucleotide polymorphism between PVYson41p-115k-GFP and the 22 PVY isolates) were identified and used to design the primers. All the primers parameters (amplicon sizes, GC contents, annealing temperatures, dimer band probabilities, probabilities of hybridization with pepper) were provided by Primer3Plus and PrimerBlast.

2.3.2. Total RNA extraction

In order to minimize RNA degradation, the leaves were separated from the plants and instantly frozen in liquid nitrogen (-196°C) in a mortar. The aliquots of ground powder were stored at -80°C. Two RNA extraction methods, TRI-Reagent® - chloroform (MRC, USA) and RNeasy®Plant Mini Kit (Qiagen, Germany) were tested in order to find the best compromise between RNA yield (measured via Nanodrop®ND-1000 Spectrophotometer, Thermo-Scientific, USA), purity (assessed through migration on 1% agarose electrophoresis gel with 0.005% BET, and Nanodrop®ND-1000 Spectrophotometer) and the method cost. Extractions were performed according to manufacturers' instructions.

2.3.3. Primers assessment

All the primers were tested following a classical two step RT-PCR procedure (figure 9). The reverse transcription was ensured by filling a 0.2 mL microtube with 2 µL of extracted RNA, 7 µL of RNase free water and 1 µL of reverse Primer (1:10 dilution). A first RNA denaturation was achieved by incubating the tubes at 80°C for 3 min (PTC-100™ Programmable Thermal Controller, MJ Research, USA) before adding 4.8 µL of RNase free water, 0.8 µL of dNTP, 4 µL of 5X buffer RT (Promega®, USA) and 0.4 µL of reverse transcriptase AMV RT (Promega®, USA). The tubes were then incubated at 42°C for 1h for the annealing step. Then the PCR was achieved by adding 3 µL of cDNA in a 0.2 mL microtube with 21.8 µL of RNase free water, 8 µL of 5X buffer (Promega®, USA), 2.4 µL of MgCl₂, 2µL of forward primer (1:10 dilution), 2 µL of reverse primer (1:10 dilution), 0.2 µL of dNTP and 0.6 µL of Taq polymerase enzyme (Promega®, USA). The PCR program consisted in a prior denaturation at 95°C for 5 min followed by 35 cycles of denaturation, annealing and extension for respectively 30 s at 95°C, 30 s at 62°C and 1 min at 72°C. The final step was an extension during 10 min at 72°C. The

amplified cDNA sequences were then visualized on a 1% or 1.5% agarose gels with 0.005% of ethidium bromide (BET) in Tris-Acetate-Ethylenediaminetetraacetic-acid (TAE) buffer.

3. Assessing the correlation of the variables provided by different quantification methods

In this part, three plant species: *C. annuum* cv. 'Yolo Wonder', *N. benthamiana* and *N. tabacum* cv. 'Xanthi' infected with PVY_{SON41p-115K-GFP} were used to perform the tests. All the plant leaves were first analyzed by fluorescence imaging to measure GFP quantitative variables before being processed by semi-quantitative ELISA (figure 10).

4. Assessing virus accumulation in pepper

As mentioned by Tamisier and al (2020), quantifying the presence of PVY in pepper is an accurate method to characterize plant resistances against virus accumulation. Here two pepper genotypes presenting contrasted resistance profiles to PVY were used.

4.1. Fluorescence monitoring

Before my internship, a set of 11 peppers 'Yolo Wonder' plants (including 1 mock-inoculated plant and 1 healthy control) and 9 peppers 'Perennial' plants (including 1 mock-inoculated plant and 1 healthy control) had been inoculated with PVY_{SON41p-115K-GFP} via aphids. From 5 to 22 days post inoculation (dpi), the leaves of the inoculated plants were monitored by fluorescence imaging at 5, 6, 8, 9, 12, 15 and 22 dpi. However, at this time the images could not be analyzed without knowing which was the most relevant variable to assess viral accumulation (average level of fluorescence or proportion of fluorescent leaf surface, see above). Given the results of my experiments (see Results section), I took in charge the analysis of these images and used the proportion of fluorescent leaf surface to model the kinetics of viral accumulation.

4.2. Modeling the kinetics of virus accumulation

The number of fluorescent pixels followed a nonlinear 3-parameter logistic model $Y \sim \text{Bin}(N, I)$ with N representing the total number of pixels in the leaf area and

$$I = \frac{k}{1 + e^{-4 \times s \times (x - \mu)}}$$

the probability for a pixel to be fluorescent (i.e. of successful viral invasion of the corresponding part of the leaf), which depended on the number of days after aphid-mediated inoculation (x). This link function was a logistic equation previously designed by Loup Rimbaud (Rimbaud and al, 2015).

The model parameters had the following biological interpretations:

- μ was the abscissa of the inflexion point and was an estimator of the time to reach 50% of the maximum proportion of fluorescent leaf surface.
- The plateau k estimated the maximal proportion of fluorescent leaf surface

- s was the slope of the curve at the inflexion point and reflected the speed at which the proportion of fluorescent surface increases

Estimates of these parameters were obtained by the nonlinear least squares method (NLS). Then linear models were calculated in order to relate each parameter (μ , k and s) with two variables: the number of successful inoculations by aphids and the plant genotype. Finally, the best models were selected based on the Akaike Information Criterion (AIC) (which must be as low as possible). The 95% confidence intervals (CI_{95}) were also calculated for each parameter estimates.

5. Statistical analyses

All statistical analyses and graphic representations were made with the R software version 3.5.1 (R core Team 2012). All the tests were considered as significant, when the obtained p -values were below the statistical threshold of 5%.

For the optimization of the ELISA protocol, all the tested factors were analyzed separately (no interactions). Means comparison and variances homogeneity tests were performed on the variable to explain (OD values) between the modalities of the explanatory variable (sample position, light condition during incubation, washing procedure). When it was possible, in order to simplify the analysis of the tests, OD values were normalized by the average OD value of the plate, which allowed us to compare different plates filled with different leaf extract concentrations. Finally, if the validation conditions of the statistical tests were not ensured (normality of residuals, variances homogeneity and independence of residuals with respectively Shapiro-Wilk, Bartlett and Durbin-Watson tests), more adequate or non-parametric tests were performed instead (Welch's t test, Kruskal-Wallis H test).

The relationship between the viral load estimated via quantitative ELISA and via fluorescence imaging was analyzed using Pearson's correlation coefficient and a generalized linear model (GLM) with a modified logarithm link function.

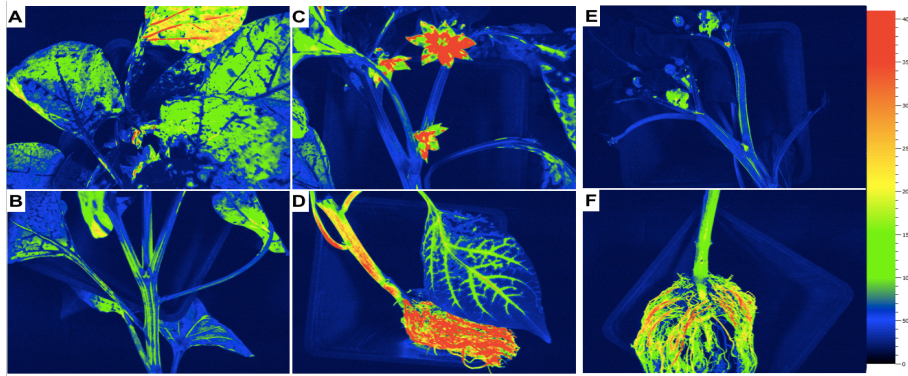


Figure 11: Observed fluorescence on *C. annuum* cv. ‘Yolo Wonder’ mechanically inoculated with PVY-son41p-115K-GFP (A: leaves, B: stems, C: flowers, D: roots) and mock inoculated (E: stems, F: roots) at 42 dpi. Fluorescence average level is given by virtual colors from deep-blue (null) to red (high intensity).

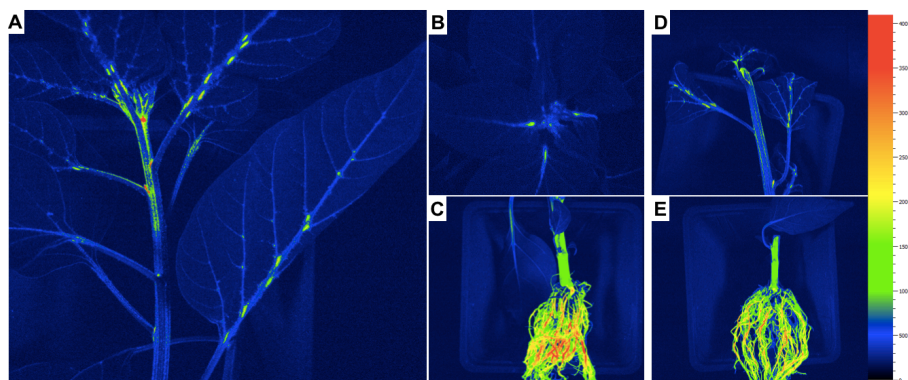


Figure 12: Observed fluorescence on *C. annuum* cv. ‘Perennial’ mechanically inoculated with PVY-son41p-115K-GFP (A: stems, B: leaves, C: roots) and mock inoculated (D: stems, E: roots) at 42 dpi. Fluorescence average level is shown by virtual colors from deep-blue (null) to red (high intensity).

Table 2: Detection of PVY-son41p-115K-GFP by ELISA in different plant organs for two *C. annuum* cultivars (‘Yolo Wonder’ and ‘Perennial’).

Tissue extracted	Pepper (<i>Capsicum annuum</i>) cultivars ^a		Positivity threshold ^b
	‘Yolo Wonder’	‘Perennial’	
Leaves	1.87 (1)	0.06 (6)	0.63
Stems	0.65 (1)	0.06 (6)	0.71
Roots	1.67 (1)	0.1 (6)	0.49
Flowers	0.27 (1)	0.19 (1)	0.74

^a Mean ΔOD values (subtraction of the blank OD values to the OD values) measured at 405 nm after 4h of substrate incubation. Numbers in parentheses are the number of samples.

^b Positivity threshold = $2x \frac{\sum(OD_{negative\ control} - OD_{blank})}{Number\ of\ negative\ control}$

Results

1. Efficiency of mechanical inoculation of PVY_{SON41p-115K-GFP} on two pepper genotypes

Plants from two different cultivars of pepper ('Yolo Wonder' and 'Perennial') were mechanically inoculated with PVY_{SON41p-115K-GFP}. The proportion of infected plants was assessed by fluorescence imaging and serological diagnostic 42 days post inoculation (dpi). All 'Yolo Wonder' leaves presented the typical fluorescence infection pattern (figure 11A) whereas no 'Perennial' leaf was fluorescent (figure 12B). To investigate if the virus could be stored in other organs of the plant, especially in 'Perennial', fluorescence imaging was taken on stems, roots and flowers. However, for all the plants genotypes and inoculation procedures (inoculated and mock inoculated), the roots and the stems fluoresced (figures 11B, 11D, 11E, 11F, 12A, 12C, 12D, 12E). Flowers were only present in an infected Yolo Wonder and were found fluorescent (figure 11C).

In distinct plants, serological detections of PVY_{SON41p-115K-GFP} were performed on different plant organs. Here, only one plant of 'Yolo Wonder' was used as a positive control (table 2). As expected, the leaves of the positive control 'Yolo Wonder' showed a ΔOD value above the positivity threshold which confirmed its infected state ($1.87 > 0.63$). Moreover, only the roots and the leaves of 'Yolo Wonder' were infected according to the positivity threshold ($1.86 > 0.49$). As the OD values for 'Perennial' tissues were always under the positivity thresholds ($0.06 < 0.63$), no 'Perennial' leaves or other tissues were considered infected. In conclusion, the fluorescence of the roots and the stems cannot be considered as good indicators of infection.

Considering the failure to mechanically infect the 'Perennial' cultivar, this genotype was not included in further experiments.

2. Optimizing the semi quantitative ELISA protocol

To determine the influences of three factors (well position, light condition during substrate incubation and washing procedure) on OD values, leaf samples of *C. annuum* cv. 'Yolo Wonder' and *N. tabacum* cv. 'Xanthi' infected with PVY_{SON41p-115K-GFP} were used to perform DAS-ELISA tests.

2.1. Well position influence on the OD values

In order to synthesize the results, the normalized OD values of each well of 3 plates loaded with *N. tabacum* cv. 'Xanthi' extracts and 9 plates loaded with *C. annuum* cv. 'Yolo Wonder' were averaged separately. According to the heat map obtained for the plates loaded with *N. tabacum* cv. 'Xanthi' leaf extracts (figure 13), the highest values are obtained on the first line and first column only. The Welch's *t*-test didn't show significant difference between the means of the average normalized OD values from the periphery and the center (*p*-value: 0.19). On the contrary, in the heat map obtained for the plates loaded with *C. annuum* cv. 'Yolo Wonder' leaf extracts (figure 14), the highest average normalized OD values (1.05 to 1.1) were reached by the peripheral wells from the first and particularly the eighth line, as

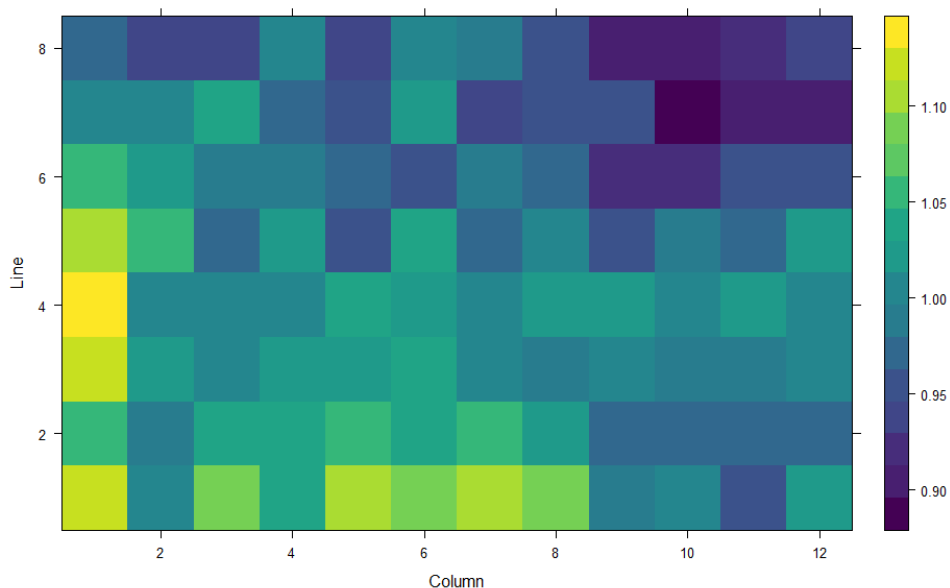


Figure 13: Heat map of the normalized OD values, averaged from 3 plates (loaded with *N. tabacum* cv. 'Xanthi' leaf extracts) after 4h of incubation with *p*-nitrophenyl-phosphate at ambient temperature. According to a Welch's *t* test, no significant difference was observed between the mean of the average normalized OD values from the center and periphery of the plate (p-value = 0.19).

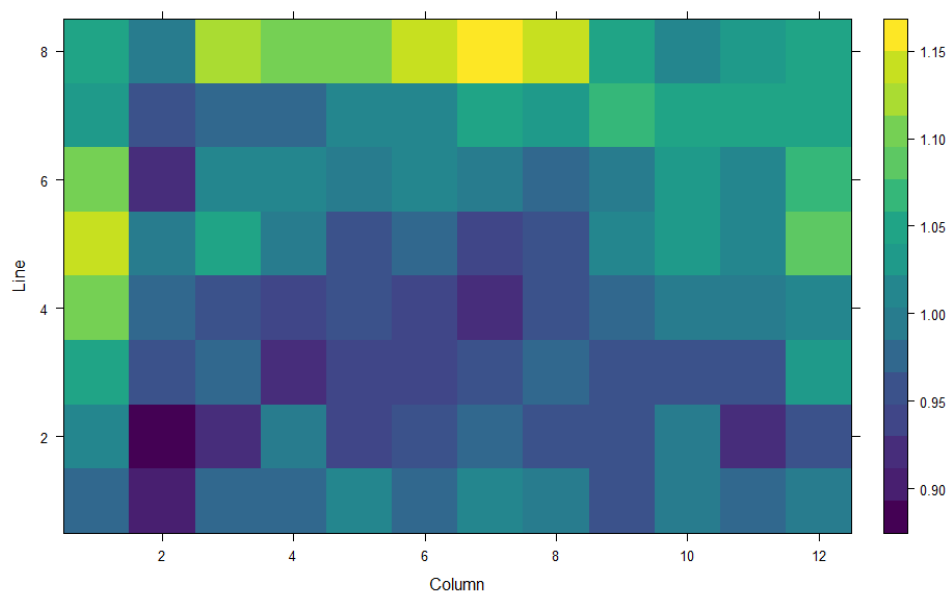


Figure 14: Heat map of the normalized OD values, averaged from 9 plates (loaded with *C. annuum* cv. 'Yolo Wonder' leaf extracts) after 4h of incubation with *p*-nitrophenyl-phosphate at ambient temperature. According to a Welch's *t* test, a significant difference was observed between the mean of the average normalized OD values from the center and periphery of the plate (p-value = 9.13×10^{-7}).

well as the first and the twelfth column. However, we noted that 6 wells present very low average normalized OD values (0.90 to 1). A Welch's *t*-test showed that the means of the average normalized OD values from the periphery and the center were significantly different (p-value: 9.13×10^{-7}). Nevertheless, when the plates are analyzed separately, 1 of the 3 and 6 of the 9 plates loaded with respectively *N. tabacum* cv. 'Xanthi' and *C. annuum* cv. 'Yolo Wonder' showed significant differences between the average normalized OD values of the center and the peripheral wells (table 3; p-value ranging from 3.77×10^{-9} to 0.03). The figures 15 to 18 showed the general distributions of the mean OD values obtained for each line and each column of an ELISA microtiter plate. For the plates loaded with *N. tabacum* cv. 'Xanthi' leaf extracts (figure 15), the curves corresponding to the lowest concentrations (1:625 and 1:15625) showed flat distributions of the mean OD values whereas the highest concentration (1:25) showed a slight decrease of the mean OD values through the lines and columns of the plate. Among the plates loaded with *C. annuum* cv. 'Yolo Wonder' leaf extracts (Figures 16 to 18), six plates showed U- or n-shape curves representing respectively higher or lower mean OD values for the peripheral wells (table 3).

2.2. Light influence on the normalized OD values

The OD values were normalized by dividing the OD value of each well by the mean OD value of the whole plate which allowed the comparison of all plates. The influence of light during the incubation period of the *p*-nitrophenyl phosphate showed no significant differences (figure 19; p-value = 1) on the normalized OD values whether the plates were placed in the light during incubation or in the dark.

2.3. Influence of the washing method on OD values

The comparison between the two washing methods was based on the normalized OD values associated with three sample types: infected sample, blank and negative control. As the p-values ranged from 0.45 to 1 (table 4), the influence of the washing method showed no significant differences between the normalized OD values for all sample types (figure 20).

3. Determination of the variable of interest for fluorescence imaging

In this part, the results were obtained for three plant species: *C. annuum* cv. 'Yolo Wonder', *N. benthamiana* and *N. tabacum* cv. 'Xanthi' infected with PVY_{SON41p-115K-GFP}. The tobacco plants were added as additional data to expand results obtained with pepper. All the plant leaves were first analyzed by fluorescence imaging to measure GFP quantitative variables before being processed by quantitative ELISA.

Unless for *N. benthamiana* samples, each leaf viral coat protein concentration was positively and significantly (5% threshold) correlated with their proportion of fluorescent leaf surface and their average level of fluorescence (table 5). Moreover, Pearson's correlation coefficient between virus coat protein concentration and the proportion of fluorescent leaf surface are ranging from 0.56 to 0.63 (for *N. tabacum* cv. 'Xanthi' and *C. annuum* cv. 'Yolo Wonder', respectively) which is higher than between coat protein concentration and average level of

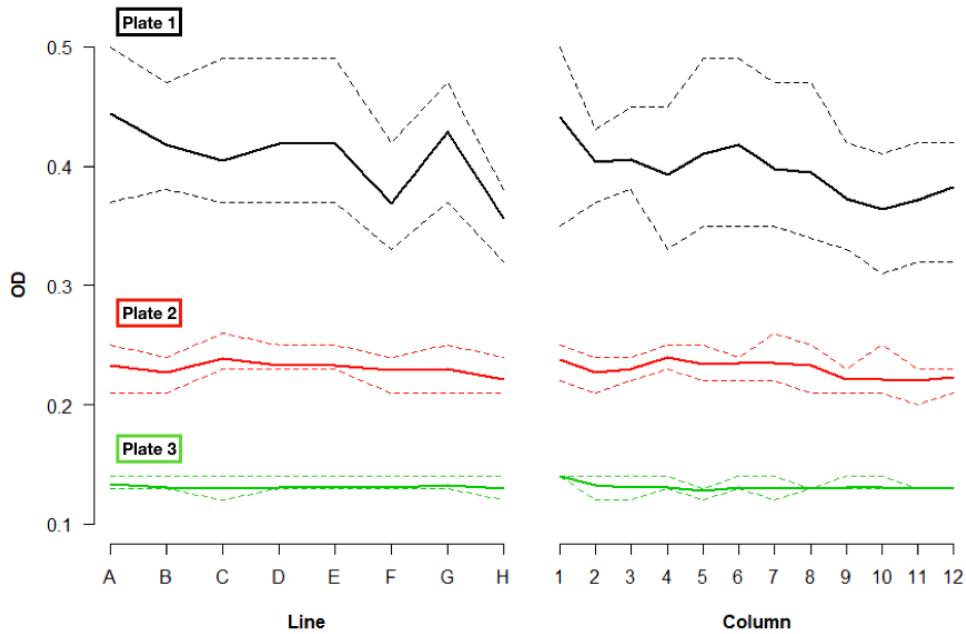


Figure 15: Mean OD values recorded for the 12 wells of each line (from A to H) or the 8 wells of each column (from 1 to 12) of a microtiter plate loaded with 3 different *N. tabacum* cv. 'Xanthi' leaf extract concentrations (Plate 1 = 1:25, Plate 2 = 1:625, Plate 3 = 1:15625) and incubated in light. Solid line: mean OD values; dashed lines: maximum and minimum OD values among the plates.

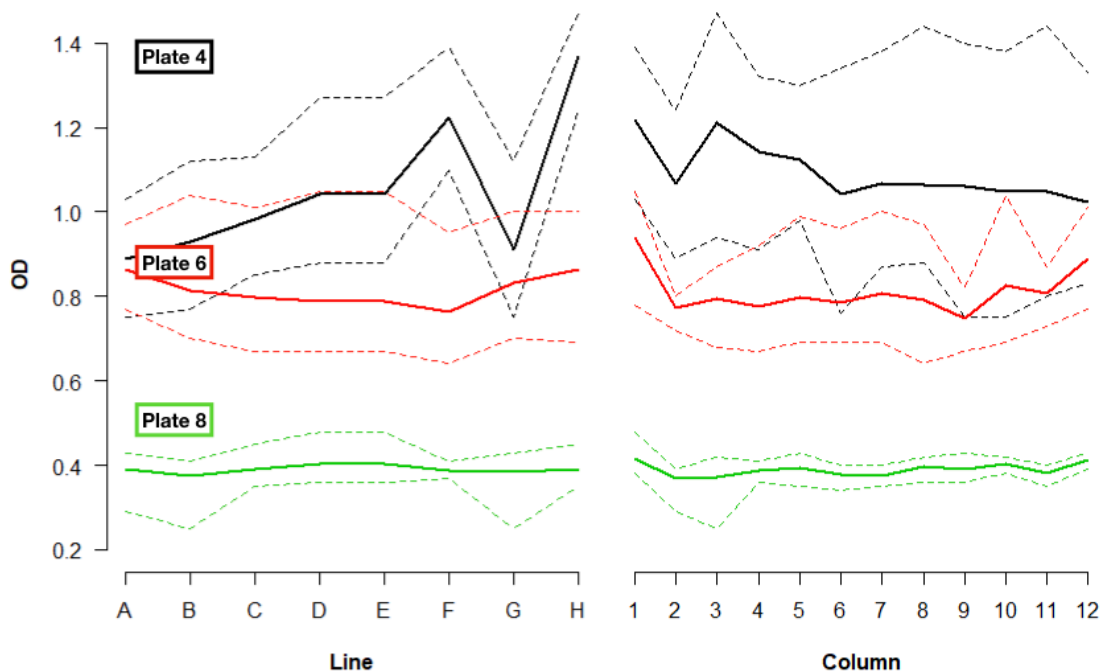


Figure 16: Mean OD values recorded for the 12 wells of each line (from A to H) or the 8 wells of each column (from 1 to 12) of a microtiter plate loaded with 3 different *C. annuum* cv. 'Yolo Wonder' leaf extract concentrations (Plate 4 = 1:5, Plate 6 = 1:25, Plate 8 = 1:125) and incubated in light. Solid line: mean OD values; dashed lines: maximum and minimum OD values among the plates.

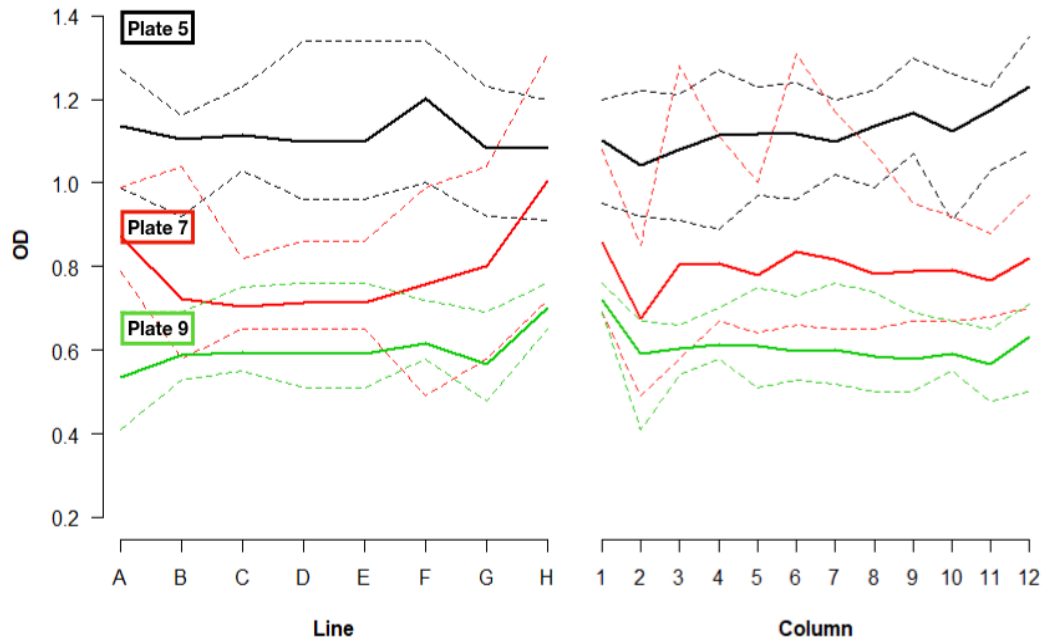


Figure 17: Mean OD values recorded for the 12 wells of each line (from A to H) or the 8 wells of each column (from 1 to 12) of a microtiter plate loaded with 3 different *C. annuum* cv. 'Yolo Wonder' leaf extract concentrations (Plate 5 = 1:5, Plate 7 = 1:25, Plate 9 = 1:125) and incubated in the dark. Solid line: mean OD values; dashed lines: maximum and minimum OD values among the plates.

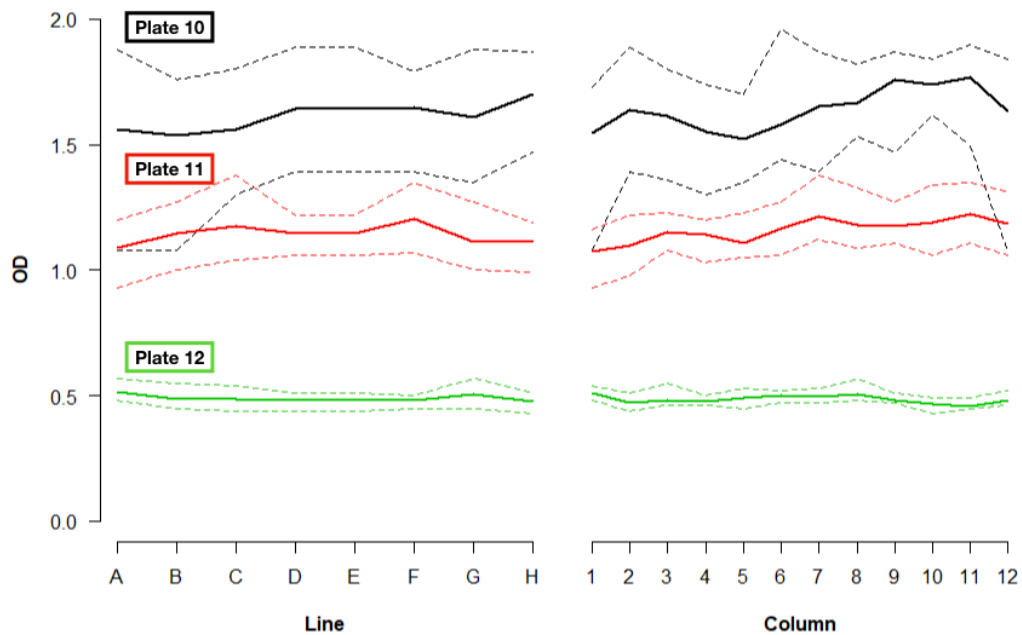


Figure 18: Mean OD values recorded for the 12 wells of each line (from A to H) or the 8 wells of each column (from 1 to 12) of a microtiter plate loaded with 3 different *C. annuum* cv. 'Yolo Wonder' leaf extract concentrations (Plate 10 = 1:5, Plate 11 = 1:125, Plate 12 = 1:3125). Solid line: mean OD values; dashed lines: maximum and minimum OD values among the plates.

Table 3: Summary of the results of Welch's t-test assessing the edge effect on OD values and the characterization of the mean OD values curve (Df: Degree of freedom)

Species	Plate number	Light condition for substrate incubation	Dilution factor	Df	Welch's t test	p-value	Mean OD values curve shape	
							Line	Column
<i>N. tabacum</i> cv. 'Xanthi'	1	Light	1:25	52.96	-1.47	0.15	Saw-tooth	Saw-tooth
<i>N. tabacum</i> cv. 'Xanthi'	2	Light	1:625	70.66	0.57	0.57	Plane	Plane
<i>N. tabacum</i> cv. 'Xanthi'	3	Light	1:15625	54.84	-2.13	0.04	Plane	Plane
<i>C. annuum</i> cv. 'Yolo Wonder'	4	Light	1:5	53.64	-1.12	0.27	Saw-tooth	Saw-tooth
<i>C. annuum</i> cv. 'Yolo Wonder'	5	Obscurity	1:5	65.19	-75	0.45	Saw-tooth	U
<i>C. annuum</i> cv. 'Yolo Wonder'	6	Light	1:25	60.9	-6.88	3.77×10^{-9}	U	U
<i>C. annuum</i> cv. 'Yolo Wonder'	7	Obscurity	1:25	52.43	-6.14	4.11×10^{-8}	U	U
<i>C. annuum</i> cv. 'Yolo Wonder'	8	Light	1:125	55.61	-2.28	0.03	Plane	Plane
<i>C. annuum</i> cv. 'Yolo Wonder'	9	Obscurity	1:125	38.98	-3.27	0.002	Saw-tooth	U
<i>C. annuum</i> cv. 'Yolo Wonder'	10	Light	1:5	62.59	0.68	0.5	Plane	n
<i>C. annuum</i> cv. 'Yolo Wonder'	11	Light	1:125	74.54	3.54	6.91×10^{-4}	n	n
<i>C. annuum</i> cv. 'Yolo Wonder'	12	Light	1:3125	60.60	-3.12	0.003	Plane	Plane

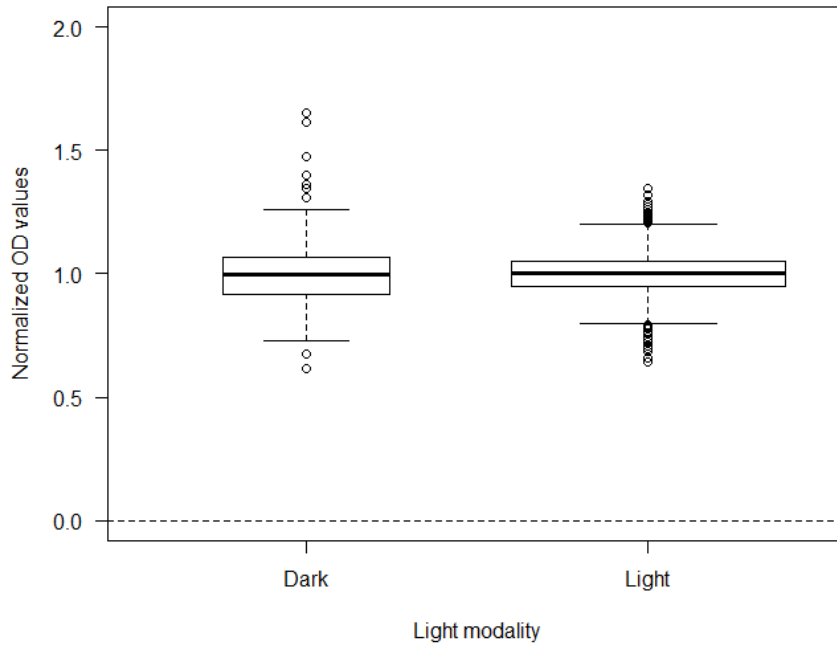


Figure 19: Boxplots of normalized OD values measured after 4h of substrate incubation in the light or in the dark. According to a Welch's t test, no significant difference was observed between the mean of the normalized OD values obtained when the plates were incubated in the light or in the dark (p -value = 1)

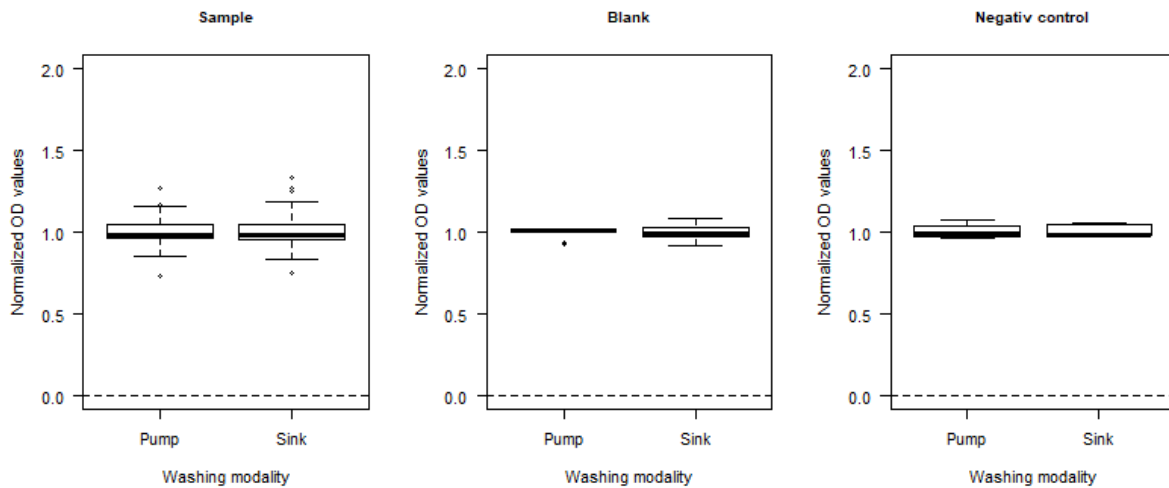


Figure 20: Boxplots of normalized OD values measured after 4h of substrate incubation for each sample type (Sample, Blank, Negative control) when plant extracts were removed from plates directly in the sink or using a vacuum a pump

Table 4: Results of Welch's *t* test and Kruskal-Wallis *H* test assessing the washing effect on normalized OD values

Sample type	Degree of freedom	Welch's <i>t</i> -test ^a	Kruskal-Wallis <i>H</i> test ^b	p-value
Sample (N = 96)	1	5.7x10 ⁻¹⁵	-	1
Blank (N = 48)	0.24	0	-	1
Negative control (N = 48)	2.9	-	0.56	0.45

^a Welch's *t* test was preferred as Student's *t* test because the data didn't respect the variances homogeneity hypothesis

^b Kruskal-Wallis *H* test was performed because the data didn't have a normal distribution

Table 5: Pearson's correlation coefficient (*r*) between coat protein concentrations and GFP fluorescence (proportion of fluorescent surface and average level of fluorescence) for *C. annuum* cv. 'Yolo Wonder', *N.benthamiana*, *N.tabacum* cv.'Xanthi'.

Plant species	Relationship between coat protein concentrations and proportion of fluorescent leaf surface		Relationship between coat protein concentrations and average level of leaf fluorescence	
	<i>r</i>	p-value	<i>r</i>	p-value
<i>C. annuum</i> cv.'Yolo Wonder' (N = 74)	0.63	3.128x10 ⁻⁹	0.39	5.8x10 ⁻⁴
<i>N.benthamiana</i> (N = 19)	0.32	0.19	0.70	0.001
<i>N.tabacum</i> cv.'Xanthi' (N = 19)	0.56	0.013	0.55	0.014

Table 6: Summary of RNA isolation from leaf samples using the TRI-Reagent® or the RNeasy®Plant Mini Kit procedure

TRI-Reagent®			RNeasy®Plant Mini Kit		
Average concentration (ng/μL)	Average A260/230 ratio	Average A260/280 ratio	Average concentration (ng/μL)	Average A260/230 ratio	Average A260/280 ratio
387.88 ^a	0.61	1.93	204.83 ^a	1.57	2.13

^a According to a Welch's *t* test a significant difference was observed between the average RNA concentration provided by the two extraction methods (p-value = 0.031)

fluorescence (0.39 and 0.55 for *C. annuum* cv. 'Yolo Wonder' and *N. tabacum* cv. 'Xanthi', respectively).

Moreover, the general distributions of the data (figure 25) highlighted that for all plant species the relative virus coat protein concentration could be described by a monotonic and increasing function of the proportion of fluorescent leaf surface. In contrast, the relationship between virus coat protein concentration and the average level of fluorescence was non-monotonic (see figure S4 in appendices), so there was no logical "mathematical pattern" between the two variables. As a result, in the following we decided to use only the proportion of fluorescent leaf surface as an estimator of the viral load in fluorescence imaging.

4. Prior results for the future quantification of viral RNA

As the development of a RT-qPCR remained incomplete, the following results were obtained according to the prior tests of RNA extraction and the specificity assessment of the designed primers.

4.1. Validation of a RNA extraction method

As a first step, we extracted total RNA from each sample using two different extraction protocols: a "home-made" protocol using TRI-Reagent® (MRC, USA) and a three-year old RNeasy®Plant Mini Kit (Qiagen, Germany). These protocols were compared based on criteria such as final concentration of total RNA and purity ratios. The comparison of average RNA concentrations (table 6) revealed significantly higher yields in samples extracted with TRI-Reagent® than these obtained with the RNeasy®Plant Mini Kit (p-value = 0.031). However, RNA purity (table 6) was better with RNeasy®Plant Mini Kit, as demonstrated by the average A260/230 and A260/280 of respectively 1.57 and 2.13 which were together much closer to the optimum value of 2.00 for RNA samples. This observation was completed by an electrophoresis migration showing that more RNA samples (77% of the 30 tested samples) were visible (or less degraded) with the RNeasy®Plant Mini Kit (figure 21) than with the other kit. It is noteworthy that no DNA contamination was observed for either kits. As a consequence of all these results, we used the RNeasy®Plant Mini Kit for further RNA extractions.

4.2. Validation of primers specificity for PVY_{SON41p-115K-GFP} detection

Five pairs of primers were designed to amplify a conserved region of the PVY genome, located at the junction between the coat protein sequence and the untranslated region (3'UTR) (table 7). The size of the respective PCR amplification products were 146 bp (PM2014), 150 bp (PM202 and PM2011), 176 bp (PM2012) and 184 bp (PM2013). When tested on RNA extract from peppers ('Yolo Wonder') infected by PVY_{SON41p-115K-GFP}, amplicons of the expected sizes were obtained for all the primers (figure 22).

The range of specificity of primers was evaluated using 14 PVY isolates in addition to PVY_{SON41p-115K-GFP}. These tests were performed using only the PM202F-PM202R and

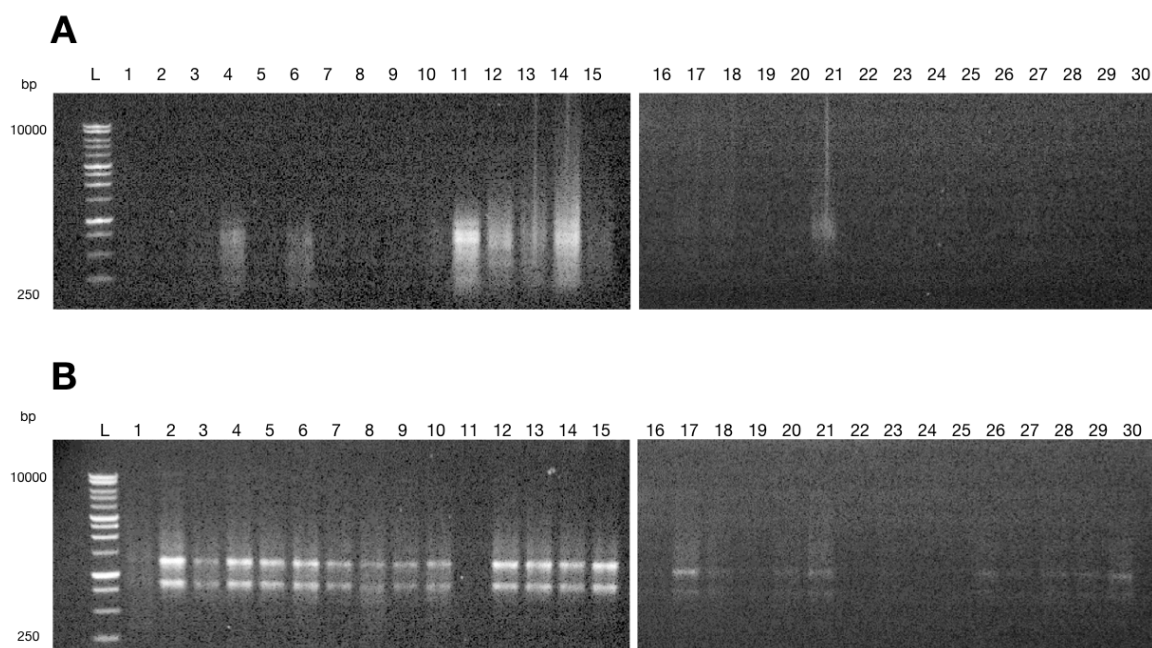


Figure 21: The 1.0% agarose gel electrophoresis analysis showing the quality of the RNA samples extracted by the TRI-Reagent®-chloroform method (A) or by the RNeasy® Plant Mini kit (B). Lanes 1 to 30 are different RNA samples extracted from 30 different PVY infected *C.annuum* cv.'Yolo Wonder' leaves. L = 1kb DNA ladder (Promega®, USA)

Table 7: Nucleotide sequences of primers designed and used for RT-PCR to detect PVYson41p-115k-GFP and 22 other PVY isolates

Name	Amplified region	Primer sequences	Length (pb)	Tm (°C)	Expected size
PM202F	CP	5'-TACACAAGAGGAGAACACAGAGAGG-3'	25	61.2	150
PM202R	3'UTR	5'-CAGGAAAAGCCAAAATACTTACTGC-3'	25	61.6	150
PM2011F ^a	CP	5'-GGGCTTATGGTTTGGTGCAT-3'	20	62	150
PM2011R	CP	5'-GAAATGTGCCATGATTTGCCTA-3'	22	62.1	150
PM2012R	CP	5'-TCTATATACGCTTCTGCAACATCTGAG-3'	27	62.1	176
PM2013R	CP	5'-TGCGCATTCTATATACGCTTCTG-3'	24	62.6	184
PM2014R	CP	5'-TGTGCCATGATTTGCCTAAG-3'	20	59.7	146

^a PM2011F is the adequate forward primer for four different reverse primers (PM2011R, PM2012R, PM2013R, PM2014R)

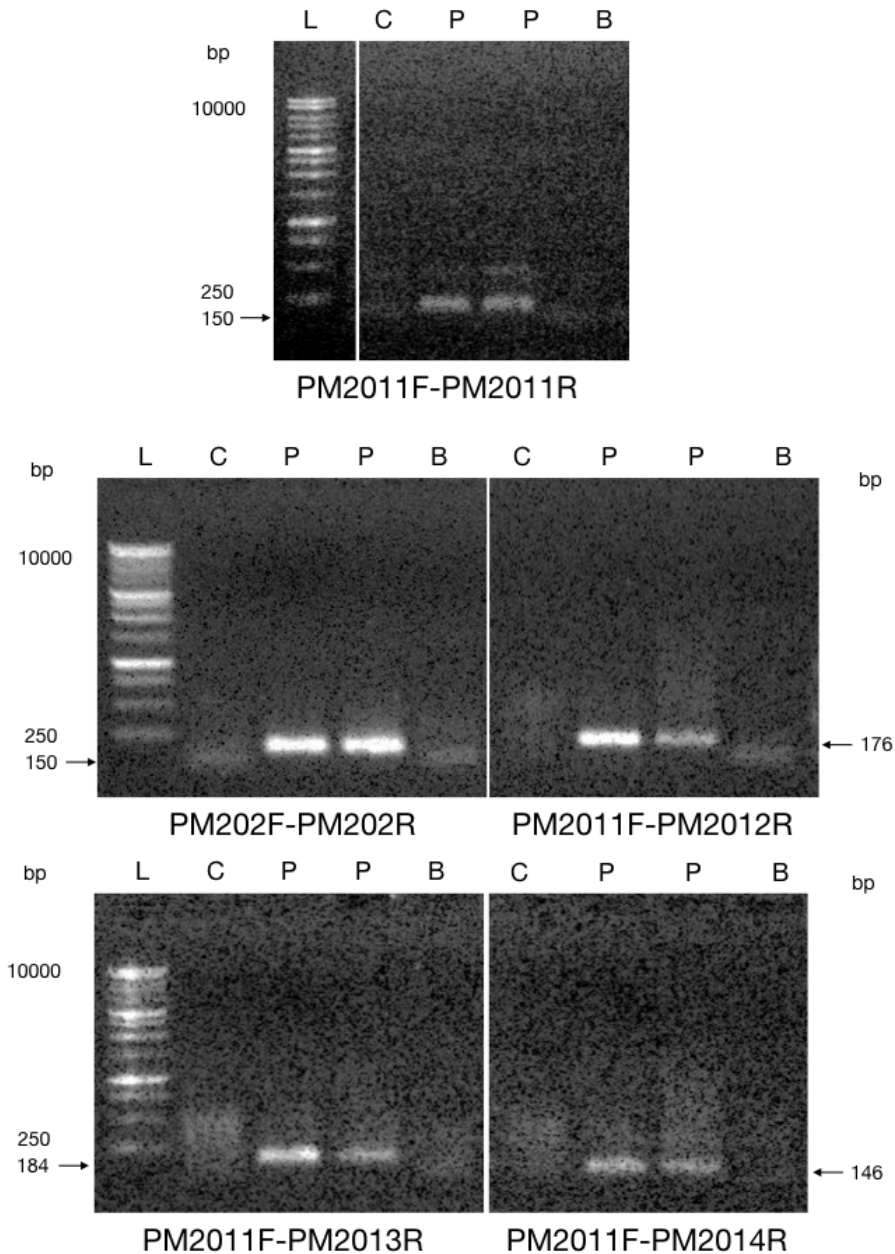


Figure 22: The 1.0% agarose gel electrophoresis analysis showing the detection of PVYson41p-115K-GFP from infected leaf samples of *C. annuum* cv. 'Yolo Wonder' by different primer couples using a RT-PCR assay targeting the coat protein gene and the untranslated 3' region. C = control (RNA extract of a healthy *C. annuum* cv. 'Yolo Wonder'). P = positive samples (RNA extracts of two PVY infected *C. annuum* cv. 'Yolo Wonder'). B = Blank. L = 1kb DNA ladder (Promega®, USA)

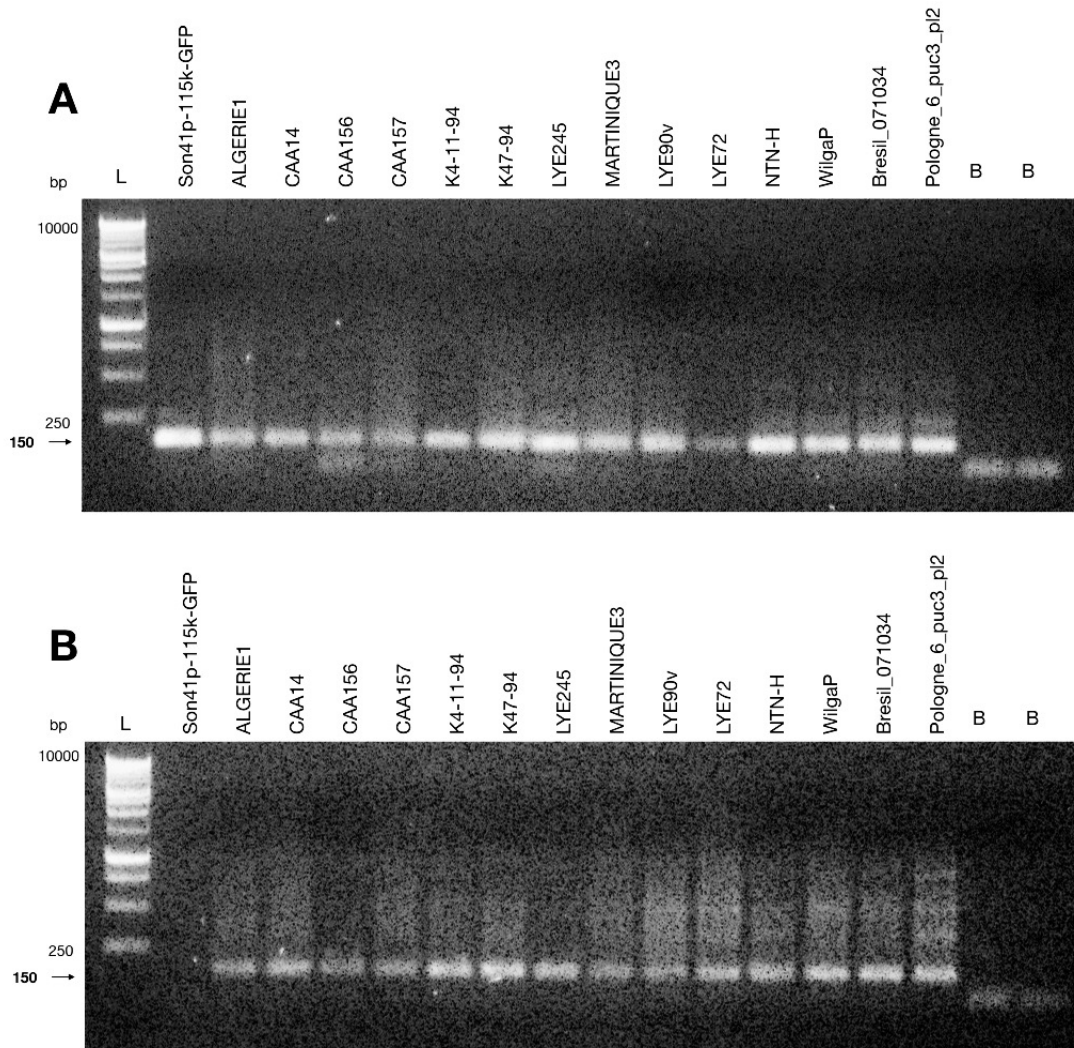


Figure 23: The 1.5% agarose gel electrophoresis analysis showing the detection of 15 PVY isolates using a RT-PCR with the PM202 (A) and PM2011 (B) primer couple. B = Blank. L = 1kb DNA ladder (Promega®, USA)

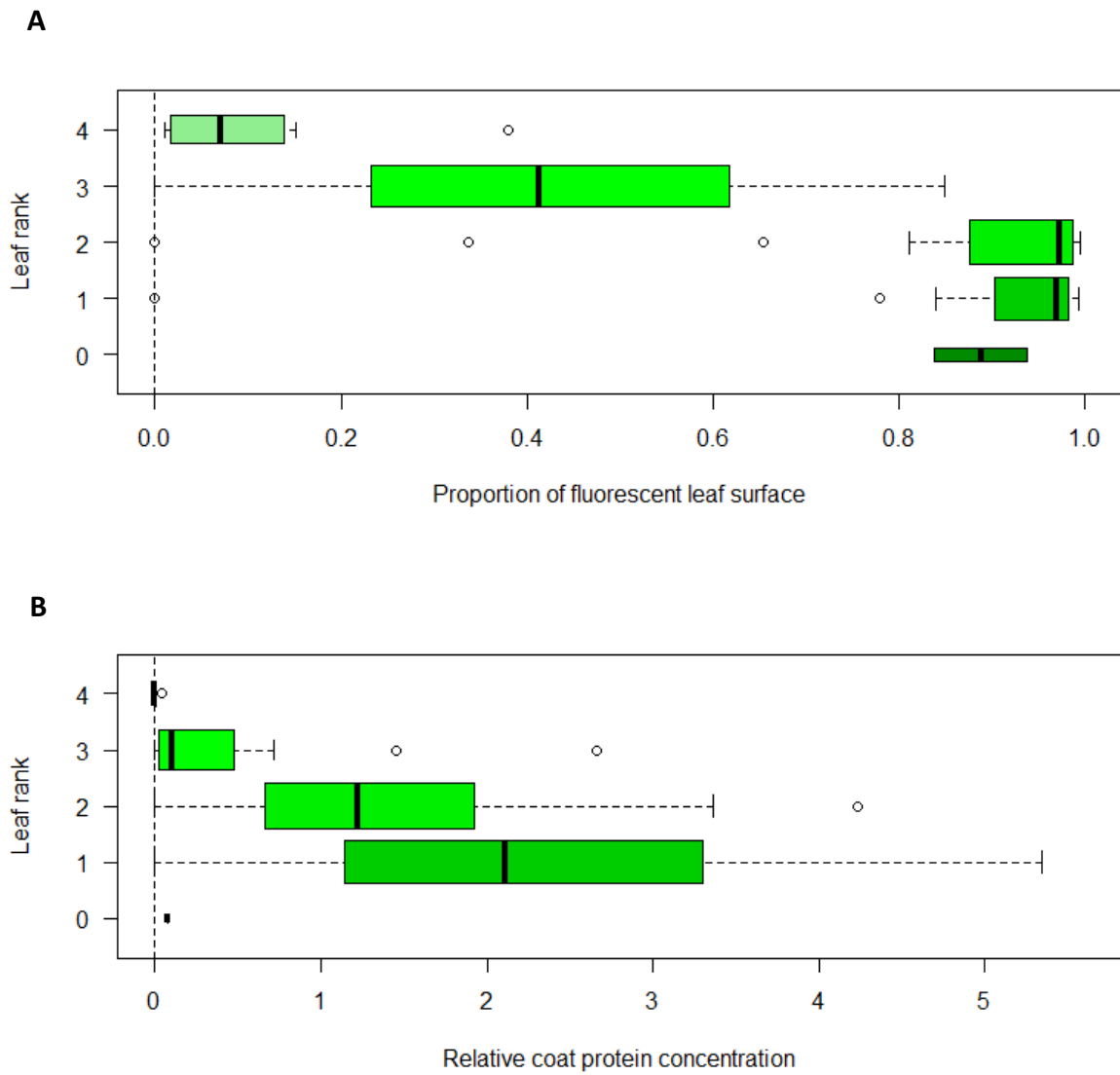


Figure 24: Proportion of fluorescent leaf surface (A) and relative coat protein concentration (B) of *C. annuum* cv. 'Yolo Wonder' leaves in relation to their rank (0, cotyledon; 1, first leaf rank; 2, second leaf rank; 3, third leaf rank; 4, fourth leaf rank).

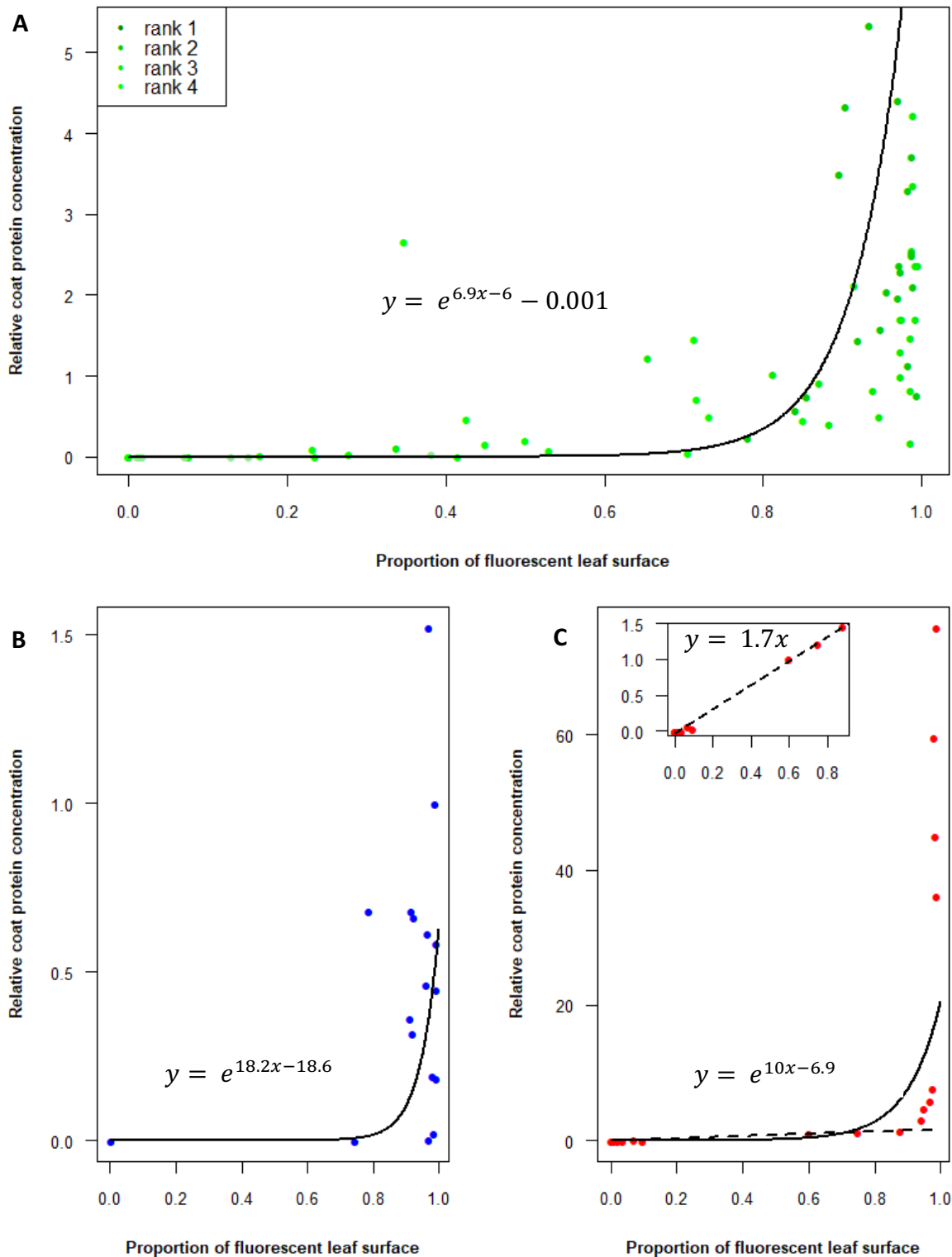


Figure 25: Regression curves between coat protein concentration and the proportion of fluorescent surface in PVYson41p-115K-GFP infected leaves of (A) *C. annuum* cv. 'Yolo Wonder', (B) *N. benthamiana*, (C) *N. tabacum* cv. 'Xanthi'. Circles: experimental data; solid line: best-fitting nonlinear model; dashed line: best fitting linear model for *N. tabacum* cv. 'Xanthi'. R^2 values are 0.85, 0.89 and 0.86 for A, B and C, respectively.

PM2011F-PM2011R primer couples as they both have 150 bp amplicons and the lowest probabilities to form primer dimers and to hybridize with *C. annuum* sequences. The electrophoresis (figure 23) revealed that both primer couples were able to detect all tested isolates although this time the PM2011F-PM2011R couple failed to detect PVY_{SON41p-115K-GFP}.

5. Relationship between leaf relative virus coat protein concentrations and proportion of fluorescent leaf surface

As the RT-qPCR was still in development and also as the proportion of fluorescent leaf surface was determined as the best variable for fluorescence imaging, the relationship between the virus coat protein concentration and the proportion of fluorescent leaf surface could be assessed. The relationships were established on the same data as before to compute Pearson's correlation coefficient (table 5). Considering these two variables for *C. annuum* cv. 'Yolo Wonder', the boxplots (figure 24) helped to identify the outlier leaf samples among the leaf ranks. Indeed, for both variables, the highest values, proportion of fluorescent leaf surface between 0.84 and 0.98, and relative coat protein concentrations between 0 and 5.34, were achieved by leaves from the first leaf rank followed by the leaves of the second leaf rank. On the contrary, the lowest values of both variables, proportion of fluorescent leaf surface between 0 and 0.85, and relative coat protein concentrations between 0 and 4.23, were achieved by the more apical leaf ranks (the third and the fourth). Surprisingly, two leaf samples (cotyledons) showed high proportions of fluorescent leaf surface but very low relative coat protein concentrations. Because this was probably due to the fact that cotyledons presented wounds induced by the mechanical inoculation (and wounds emitting a spontaneous fluorescence), cotyledons were removed from further analyses.

Then to linearize the relationship between relative coat protein concentration and the proportion of fluorescent leaf surface for each plant species, we used the logarithm of the coat protein concentrations (as frequently done for concentration values), including a constant of 0.001 for *C. annuum* cv. 'Yolo Wonder' to avoid infinite values when the concentration is zero (figure 25). The calculated R² values are 0.85, 0.86 and 0.89 for *C. annuum* cv. 'Yolo Wonder', *N. tabacum* cv. 'Xanthi' and *N. benthamiana*, respectively. In addition, for *N. tabacum* cv. 'Xanthi' a linear model fitted on fluorescent surface values between 0 and 0.92 provided a R² value equal to 0.98. The general distribution of the data showed that for all plant species, the coat protein concentration variances becomes larger as the proportion of fluorescent leaf surface increases. Indeed for *C. annuum* cv. 'Yolo Wonder', the coat protein concentrations measured when the leaves showed between 97 and 100% of fluorescent surface range from 0.17 to 4.41. The same pattern could be observed for *N. benthamiana* and *N. tabacum* cv. 'Xanthi' where the coat protein concentrations ranged respectively from 0.18 to 1.52 and 5.8 to 77.8 and for proportions of fluorescent leaf surface between 97 and 100%.

Table 8: Mean and 95% confidence interval for the parameters of the non-linear logistic equations estimated for two cultivars of *C. annuum*, 'Yolo Wonder' and 'Perennial'

Cultivar	μ^a	k^b	s^c
'Yolo Wonder'	11.48 (10.8 - 12.19)	0.77 (0.67 - 0.88)	0.19 (0.18 - 0.22)
'Perennial'	16.31 (15.22 - 17.4)	0.098 (0 - 0.2)	0.13 (0.098 - 0.17)

^a Time to reach 50% of the maximum proportion of fluorescent leaf surface (days)

^b Maximum proportion of fluorescent leaf surface

^c Slope at the inflection point

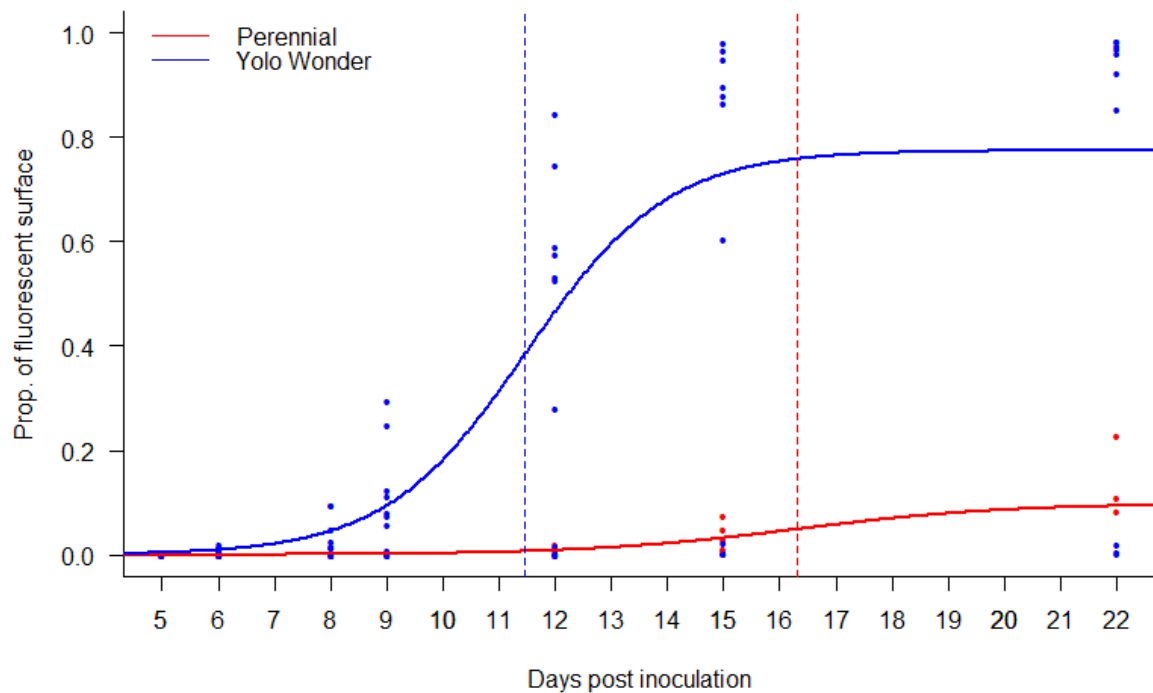


Figure 26: Kinetics of the proportion of fluorescent leaf surface in PVYson41p-115k-GFP infected leaves of *C. annuum* cv. 'Yolo Wonder' and 'Perennial'. Circles: experimental data; solid lines: prediction of the dynamics following a single and successful aphid mediated inoculation using the best-fitting logistic model; dashed vertical lines: time to 50% of the maximum value of fluorescent leaf surface.

6. Assessing PVY_{SON41p-115K-GFP} accumulation in two contrasted pepper genotypes

These results were obtained by monitoring the GFP fluorescence on pepper plants after aphid-mediated inoculation of PVY_{SON41p-115K-GFP} (figure 26). Fluorescence imaging was performed on 5, 6, 8, 9, 12, 15 and 22 days post inoculation (dpi). According to the results (table 8), 'Perennial' showed a lesser, slower and delayed viral accumulation in comparison to 'Yolo Wonder'. Indeed, the maximum proportion of fluorescent leaf surface was 77% for 'Yolo Wonder' and only 9.8% for 'Perennial'. The infected leaves of 'Yolo Wonder' reached 50% of their maximum fluorescent surface proportion about 11.5 days post inoculation, while it was about 16 days post inoculation for 'Perennial'. Finally, the slope at the inflection point was about 19% per day for 'Yolo Wonder' and 13% per day for 'Perennial'.

Discussion

1. A robust quantitative approach to estimate viral load

In a context of sustainable use of plant resistances against viruses, several methodologies for quantifying the viral load in plants in order to assess their resistance level could have been used. Indeed, a strategy could have been the establishment of a correlation between a symptom expression quantitative variable (non-destructive method) and virus coat protein concentration (destructive method). However, some authors reported difficulties to closely correlate virus titer to symptom expression (Zhu and al, 2010) and distinct resistance mechanisms may govern symptom expression and virus accumulation leading to a break in the correlation (Kaweesi and al, 2014). Here two methods for quantifying the virus in plants infected by a modified virus were tested and compared. The first one based on fluorescence imaging focuses on GFP emission measurements while the second based on quantitative ELISA focuses on virus coat proteins. A major result was the monotonic relationship between relative coat protein concentration and the proportion of fluorescent leaf surface on pepper and tobacco leaf samples. Biologically it seemed intuitive that as the modified virus isolate multiplied within its host, it increased the coat protein concentration in the infected tissues and simultaneously the concentration of GFP. It should be noted that no GFP titer was actually performed, but it was estimated by fluorescence imaging. Indeed, when GFP is purified from a sample, its fluorescence intensity is directly linked to its concentration, which allows the design of non-destructive quantitative methods (Remans and al, 1999; Richards and al, 2003). However here we decided to use the proportion of fluorescent leaf surface instead of the average level of fluorescence because the link between the coat protein concentration and the proportion of fluorescent surface was unequivocally exponential for all studied plant species. The Pearson's correlation coefficient (r) of the linearized models were all above 0.92 which indicates a very strong correlation between the coat protein concentrations and the proportions of fluorescent leaf surface. In addition, for *N. tabacum* cv. 'Xanthi', the fit of a linear model was good enough to provide a r value equal to 0.99 when the proportion of fluorescent surface values are between 0% and 92%. It highlighted that when the proportion of fluorescent leaf surface became close to 100%, there is a saturation effect of this variable while the other (coat protein concentration) kept increasing. Thus, the linearity was lost and the value of fluorescence had to be considered with care.

This work is destined to be complemented by other experiments, as the relationship between the two presented quantification methods concerns only viral proteins. In fact, when a virus replicates in the host cell, the viral proteins are separated from the nucleic acids (Walkey, 1991; Astier and al, 2001). As a complete virus particle is defined by the viral RNA surrounded by its related proteins, quantifying both viral proteins and nucleic acids would nicely complete this work.

2. Promising prior results for an entire RT-qPCR protocol development

The development of a RT-qPCR method would be useful to link these virus related protein quantitative variables to the RNA quantity. Such correlation has already been made on *N. tabacum* cv. 'Xanthi' infected with a GFP labelled PVY isolate where the measured GFP fluorescence intensity showed a linear correlation ($R^2 = 0.76$) with virus RNA concentration (Rupart and al, 2015). Such result is essential to get a fine understanding of viral quantification by RT-qPCR which has a higher specificity than ELISA (Webster and al, 2004; Bustin and al, 2009; Varveri and al, 2015). However, the entire RT-qPCR protocol had to be developed. To date the target region chosen for quantification was the contiguous sequences of the coat protein gene and the 3' untranslated region which is highly conserved among PVY isolate strain groups (Kim and al, 2016). Here all the designed primers successfully amplified the targeted sequence in the coat protein region (PM2011, PM2012, PM2013 and PM2014) as well as the 3' untranslated region (PM202) of the isolate PVYson41p-115K-GFP. Moreover, two of the primer pairs (PM202F-PM202R and PM2011F-PM2011R) were tested on 14 other PVY isolates and were able to detect all of them. These primers are thus good candidates for the laboratory to detect and quantify any PVY isolate. More specifically the primer pair, PM202F-PM202R must apparently be preferred as it also presented the lowest probability to form primer dimer bands and to hybridize with pepper sequences. In addition, the next experiments will also use the RNeasy®Plant Mini Kit for RNA extraction given the quality of extracted RNA even though the yield is significantly lower and the price is higher than with the TRI-Reagent®-chloroform method (1.48€ vs 1.00€ per extracted sample respectively). Finally, the assessment of the relationship between viral RNA concentration and the proportion of fluorescent leaf surface will require further adjustments like choosing the most suitable protocol for reverse transcription (one or two steps) and the best candidate reference gene for normalization among the three candidates (actin, ubiquitin and tubulin identified based on literature). In addition, as a primer pair which amplifies a PCR product in standard RT-PCR may have a poor efficiency in RT-qPCR, the quantification efficiency of the primers will also require further analysis. The method for gene expression analysis will be based on SYBR Green as it is relatively cost effective (Tajadini and al, 2014).

3. Fluorescence imaging: a non-destructive and reliable method for virus quantification

The proportion of fluorescent leaf surface appears to be a good estimator of the viral load (at least the amount of coat proteins), which can therefore be monitored in a non-destructive way by fluorescence imaging. A non-destructive method presents the main advantage to allow a direct quantification of the virus without any sample processing in contrast to serological or molecular methods. Moreover, compared to ELISA and RT-qPCR, fluorescence imaging is well less labor intensive (at least for capturing images) and is cheaper (no need for expensive extraction kits or antibodies) (Bustin, 2000; Sakamoto and al, 2018). However, as shown by the figures, the auto fluorescence of plant tissues was a serious drawback to have reliable results. Indeed, auto fluorescence may be linked to the

plant tissues (stems, roots), to the presence of necrotic spots or to damages caused by the inoculation procedure (Baulcombe and al, 1995). Here, the achievement of a complementary ELISA test for virus detection showed that only the leaves and the roots were effectively infected in 'Yolo Wonder'. However, the roots of healthy plants presented high auto fluorescence response. This highlighted that not all plant organs were good targets for virus detection or quantification by fluorescence imaging; leaves were definitely the organ to favor. Indeed, the auto fluorescence is a known as a recurrent limit in fluorescence imaging and generally encourages scientists to design specific strategies to overcome auto fluorescence of living tissues (Kodama, 2016). Likewise, severe interference of chlorophyll with GFP are known to disrupt the proportional relationship between GFP titer and fluorescence leading to substantial errors in estimating the target concentration (Zhou and al, 2005). In our experiments, these issues were limited in estimating the proportion of fluorescent leaf surface by adding an auto fluorescence threshold. Nevertheless, some uncertainty may lie in the fluorescence measurements because the calculation of the proportion of fluorescent leaf surface is provided by manually cutting-our surfaces on images (which is, in addition, labor intensive). In order to evaluate the reliability of this measurement, we tested the correlations between the estimated total leaf area and the actual weight of each leaf. The obtained Pearson's correlation coefficients were always above 0.76, which suggested that our measurements were accurate. Further works is needed to automate image analysis using an image processing software like ImageJ to speed up the analysis and improve the precision of the results.

Finally, as the proportion of fluorescent leaf proportion was not impacted by leaf size and allowed comparisons of phenotypically different plant cultivars, this method may be extended to the phenotyping of virus accumulation in different genotypes.

4. The proportion of fluorescent surface allows to monitor virus accumulation dynamics confirming known resistance characteristics of pepper cultivars

As demonstrated above, the proportion of fluorescent leaf surface could thus be used to assess resistances targeting viral accumulation. In this context, *C. annuum* cv. 'Yolo wonder' and 'Perennial' were chosen for their contrasted resistance profile to PVY and were inoculated via aphids with the isolate PVY_{SON41p-115K-GFP}. Unsurprisingly, 'Yolo Wonder' presents a higher level of virus accumulation ($k = 77\%$) and a faster virus accumulation ($\mu = 11.5$ days) than 'Perennial' ($k = 9.8\%$ and $\mu = 16.31$ days). Consequently, all the non-linear logistic model estimators highlight the higher susceptibility of the cultivar 'Yolo Wonder' than 'Perennial'. Biologically, it seemed that PVY accumulated more in 'Yolo Wonder' than in 'Perennial' which are known to present respectively a susceptibility allele ($pvr2^+$) and a resistance allele ($pvr2^3$) combined with three QTLs. These observations confirmed the characteristics of these cultivars, and in the case of 'Perennial' they allowed to assess the level of resistance on PVY accumulation (Montarry and al, 2012; Quenouille and al, 2013). Here the low accumulation PVY_{SON41p-115K-GFP} in 'Perennial' shows that the quantitative resistance to PVY occurs at an early step of the viral infection process (Moury and al, 2004).

Nevertheless, it is important to bear in mind that this method only allowed the assessment of resistance to virus accumulation; as mentioned in the introduction other steps of the viral cycle could be targeted by plant resistances.

5. *C. annuum* cv. 'Perennial' resistance to mechanical inoculation of PVY_{SON41p-115K-GFP}

Comparing the results of two different virus inoculation procedures (mechanical and aphid mediated) obtained with two pepper cultivars, it was very surprising to measure viral accumulation in 'Perennial' following an aphid-mediated inoculation even though a mechanical inoculation never succeeded in efficiently infecting this cultivar. To our knowledge, 'Perennial' is described to be completely resistant to the isolate PVY_{SON41p}. Nevertheless, a mutation in the VPg (at 115th amino acid) restores infectivity and breaks down the major resistance gene (*pvr2*³). Thus, the failure of virus infection after mechanical inoculation wasn't expected, especially because potyviruses are notorious to be easily transmitted via mechanical inoculations (Kerlan, 2006, Quenouille and al, 2013). Our current hypothesis relies on the anatomic differences between the two pepper cultivars. Indeed, leaves of *C. annuum* cv.'Perennial' are harder and twice smaller than these of *C. annuum* cv.'Yolo Wonder'. Moreover, on other pathosystems, authors reported several factors affecting mechanical transmission of plant viruses such as the presence of a high wax layer on the leaves which could be overcome by the use of Na₂SO₃ and mercaptoethanol in the inoculation buffer (Mandal and al, 2001). They also recommended the use of more abrasive powders like diatomaceous earth to ensure more injuries on the leaves (Mandal and al, 2001). These ideas could be confirmed by further adjustments of the inoculation procedure of PVY on 'Perennial' or by scanning electron microscope. In any case, the evident success of aphid mediated inoculation confirmed that aphid mouthparts and feeding process are remarkably adapted to virus inoculation (Brault and al, 2010).

6. Ambiguous effects inducing OD variations in ELISA plates

The lack of reproducibility of the ELISA method may be explained by numerous factors that could interfere at different steps of the test and highly depends on the studied pathogen (Cardin and al, 1984). However, as at the "Pathologie Végétale" research unit, manipulators perform ELISA on a daily basis, they reported divergences in achieving an entire ELISA, like the light conditions for substrate incubation and the washing method for removing plant extracts. Here, the assessment of possible factors influencing OD values in ELISA was investigated on PVY. First, the effect of the method to remove plant extracts from the plates was not significant and no contamination leading to false positive results was observed. This meant that the sensibility of the ELISA tests for PVY diagnostic and quantification on pepper was not compromised by the washing method. In addition, the light effect showed no significant effect on the normalized OD values measured on plates incubated in the light or in the dark even though it is in contradiction with the supplier recommendations (Esser, 2014). With regard to the washing method and light condition for substrate incubation, the

methods requiring the least effort (sink washing and substrate incubation in light) were retained for all subsequent ELISA measurements.

According to Cardin and al (1984), the OD variations among the wells of a plate are not randomly assigned. This observation was supported by the determination of a significant difference between the mean of the normalized OD values from the peripheral wells and the center wells of the plates loaded with *C. annuum* cv. 'Yolo Wonder' leaf extracts. However, no significant difference was detected between the mean of the normalized OD values from the peripheral and the center wells of the plates loaded with *N. tabacum* cv. 'Xanthi'. As these tests using *N. tabacum* cv. 'Xanthi' leaf extracts were performed first during my internship, it led to the use of the 96 wells for all semi-quantitative ELISA tests. This avoided the loss of the 36 peripheral wells and limited therefore the number of required plates which matched the SME (Environment Management System) certification of the research unit and its global procedure of waste reduction. Indeed, the use of the whole microtiter plates reduced by half the number of plates required for the whole internship (56% of reduction). In addition, as shown by the figures the general distributions of the OD values varied sharply between the plates which made more difficult the establishment of a final conclusion. Indeed, the determination of a significant difference in the normalized OD means between the center and the peripheral wells wasn't always linked to a U- or n-shape tendency of the mean OD values along lines and columns. Nevertheless, we kept analyzing the influence of the well position until the end of my internship and finally identified an "Edge" effect within microtiter plates. This justifies the traditional avoidance of the peripheral wells. According to several authors, the variations between the OD measured from the peripheral to the center wells can be attributed to differences in thermic isolation and plastic characteristics within the plates, leading to differences in enzyme activity and in antigen attachment, respectively (Burt and al, 1979; Oliver and al, 1981; Shekarchi and al, 1984).

Conclusion

Breeding for resistance with conventional approaches remains a long and expensive process. Therefore, in order to be cost-efficient and to maximize the success probability of plant resistances use, the prior assessment of plant resistances is essential. And yet, despite the recent development and spread of easy and reliable serological and molecular techniques for virus detection and quantification, the phenotyping of plant resistances among plant accessions bank using laboratory methods is still labor intensive. In order to face these main issues, this report presented the first evaluation of a non-destructive method for quantifying virus accumulation, based on fluorescence imaging. Measures of viral accumulation in pepper (*C. annuum* cv. 'Yolo wonder') and tobacco (*N. benthamiana* and *N. tabacum* cv. 'Xanthi') plants inoculated by a modified PVY isolate (PVY_{SON41p-115K-GFP}) were significantly and positively correlated when obtained by ELISA (to quantify coat proteins) and fluorescence imaging (to estimate the proportion of fluorescent leaf surface). Hence, the estimation of the viral load by fluorescence imaging allowed to observe the phenotypic expression of resistance to PVY accumulation in a resistant cultivar ('Perennial') compared to susceptible one ('Yolo Wonder'). Thus, if the relationship between virus RNA concentrations and the proportion of fluorescent leaf surface lead to the same observations, it will corroborate that the quantification of GFP appears as a promising macroscopic and non-destructive method which may be used for further phenotyping pepper resistances to PVY accumulation. Indeed, thirteen pepper double haploid lines issued from the F₁ hybrid (Perennial x Yolo Wonder) went through the same protocol as 'Perennial' and 'Yolo Wonder' plants in order to assess PVY_{son41p-115K-GFP} virus accumulation. According to their genotypes characteristics, their response to virus accumulation may provide different resistance profiles. Finally, the quantification of virus remains a reliable method for phenotyping plant resistances against virus accumulation. However, the characterization of plant resistances on other viral cycle steps (inoculation, systemic colonization, acquisition) would require the design of other specific methodologies.

Cited literature

Astier, S., J. Albouy, Y. Maury, et H. Lecoq. Principes de virologie végétale, génome, pouvoir pathogène, écologie des virus. INRA., 2001.

Baulcombe, D.C., S. Chapman, et S. Santa Cruz. « Jellyfish green fluorescent protein as a reporter for virus infections ». *The Plant Journal* 7, n° 6 (1995): 1045-53.

Boissot, N., S. Thomas, N. Sauvion, C. Marchal, C. Pavis, et C. Dogimont. « Mapping and validation of QTLs for resistance to aphids and whiteflies in melon ». *Theoretical and Applied Genetics* 121 (2010): 9-20.

Boonham, N., J. Kreuze, S. Winter, R. Van der Vlugt, J. Bergervoet, J. Tomlinson, et R. Mumford. « Methods in virus diagnostics from ELISA to next generation sequencing ». *Virus Research*, n° 65 (2014): 473-503.

Boote, K.J., J.W. Jones, J.W. Mishoe, et R.D. Berger. « Coupling pests to crop growth simulators to predict yield reductions ». *Phytopathology*, n° 73 (1983): 1581-87.

Boualem, A., C. Dogimont, et A. Bendahmane. « The battle for survival between viruses and their host plants ». *Current Opinion in Virology*, n° 17 (2016): 32-38.

Brault, V., M. Uzest, B. Monsion, E. Jacquot, et S. Blanc. « Aphids as transport devices for plant viruses ». *Compte Rendus Biologie* 333, n° 6-7 (2010): 524-38.

Burt, S.M., T.J.N. Carter, et L.J. Kricka. « Thermal characteristics of microtitre plates used in immunological assays ». *Journal of Immunological Methods* 31 (1979): 231-36.

Bustin, S.A. « Absolute quantification of mRNA using real-time reverse transcription polymerase chain reaction assay ». *Journal of Molecular Endocrinology*, n° 25 (2000): 169-93.

Bustin, S.A., V. Benes, J.A. Garson, J. Hellems, J. Huggett, M. Kubista, R. Mueller, et al. « The MIQE Guidelines: Minimum Information for Publication of Quantitative Real-Time PCR Experiments ». *Clinical Chemistry* 55, n° 4 (2009): 611-22.

Bustin, S.A., et J. Huggett. « qPCR primer design revisited ». *Biomolecular Detection and Quantification*, n° 14 (2017): 19-28.

Cardin, L., J.C. Devergne, et M. Pitrat. « Dosage immunoenzymatique (ELISA) du virus de la mosaïque du concombre. I. Aspect méthodologique ». *Agronomie* 4, n° 2 (1984): 125-35.

Charron, C., M. Nicolai, J.L. Gallois, C. Robaglia, B. Moury, et C. Caranta. « Natural variation and functional analyses provide evidence for co-evolution between plant eIF4E and potyviral VPg: Co-evolution between eIF4E and VPg ». *The Plant Journal* 54, n° 1 (2008): 56-68.

Chisholm, S.T., M.A. Parra, R.J. Anderberg, et J.C. Carrington. « Arabidopsis RTM1 and RTM2 genes function in phloem to restrict long-distance movement of tobacco etch virus ». *Plant Physiology* 127 (2001): 1667-75.

Clark, M.F., et A.N. Adams. « Characteristics of the microplate method of enzyme-linked immunosorbent assay for the detection of plant viruses ». *Journal of General Virology*, n° 34 (1977): 475-83.

Crowther, J.R. ELISA Theory and Practice. Vol. 42. Methods in Molecular Biology. Humana Press Inc., 1995.

Dawson, W.O., et M.E. Hilf. « Host-range determinants of plant viruses ». *Annual Review of Plant Physiology*, n° 43 (1992): 527-55.

Devergne, J.C., et J. Albouy. *Maladies à virus des plantes ornementales*. INRA., 1998.

Díaz-Pendón, J.A., R. Fernández-Muñoz, M.L. Gómez-Guillamón, et E. Moriones. « Inheritance of resistance to Watermelon mosaic virus in cucumis melo that impairs virus accumulation, symptom expression and aphid transmission ». *Phytopathology* 95, n° 7 (2005): 840-46.

Dogimont, C., A. Palloix, A.M. Daubèze, G. Marchoux, K. Gebre Selassie, et E. Pochard. « Genetic analysis of broad spectrum resistance to potyviruses using diabled haploid lines of pepper (*Capsicum annuum* L.) ». *Euphytica* 88 (1996): 231-39.

Esser, P. « Edge effect in Thermo Scientific Nunc Microwell ELISA ». Thermo Scientific, 2014.

Fereres, A., C. Avilla, J.L. Collar, M. Duque, et C. Fernandez-Quintanilla. « Impacts of various yield-reducing agents on open-field sweet peppers ». *Environmental Entomology* 25 (1996): 983-86.

Fraser, R.S.S. « The genetics of plant-virus interactions: implications for plant breeding ». *Euphytica* 63 (1992): 175-85.

Gago, S., S.F. Elena, R. Flores, et R. Sanjuán. « Extremely high mutation rate of a hammerhead viroid ». *Science* 323 (2009): 1308-1308.

Hipper, C. « Nature du complexe viral dans le mouvement à longue distance du virus de la jaunisse du navet ». Université de Strasbourg, 2013.

Jones, R.A.C. « Control of Plant Virus Diseases ». *Advances in Virus Research* 67 (2006): 205-44.

Kaweesi, T., R. Kawuki, V. Kyaligonza, Y. Baguma, G. Tusiime, et M.E. Ferguson. « Field evaluation of selected cassava genotypes for cassava brown streak disease based on symptom expression and virus load ». *Virology journal* 11, n° 216 (2014): 1-14.

Khelifa, M. « Detection and quantification of Potato virus Y in Singel Aphid Stylets ». *Plant Disease*, n° 103 (2019): 2315-21.

Kerlan, C. « Potato virus Y ». In *Descriptions of plant viruses*, Wellesbourne UK association. *Applied Biology* 414, s. d.

Kodama, Y. « Time gating of chloroplast autofluorescence allows clearer fluorescence imaging in planta ». *Plos One* 11, n° 3 (2016): 1-8.

Kim, S., W. Kang, H.N. Huy, S. Yeom, J. An, S. Kim, M. Kang, H.J. Kim, Y.D. Jo, et Y. Ha. « Divergent evolution of multiple virus-resistance genes from a progenitor in *Capsicum* spp. ». *New Phytologists* 213 (2017): 886-99.

Lecoq, H., B. Moury, C. Desbiez, A. Palloix, et M. Pitrat. « Durable virus resistance in plants through conventional approaches: a challenge ». *Virus Research* 100, n° 1 (2004): 31-39.

Lindhout, P. « The perspectives of polygenic resistance in breeding for durable disease resistance ». *Euphytica* 124 (2002): 217-26.

- Lucas, W.J. « Plant viral movement proteins: agents for cell-to-cell trafficking of viral genomes ». *Virology* 344, n° 1 (2006): 169-84.
- Mandal, B., H.R. Pappu, et A.K. Culbreath. « Factors affecting mechanical transmission of Tomato spotted wilt virus to Peanut (*Arachis hypogea*) ». *Plant Disease* 85, n° 12 (2001): 1259-63.
- Martin, B., Y. Rahbé, et A. Fereres. « Blockage of stymet tips as the mechanism of resistance to virus transmission by *Aphis gossypii* in melon lines bearing the Vat gene ». *Annal of Applied Biology* 142, n° 2 (2005): 245-50.
- Matthews, R.E.F. *Plant Virology*. Academic Press. London, 1981.
- Montarry, J., M. Cartier, M. Jacquemond, A. Palloix, et B. Moury. « Virus adaptation to quantitative plant resistance: erosion or breakdown? ». *Journal of Evolutionary Biology*, n° 25 (2012): 2242-52.
- Moscone, E.A., M.A. Scaldaferrò, M. Grabièle, N.M. Cecchini, Y. Sanchez Garcia, R. Jarret, J.R. Daviña, D.A. Ducasse, G.E. Barboza, et F. Ehrendorfer. « The evolution of Chili Peppers (*Capsicum-Solanaceae*): a cytogenetic perspective ». *Acta Horticulturae* 745 (2006): 137-70.
- Moury, B., F. Fabre, J. Montarry, B. Janzac, V. Ayme, et A. Palloix. « L'adaptation des virus de plantes aux résistances variétales ». *Virologie* 14, n° 4 (2010): 227-39.
- Moury, B., A. Palloix, C. Caranta, P. Gognalons, S. Souche, K.G. Selassie, et G. Marchoux. « Serological, molecular, and pathotype diversity of Pepper veinal mottle virus and Chili veinal mottle virus », *Phytopathology*, 95 (2005): 227-32.
- Moury, B., C. Morel, E. Johansen, C. Guibaud, S. Souche, V. Ayme, C. Caranta, A. Palloix, et M. Jacquemond. « Mutation in Potato virus Y genome-linked protein determine virulence toward recessive resistances in *Capsicum annuum* and *Lycopersicon hirsutum* ». *Molecular Plant Microbe Interactions* 17 (2004): 322-29.
- Ng, J.C.K., et K.L. Perry. « Transmission of plant viruses by aphid vectors ». *Molecular Plant Pathology*, 2004.
- Nicaise, V. « Crop immunity against viruses: outcomes and future challenges ». *Frontiers in Plant Science* 5, n° 660 (2014): 1-18.
- Oerke, E.C. « Crop losses to pests ». *Journal of Agriculture Science*, n° 144 (2005): 31-43.
- Oliver, D.G., A.H. Sanders, D. Hogg, et J. Woods Hellman. « Thermal gradients in microtitration plates. Effects on enzyme-linked immunoassay ». *Journal of Immunological Methods*, n° 42 (1981): 195-201.
- Palloix, A., V. Ayme, et B. Moury. « Durability of plant major resistance genes to pathogens depends on the plant genetic background, experimental evidence and consequences for breeding strategies ». *New Phytologists* 183 (2009): 190-99.
- Penella, C., et A. Calatayud. « Pepper crop under climate change: grafting as an environmental friendly strategy ». In *Climate Resilient Agriculture - Strategies and Perspectives*, 2018.
- Perring, T.M., N.M. Gruenhagen, et C.A. Farrar. « Management of plant viral diseases through chemical control of insect vectors ». *Annual Review of Entomology* 44 (1999): 457-81.

Pochard, E. « Méthodes pour l'étude de la résistance partielle au virus du concombre chez le piment », 93-104, 1977.

Quenouille, J., J. Montarry, A. Palloix, et B. Moury. « Farther, slower, stronger: how the plant genetic background protects a major resistance gene from breakdown ». *Molecular Plant Pathology* 2, n° 14 (2013): 109-18.

Quenouille, J., L. Saint-Felix, B. Moury, et A. Palloix. « Diversity of genetic backgrounds modulating the durability of a major resistance gene; Analysis of a core collection of pepper landraces resistant to Potato virus Y ». *Molecular Plant Pathology* 2, n° 17 (2016): 296-302.

Remans, T., P.M. Schenk, J.M. Manners, C.P.L. Grof, et A.R. Elliott. « A protocol for fluorometric quantification of mGFP5-ER and sGFP (S65T) in transgenic plants ». *Plant Molecular Biology Reporter* 17 (1999): 385-95.

Richards, H.A., M.D. Halfhill, R.J. Millwood, et C.N. Stewart. « Quantitative GFP fluorescence as an indicator of recombinant protein synthesis in transgenic plants ». *Plant Cell Reports* 22 (2003): 117-21.

Rimbaud, L., S. Dallot, A. Delaunay, S. Borron, S. Soubeyrand, G. Thébaud, et E. Jacquot. « Assessing the Mismatch Between Incubation and Latent Periods for Vector-Borne Diseases : The case of Sharka ». *Phytopathology* 105, n° 11 (2015): 1408-16.

Rubio, L., L. Galipienso, et I. Ferriol. « Detection of plant viruses and disease management: relevance of genetic diversity and evolution ». *Frontiers in Plant Science* 11 (2020): 1-23.

Ruffel, S., M. Dussault, M. Lesage, A. Moretti, A. Palloix, M. Daunay, B. Moury, A. Bendahmane, C. Robaglia, et C. Caranta. « Involvement of the eukaryotic translation initiation factor eIF4E in Solanaceae-Potyvirus interactions. » *European Association for Research on Plant Breeding*, 2004, 167-70.

Rupart, M., F. Faurez, M. Tibodet, I. Gutiérrez-Aguirre, A. Delaunay, L. Glais, M. Kriznik, et al. « Fluorescently tagged Potato Virus Y: a versatile tool for functional analysis of plant-virus interactions ». *The American Phytopathological Society* 28, n° 7 (2015): 739-50.

Sakamoto, S., W. Putalun, S. Vimolmangkang, W. Phoolcharoen, Y. Shoyama, H. Tanaka, et S. Morimoto. « Enzyme-linked immunosorbent assay for the quantitative/qualitative analysis of plant secondary metabolites ». *Journal of Natural Medicines* 72, n° 1 (2018): 32-42.

Salem, N., A. Mansour, M. Ciuffo, B.W. Falk, et M. Turina. « A new tobamovirus infecting tomato crops in Jordan ». *Archives of Virology*, n° 161 (2016): 503-6.

Savary, S., L. Willocquet, S.J. Pethybridge, P. Esker, N. McRoberts, et A. Nelson. « The global burden of pathogens and pests on major food crops ». *Nature Ecology and Evolution*, n° 3 (2019): 430-39.

Scholthof, K.B.G., S. Adkins, H. Czosnek, P. Palukhaitis, E. Jacquot, T. Hohn, B. Hohn, et al. « Top 10 plant viruses in molecular plant pathology ». *Molecular Plant Pathology* 12, n° 9 (2011): 938-54.

Sharma, N., P.P. Sahu, S. Puranik, et M. Prasad. « Recent Advances in Plant-Virus Interaction with Emphasis on Small Interfering RNAs (siRNAs) ». *Molecular Biotechnology*, n° 55 (2013): 63-77.

- Shekarchi, I.C., J.L. Sever, Y.J. Lee, G. Castellano, et D.L. Madden. « Evaluation of various plastic microtiter plates with measles, toxoplasma, and gamma globulin antigens in enzyme-linked immunosorbent assays ». *Journal of Clinical Microbiology* 19, n° 2 (1984): 89-96.
- Strange, R.N., et P.R. Scott. « Plant Disease: A threat to Global Food Security ». *Annual Review of Phytopathology*, n° 43 (2005): 83-116.
- Sylvester, E.S. « Circulative and propagative virus transmission by aphids ». *Annual Review of Entomology*, n° 25 (1980): 257-86.
- Tamisier, L., M. Szadkowski, G. Nemouchi, V. Lefebvre, E. Szakowski, R. Duboscq, S. Santoni, et al. « Genome-wide association mapping of QTLs implied in Potato virus Y population sizes in pepper: evidence for widespread resistance QTL pyramiding ». *Molecular Plant Pathology* 21, n° 1 (2020): 3-16.
- Tajadini, M., M. Panjehpour, et S.H. Javanmard. « Comparison of SYBR Green and TaqMan methods in quantitative real-time polymerase chain reaction analysis of four adenosine receptor subtypes ». *Advanced Biomedical Research* 85, n° 3 (2014).
- Thompson, J.R., et M. Tepfer. « Assessment of the benefits and risks for engineered virus resistance ». In *Advances in Virus Research*, Academic Press., 76:33-56. Burlington, 2010.
- Tse, C., et J. Capeau. « Quantification des acides nucléiques par PCR quantitative en temps réel ». *Annales de Biologie Clinique* 61, n° 3 (2003): 279-93.
- Valverde, R.A., S. Sabanadzovic, et J. Hammond. « Viruses that Enhance the Aesthetics of some Ornamental Plants: Beauty or Beast? ». *Plant Disease* 96, n° 5 (2012): 600-611.
- Van Stralen, K.J., V.S. Stel, J.B. Reitsma, F.W. Dekker, C. Zoccali, et K.J. Jager. « Diagnosis methods I: sensitivity, specificity, and other measures of accuracy ». *Kidney international* 75, n° 12 (2009): 1257-63.
- Varveri, C., V.I. Maliogka, et T. Kapari-Isaia. « Principles for supplying virus-tested material ». In *Control of Plant Virus Diseases*, Academic Press., 2-24, 2015.
- Walkey, D. *Applied Plant Virology*. Chapman and Hall. Kluwer Academic Publishers, 1991.
- Wang, M.R., Z.H. Cui, J.W. Li, X.Y. Hao, L. Zhao, et Q.C. Wang. « In vitro thermotherapy-based methods for plant virus eradication ». *Plant Methods* 14, n° 87 (2018): 1-18.
- Webster, C.G., S.J. Wylie, et M.G.K. Jones. « Diagnosis of plant viral pathogens ». *Current Science* 86, n° 12 (2004): 1604-7.
- Zhou, Y.J., S.T.S. Lim, S. Schenck, A. Arcinas, et E. Komor. « RT-PCR and quantitative real-time RT-PCR detection of symptomatic Sugarcane Yellow Leaf Virus (SCYLV) in symptomatic and asymptomatic plants of Hawaiian sugarcane cultivars and the correlation of SCYLV titre to yield ». *European Journal of Plant Pathology*, n° 127 (2010): 263-73.

Appendices

Table S1: Composition of the inoculation/grinding buffer

Reagents	Volume or mass for 10 mL of buffer
Na ₂ HPO ₄ 12H ₂ O	0,1074 g
C ₅ H ₁₀ NS ₂ (Diethyldithiocarbamate)	0,02 g
H ₂ O	Qsp 10mL

Table S2: Composition of the inoculation buffer of the first IgG dilution buffer

Reagents	Volume or mass for 1 L of buffer
NA ₂ CO ₃	1.6 g
NAHCO ₃	3 g
H ₂ O	qsp 1L

Table S3: Composition of the inoculation buffer of the second IgG dilution buffer

Reagents	Volume or mass for 1 L of buffer
Polyvinylpyrrolidone	20 g
Ovalbumine	2 g
NaN ₃	0.2 g
H ₂ O	qsp 1L

Table S4: Composition of the *p*-nitrophenyl-phosphate buffer (pH adjusted to 9.8 with fuming HCl)

Reagents	Volume or mass for 1 L of buffer
H ₂ O	800 mL
Diethanolamine	97 mL
H ₂ O	qsp 1 L

Table S5: Composition of a 1% agarose gel

Reagents	Volume or mass for 700 mL of gel
TAE	700 mL
Agarose	7g

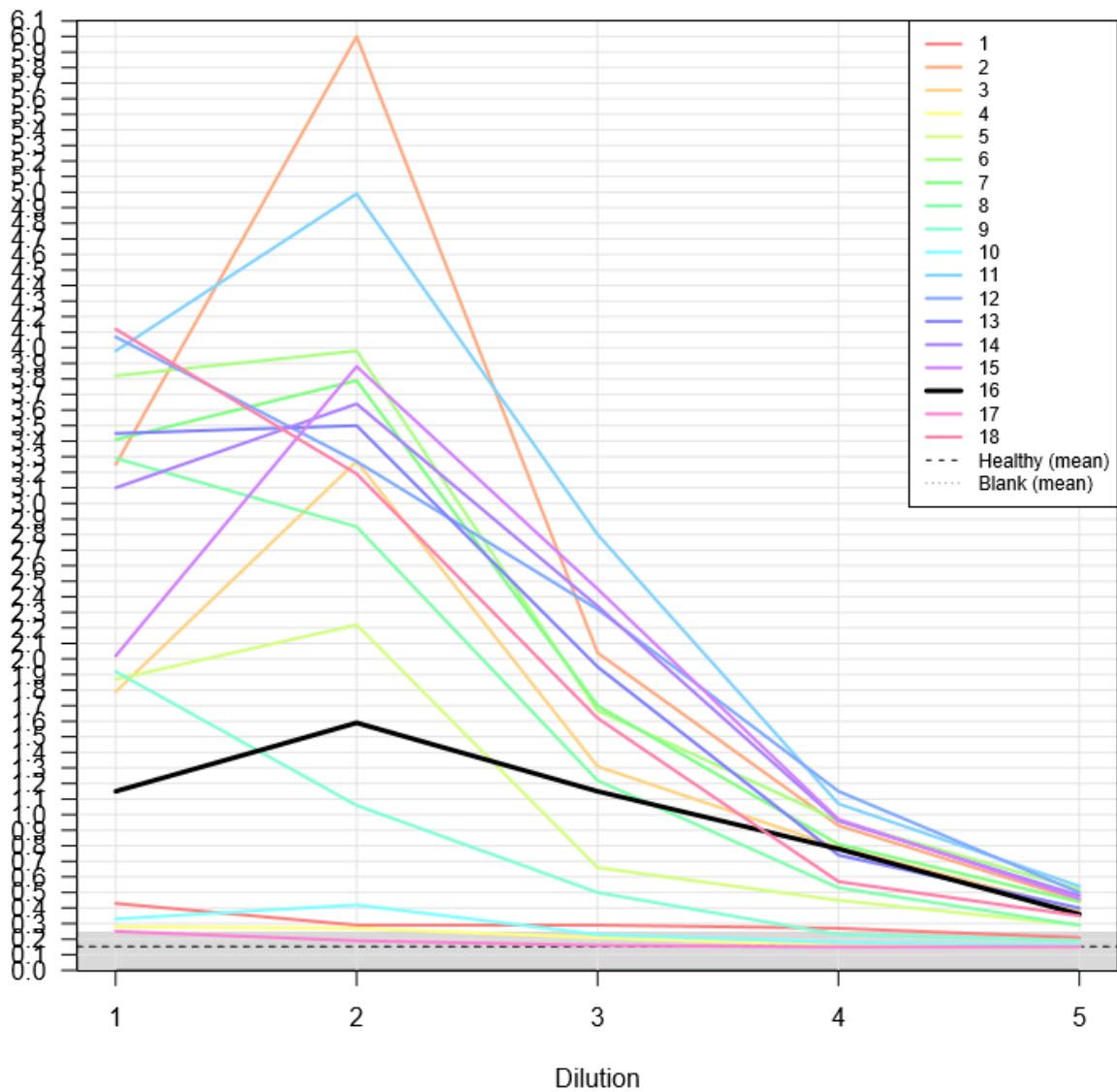


Figure S1: OD values in function of the dilution factor for the 18 samples of a plate (16th sample: reference sample). Dilution factors, 1: 1:5, 2: 1:25, 3: 1:125, 4: 1:625, 5: 1:3125)

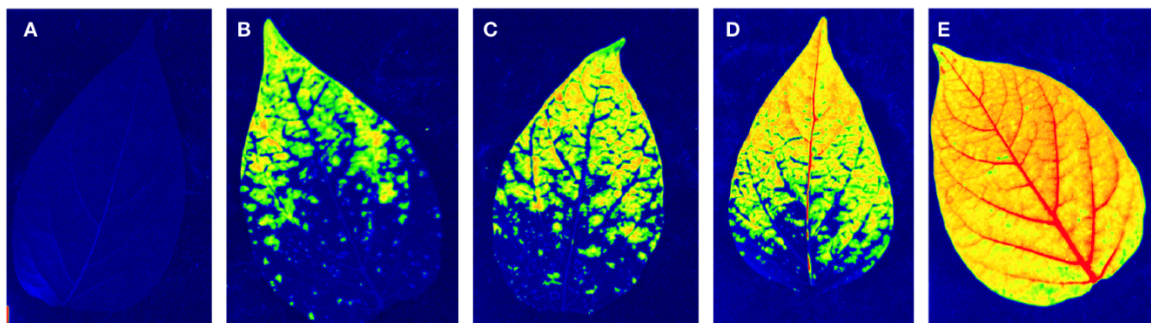


Figure S2: Illustration of the proportion of fluorescent leaf surface (A = 0%; B = 26.5%; C = 50%; D = 71.6% and E = 99.5%).

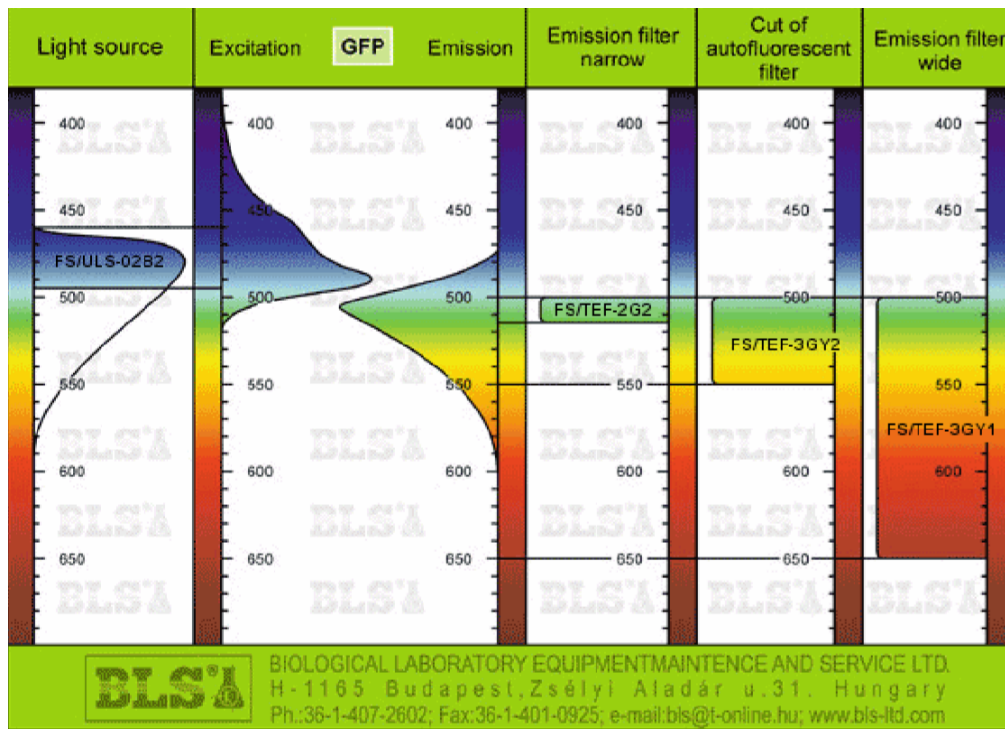


Figure S3: GFP excitation and emission spectrum (BLS®, Hungary)

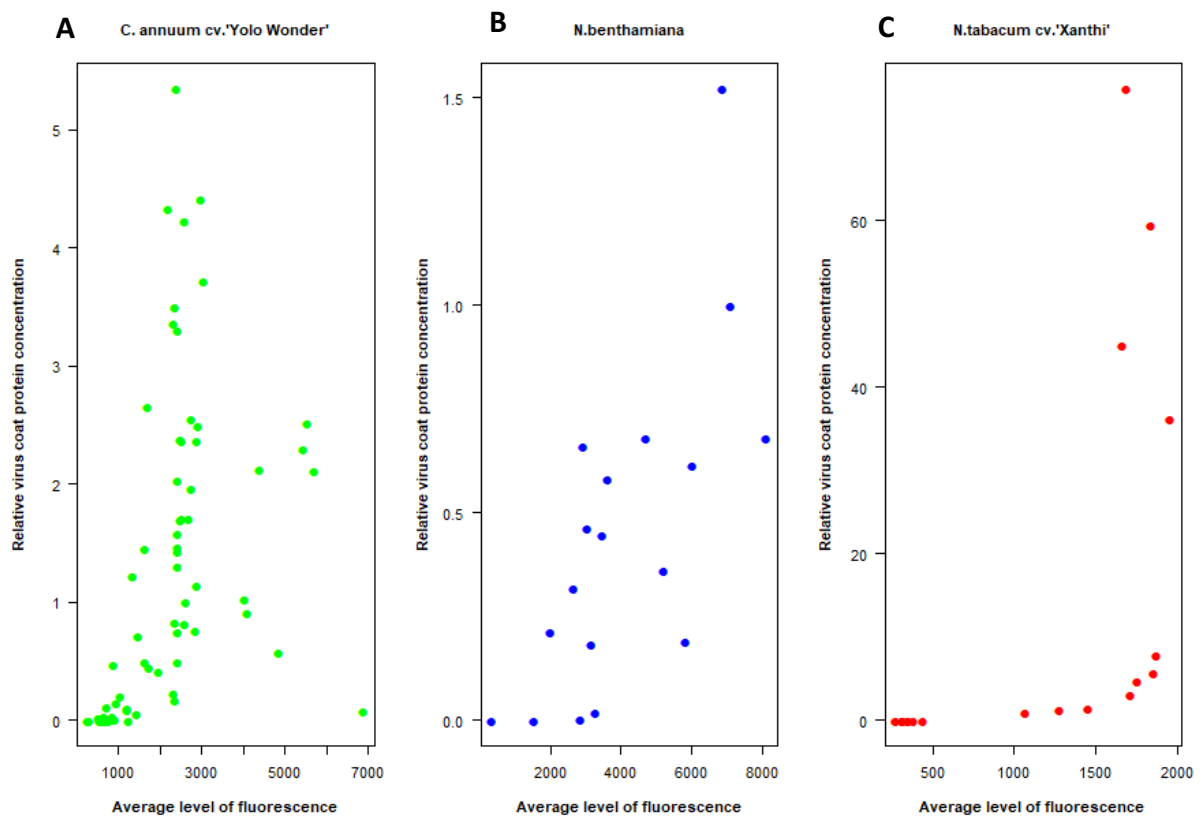


Figure S4: Relative coat protein concentrations in function of average level of fluorescence of the leaves of (A) *C. annuum* cv. 'Yolo Wonder', (B) *N. benthamiana*, (C) *N. tabacum* cv. 'Xanthi'.

Table S6: Pearson's correlation coefficient (r) between leaf weight (g) and leaf total size (in pixels) for *C. annuum* cv. 'Yolo Wonder', *N.benthamiana*, *N.tabacum* cv.'Xanthi'.

Plant species	Relationship between leaf weight and leaf total size	
	r	p-value
<i>C. annuum</i> cv.'Yolo Wonder' (N = 74)	0.75	1.94×10^{-14}
<i>N.benthamiana</i> (N = 19)	0.83	1.26×10^{-5}
<i>N.tabacum</i> cv. 'Xanthi' (N = 19)	0.79	8.59×10^{-5}

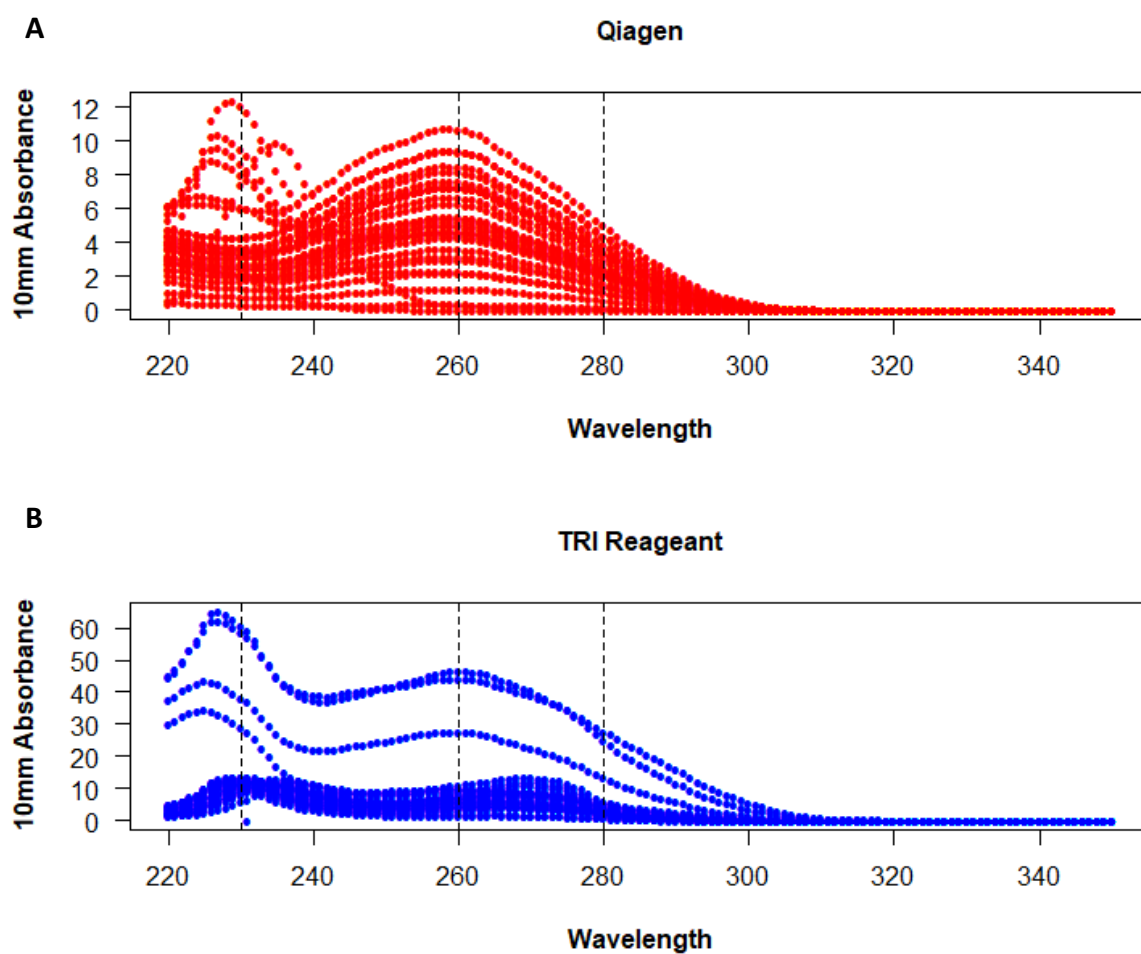


Figure S5: Absorption in function of wavelength of 30 RNA samples extracted with two extraction methods: (A) RNeasy® Plant Mini Kit (Qiagen, Germany) and (B) TRI-Reagent® - chloroform (MRC, USA). All the absorptions were measured via Nanodrop®ND-1000 Spectrophotometer (Thermo-Scientific, USA)

R script example for assessing the washing effect on normalized OD values

Student's t test

```
mod3 <- lm(Abs_norm~Lavage, data = DataELISA[DataELISA$Type == "Blanc",])  
summary(mod3)
```

Assessing the conditions of application

```
validation.test(mod = mod3, myfactor = DataELISA$Lavage)  
plot_model(mod = mod3, myfactor = DataELISA$Lavage)
```

In case of a significant Bartlett test, rejection of the variances homogeneity hypothesis

```
t.test(Abs_norm~Lavage, data = DataELISA[DataELISA$Type == "Blanc",])
```

In case of a significant Shapiro-Wilk test, rejection of the normal distribution hypothesis

```
kruskal.test(Abs_norm ~ Lavage, data = DataELISA)
```

Designed functions for automating the tests and graphic representations

```
validation.test <- function(mod,myfactor) {
```

```
  #Independency of the residues
```

```
  require(lmtest)
```

```
  dtest <- dwtest(mod)
```

```
  #Normality of the residues
```

```
  stest <- shapiro.test(residuals(mod))
```

```
  #Homogeneity of the residues
```

```
  btest <- bartlett.test(residuals(mod)  
                        ~myfactor)
```

```
  Res <- c(DurbinWatson=dtest$p.value, Shapiro=stest$p.value, Bartlett=btest$p.value)
```

```
  return(Res)}
```

```
plot_model <- function(mod,myfactor){
```

```
  # Normality of the residues and homoscedasticity
```

```
  par(mfrow=c(2,2))
```

```
  hist (residuals(mod)
```

```
    , xlab='Residue values'
```

```
    , ylab='Numbers')
```

```
  qqnorm(residuals(mod)
```

```
    , col='red'
```

```
    ,pch=16)
```

```
  qqline(residuals(mod))
```

```
  plot(residuals(mod)~fitted(mod)
```

```
    , pch=16
```

```
    , xlab = "Fitted values"
```

```
    , ylab = "Residuals"
```

```
    , main = "Homogeneity?")
```

```
  abline(h = 0, v = 0, lty = 2)
```

```
boxplot( residuals(mod)~ myfactor
        , varwidth = TRUE
        , ylab = "Residus"
        , xlab = "Factor"
        , main = "Homogeneity?")
abline(h = 0, v = 0, lty = 2)
Res <- validation.test(mod, myfactor)
return(Res)
}
```

 agriculture • alimentation • environnement	 Diplôme d'Ingénieur de l'Institut Supérieur des Sciences agronomiques, agroalimentaires, horticoles et du paysage Spécialité : Horticulture Enseignant référent : Alexandre Degrave
Auteur : Pierre Mustin Date de naissance : 08/08/1997	Organisme d'accueil : INRAE- Institut National de Recherche pour l'Agriculture, l'Alimentation et l'Environnement – UR Pathologie Végétale – Equipe Virologie
Nb pages : 38 Annexe(s) : 6	
Année de soutenance : 2020	Adresse : Domaine Saint Maurice, 67 allée des chênes, 84140, Avignon Maître de stage : Loup Rimbaud
Titre français : Caractérisation de différentes résistances du piment au <i>Potato virus Y</i> par des mesures quantitatives de la charge virale Titre anglais : Characterization of different pepper resistances to <i>Potato virus Y</i> through quantitative approaches to measure viral load	
Résumé: La résistance des plantes aux virus peut cibler différentes étapes du cycle du virus, comme l'inoculation, l'accumulation et le mouvement de cellule à cellule, la colonisation systémique et l'acquisition par un vecteur. Parmi celles-ci, l'accumulation de virus dans les plantes peut être inhibée ou diminuée par différents mécanismes de résistance. Même si elles sont bien caractérisées au niveau moléculaire, l'évaluation de l'expression phénotypique de ces résistances nécessite le développement de méthodes spécifiques. Basé sur le pathosystème piment- <i>Potato virus Y</i> (PVY), ce travail s'appuie sur 3 méthodes de mesure quantitative de l'accumulation des virus dans les plantes : l'ELISA, la RT-qPCR et l'imagerie par fluorescence. Le résultat principal est l'identification une corrélation significative entre la proportion de surface fluorescente mesurée par imagerie fluorescente (et liée à l'expression de la protéine GFP accolée au virus) et la concentration de protéines de capsid mesurée par ELISA semi-quantitative. En outre, l'utilisation de l'imagerie fluorescente (une méthode non destructive) a permis de suivre l'accumulation virale dans différentes accessions de piments et a mis en évidence une cinétique contrastée chez une variété sensible et une variété résistante.	
Abstract: Plant resistance to viruses can target different stages of the virus cycle like the inoculation, the accumulation and cell to cell movement, the systemic colonization and the virus ingestion by a vector. Among them, virus accumulation in plants can be inhibited or diminished by different resistance mechanisms. Even if they are well characterized at the molecular level, the evaluation of the phenotypic expression of these resistances requires the development of specific methods. Based on the pathosystem pepper- <i>Potato virus Y</i> (PVY), this work relies on 3 methods for the quantitative measure of virus accumulation in plants: ELISA, RT-qPCR and fluorescence imaging. The major result is the identification of a significant correlation between the proportion of fluorescent surface area measured by fluorescent imaging (and linked to the expression of a GFP protein stuck on the virus) and the concentration of coat proteins measured by semi-quantitative ELISA. In addition, the use of fluorescent imaging (a non-destructive method) allowed the monitoring of viral accumulation in different pepper accessions and highlighted contrasted kinetics in a susceptible and a resistant cultivar.	
Mots-clés : Méthodes de quantification – accumulation viral – résistance des plantes – ELISA – RT-qPCR – Imagerie par fluorescence – GFP – PVY - Piment Key Words: Quantification methods – Viral accumulation – Plant Resistance – ELISA – RT-qPCR – Fluorescence imaging – GFP –PVY - Pepper	